UNIVERSIDAD COMPLUTENSE DE MADRID
FACULTAD DE CIENCIAS QUÍMICAS

TESIS DOCTORAL

Posttranslational modifications of endosomal GTPases.
Implications in intracellular localization and traffic

Modificaciones postraduccionales de GTPasas endosomales
implicaciones en localización y tráfico intracelular

MEMORIA PARA OPTAR AL GRADO DE DOCTORA
PRESENTADA POR

Clara Lillian Oeste Villavieja

Directora

María Dolores Pérez-Sala Gozalo

Madrid, 2015

©Clara Lillian Oeste Villavieja, 2015

UNIVERSIDAD COMPLUTENSE
DE MADRID

CENTRO DE INVESTIGACIONES
BIOLÓGICAS (CSIC)

Posttranslational modifications of endosomal GTPases. Implications in intracellular localization and traffic

Modificaciones postraduccionales de GTPasas endosomales. Implicaciones en localización y tráfico intracelular

By

Clara Lillian Oeste Villavieja

A thesis
in Biochemistry and Molecular Biology

Submitted to
Universidad Complutense de Madrid
in fulfillment of the requirements for the degree of

Doctor in Philosophy

Tutor
Mª Dolores Pérez-Sala Gozalo
Centro de Investigaciones Biológicas, CSIC

Madrid, 2015

"Satisfaction of one's curiosity is one of the greatest sources of happiness in life."

Linus Pauling

ACKNOWLEDGEMENTS

This work was supported by the "Formación de Personal Investigador" doctoral fellowship program (BES-2010-033718), including the "Estancias Breves" program (EEBB-I-12-04482), from MINECO within the framework of grants SAF2009-11642 and SAF2012-36519, and by RETIC RIRAAF from ISCIII (RD07/0064/0007 and RD12/0013/0008). Funding from the CSIC JAE-Intro program as well as the FEBS Summer Fellowship program is also acknowledged.

This work wouldn't have been possible without Dr. Pérez-Sala's kind and ceaseless support. Thank you for sharing your never-ending keenness for science, and for catalyzing my transition from theoretical science to hands-on research with such patience and enthusiasm, as well as a scientific thoroughness that I hope never to stray from.

I would also like to thank the constant help of Mª Jesús Carrasco. Muchas gracias por los buenos ratos y ánimos en todos estos años. I would especially like to thank all my colleagues at the lab for their help and warmth, particularly Irene, Ruth, Bea and Marta, and more recently Fran, whose unrelenting eagerness to help has filtered into this thesis unawares.

The help of many people at the Centro de Investigaciones Biológicas (CIB) has been crucial for this work, specifically that of Maite Seisdedos at the confocal imaging unit, and Dr. Blanca Pérez Maceda and Carmen Doñoro at the cell culture facility. Furthermore, I would like to thank collaborators here at the CIB, particularly Dr. Miguel A. Peñalva for the opportunity of exploring the stunning *Aspergillus nidulans* cell trafficking model, and Mario and Elena for their help in setting it up. Thanks to Dr. Patricia Boya for autophagy studies and Esther for experimental input.

It is essential to show my gratitude towards all who helped me during stays abroad, for both their mentoring and kind welcome. Thanks to Prof. Harald Stenmark and all the members of the lab at the Radium Hospital in Oslo, including Andreas, Viola, and especially Kay for help with super-resolution imaging. I would also like to thank Prof. Marja Jäättelä as well as Dr. Nikolaj H. T. Pedersen and all other colleagues at the Kræftens Bekæmpelse in Copenhagen.

The scientific curiosity that lead me on the path to research was initially awakened by Dr. Diana Wrigley de Basanta, whom I would like to thank for so brilliantly introducing the concept of cell biology in her classes in 9th grade. I am deeply indebted to many other teachers that have awakened my awareness on many subjects.

Muchísimas gracias a mi maravillosa familia (a mis tíos Antonio, Esther, Manuel, Mary Tere, etc. y todos mis primos) por su apoyo y alegría. Es una suerte teneros cerca porque vuestra compañía me llena de felicidad. Gracias especialmente a mi prima y mejor amiga Mayte por sus arengas y por las risas. También agradecer su apoyo a mis amigos, que siempre siguen ahí a pesar de mis negligencias o de la distancia.

Querría ante todo dar las gracias a mis padres. Gracias Ma por tu amor y dulzura incondicionales, y por transmitirme tu fortaleza mental para aprender a relativizar: es la lección más importante que he aprendido en la vida. Esta tesis es por y para ti. Thanks Dad, for your love and for keeping up your delightful and charming character, just like grandma Florence, regardless of your troubles. Gracias Sister, por ser mi role model desde pequeñas con tu inteligencia y esfuerzo, además de por tu cariño y apoyo, tan presentes aun en la distancia. Gracias también por tu empeño en compartir con nosotros la alegría de esa maravilla que es Sofía.

Finalmente, quería dar las gracias a la persona que más afectada se ha visto por el desarrollo de este trabajo, sin cuyo amor y comprensión hubiese sido casi irrealizable. Adrián, mi persona favorita, me haces más feliz cada día desde hace ya tantos años que el único agradecimiento posible es esforzarme en poder hacer lo mismo por ti siempre. *The light of my life and the beat of my heart.*

ABBREVIATIONS

15d-PGJ_2	15-deoxy-$\Delta^{12,14}$-Prostaglandin J_2
2-BP	2-bromopalmitate
AP	Heterotetrameric adaptor protein complexes
BAEC	Bovine aortic endothelial cell(s)
BLOC	Biogenesis of lysosome-related organelles complex
C-terminal	Carboxy-terminal
CD	Clusters of differentiation
CHS	Chediak-Higashi Syndrome
COX	Cyclooxygenase
cyPG	Cyclopentenone prostaglandin(s)
DBB	Dibromobimane
EGFR	Epidermal growth factor receptor
ER	Endoplasmic reticulum
ESCRT	Endosomal sorting complex required for transport
FT	Farnesyl transferase(s)
GAP	GTPase-activating protein(s)
GDI	GDP dissociation inhibitor(s)
GDP	Guanosine diphosphate
GEF	Guanine nucleotide exchange factor(s)
GGT	Geranylgeranyl transferase(s)
GPCR	G-protein coupled receptor(s)
GTP	Guanosine triphosphate
HPS	Hermansky-Pudlak Syndrome
Hrs	Hepatocyte growth factor-regulated tyrosine kinase substrate
ILV	Intraluminal vesicle(s)
KD	Knock-down
Lamp1	Lysosome-associated membrane protein 1
LBPA	Lysobisphosphatidic acid (a.k.a. BMP)
LRO	Lysosome-related organelle(s)

LTR	Lysotracker® Red
Lyst	Lysosomal trafficking regulator
M6P	Mannose 6-phosphate
MHC	Major histocompatibility complex
MVB	Multivesicular body/bodies
NF-κB	Nuclear factor kappa-light-chain-enhancer of activated B cells
NPC	Niemann-Pick type C disease
PAGE	Polyacrylamide gel electrophoresis
PAO	Phenylarsine oxide
PAT	Palmitoyl transferase(s)
PE	Phosphatidylethanolamine
PI(3)P	Phosphatidylinositol 3-phosphate
PS	Phosphatidylserine
Rab	Ras-related in brain
Ras	Rat sarcoma
Rep	Rab escort protein
Rho	Ras homolog
SDS	Sodium dodecyl sulfate
SIM	Structured illumination microscopy
TEM	Tetraspanin-enriched microdomain(s)
Tsg101	Tumor susceptibility gene 101
WB	Western blot(s)
ZGA	Zaragozic acid

Other abbreviations not shown here follow IUPAC nomenclature.

TABLE OF CONTENTS

LIST OF FIGURES

LIST OF TABLES

INTRODUCTION

1. Small GTPase proteins

The Rat sarcoma (Ras) superfamily of small GTPases is made up of a plethora of 20 to 40 kDa proteins that share the ability to bind to a GTP nucleotide and hydrolyze it to GDP, which determines their activation state. The Ras, Rho, Rab, Arf and Ran protein families represent the majority of proteins in this family (Figure 1), which share some similar domains but also contain specific structural determinants that endow each protein with unique conformational and signaling characteristics, as reviewed in (Takai et al., 2001). This superfamily is named after the first small GTPases that were studied: the Ras proteins (Barbacid, 1987). Some of the first oncogenes identified are part of this family and play crucial roles in cell survival, proliferation and signaling, as reviewed in (Ridley, 2001; Schmitz et al., 2000).

The Rho protein family was identified as containing sequences homologous to Ras (**R**as **ho**molog) and includes three Rho isoforms (RhoA, B and C), three Rac isoforms (Rac1, 2 and 3) as well as Cdc42, among others (Bustelo et al., 2007; Madaule and Axel, 1985). Rho proteins regulate cytoskeletal functions such as actin stress fiber induction (RhoA) or lamellipodia and filopodia formation (Rac and Cdc42, respectively), as reviewed in (Hall, 2005; Matozaki et al., 2000). Another member, RhoB, is known to induce stress fibers but also plays a role in vesicular transport (Aspenström et al., 2004; Gampel et al., 1999), as will be discussed below in detail. The Rab GTPases (**Ra**s-related in **b**rain) comprise the largest of the Ras families, with more than 60 isoforms identified in humans (Touchot et al., 1987). They are responsible for membrane trafficking processes including endocytosis, exocytosis, transcytosis, and general vesicle maturation, as reviewed in (Stenmark, 2009).

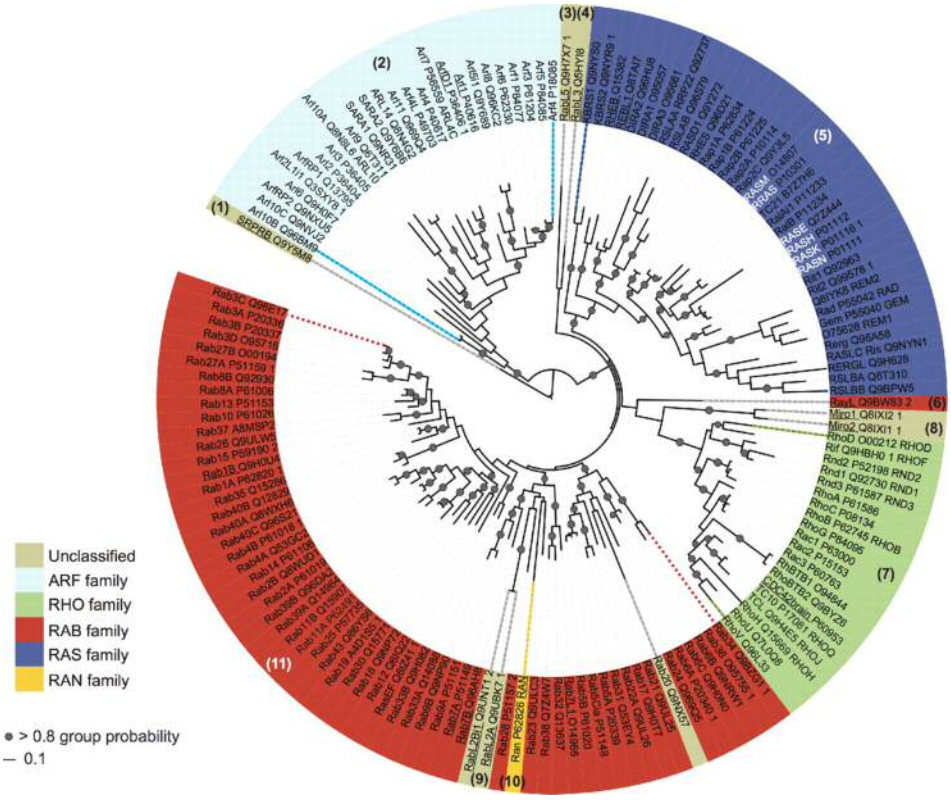

Figure 1. Human Ras superfamily phylogenetic tree.

Representation of the different Ras families from a phylogenetic standpoint, as represented by the tree inside the circle. The major Ras groups are shown in different colors, i.e. blue for the Ras family, green for Rho, red for Rab, cyan for Arf, and yellow for Ran. ©Rojas et al., 2012. Originally published in The Journal of Cell Biology. doi: 10.1083/jcb.201103008. (Rojas et al., 2012)

Small GTPases act as molecular switches, transitioning between a GDP-bound, inactive state and a GTP-bound, active state, as depicted in Figure 2. Their activation is mediated by varied stimuli, which can initiate signaling cascades affecting guanine nucleotide exchange factors (GEF), which favor GTP incorporation, as reviewed in (Geyer and Wittinghofer, 1997). Active states of small GTPases arise from conformational changes that allow these proteins to bind to effectors and hence propagate signals intracellularly. Considering that the intrinsic GTPase activity of these proteins is rather low, they require GTPase activating proteins (GAP) to effectively hydrolyze GTP to GDP, returning to their inactive state. A further level of regulation involves specific GDP dissociation inhibitors (GDI), which bind to inactive Ras superfamily proteins to detach them from membranes, thus retaining them in the cytosol (Figure 2).

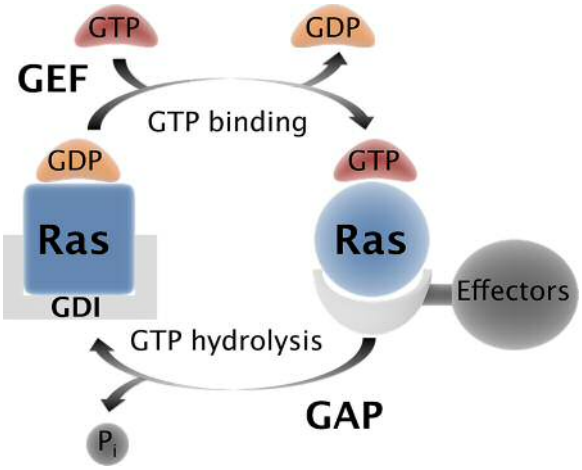

Figure 2. Small GTPase GDP/GTP cycle.

The inactive form of the Ras superfamily protein (square Ras) is bound to GDP. For some GTPases, binding to RhoGDI stabilizes this inactive form. Small GTPase binding to GTP is facilitated by GEF and allows interaction with effectors to induce signal transduction (circular Ras). Enzymatic hydrolysis of GTP for GDP is stimulated by GAP and leads to GTPase inactivation, terminating its effector binding and activation.

GEF, GAP and GDI proteins are inherent to the process of Ras protein regulation, so that each subfamily is modulated by a specific subset of activators, inhibitors or overall modulators, each with their feedback or feed-forward regulation. Thus, this complex network of Ras protein-related effectors generates fine-tuned signaling cascades within the cell, as reviewed extensively in (Cherfils and Zeghouf, 2013). It is therefore evident that small GTPases entail tight regulatory mechanisms to correctly carry out their intracellular functions (Matozaki et al., 2000).

1.1 Endolysosomal GTPases

Numerous members of the Ras superfamily appear at endolysosomal compartments, particularly Rab proteins, as well as the Ras proteins Rap2A, Rap2B, and H-Ras, or the Rho proteins TC10 and RhoB (Valero et al., 2010), as will be described throughout this work. Specific members of the Rab protein family associate at defined vesicles along the endocytic pathway and assist in the maturation of these membrane compartments by mediating vesicle budding, fusion, motility, coating and uncoating, which endows endomembranes with an extremely dynamic quality (Stenmark, 2009). The core endosomal Rabs may be laterally segregated into specific domains of the same

vesicles, which allows for a flexible flow of compartments within the cell. Except in the case of Ran proteins, which contain a nuclear import signal, lipids modify proteins belonging to the Ras superfamily posttranslationally in order to associate with membranes. The combination of these lipid anchors and other structural determinants gives rise to subcellular localizations at specific membrane compartments, as discussed below for RhoB in greater detail.

1.2 RhoB

RhoB is located on the cytoplasmic side of the plasma membrane and late endosomes, from which it plays important roles in trafficking of signaling molecules (Gampel et al., 1999). It is a short-lived protein with a half-life of approximately 2-3 hours, which differs from the relative stability of other Rho proteins (24-hour half-lives) (Engel et al., 1998; Stamatakis et al., 2002). RhoB is an immediate early response gene that is rapidly induced by DNA damage or growth factors (Fritz and Kaina, 1997; Malcolm et al., 2003). Therefore, maintaining a high RhoB turnover ensures the rapid response of RhoB levels to various stimuli. Though *in vitro* studies have shown similar effectors for RhoA and RhoB, cellular approaches have shown that each has its own set of interactors to carry out specific functions. As summarized in Figure 3, RhoB presents unique functions that set it apart from other Rho proteins by controlling endocytic traffic and affecting the sorting of growth factor receptors or signaling kinases (Fernández-Borja et al., 2005; Huang et al., 2007b; Mellor et al., 1998; Sandilands et al., 2004; Wherlock et al., 2004). Hence, there are associated consequences for growth factor signaling, cell survival, proliferation, and apoptosis, which contribute to the proposed dual role of RhoB as both a tumor suppressor and an angiogenesis inducer (Gerald et al., 2013; Huang et al., 2006; Liu et al., 2001). RhoB is involved in modulating cell death through genotoxic stress (Fritz and Kaina, 2000; Liu et al., 2001) and controlling c-myc stability (Huang et al., 2006), as well as signaling and trafficking of Akt kinase (Adini et al., 2003). Furthermore, RhoB could play a role in apoptosis following Ras inhibition (Kamasani et al., 2004; Liu et al., 2001). RhoB has also been shown to mediate actin dynamics upstream of Dia1 (Diaphanous-related formin 1), which is necessary for actin coat formation around endosomes (Fernández-Borja et al., 2005). Additionally, reduced

cell spreading and adhesion to different substrates was noted in several RhoB-depleted cell types, which could be due to the concomitant reduction of surface β1 integrin levels in these cells and accountable for decreased focal adhesions, resulting in increased migration rates (Vega et al., 2012).

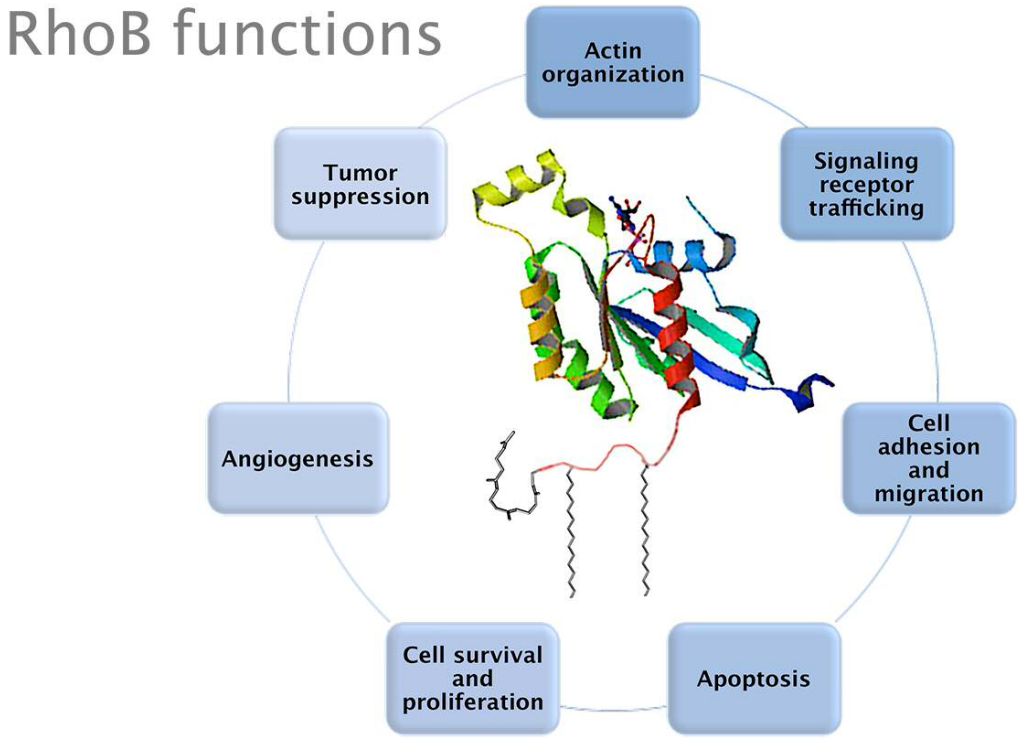

Figure 3. Schematic of RhoB functions.

A ribbon diagram of the RhoB structure attached to an isoprenoid moiety (curved, gray chain) and two palmitates (straight chains) is shown in the center. The small GTP-binding protein RhoB performs specific tasks within the cell that set it apart from other proteins of the Ras superfamily, including roles in cancer progression related to angiogenesis or apoptosis, regulating receptor trafficking or actin polymerization at endosomes, and cell migration. See text for details.

RhoB is highly homologous to RhoA in structural terms, though under resting conditions, RhoGDI retains RhoA in the cytosol (Dransart et al., 2005) whereas RhoB is bound to the plasma membrane or endolysosomal membranes (Oeste et al., 2014; Pérez-Sala et al., 2009; Stamatakis et al., 2002). These differences in localization are related to the distinct residues present at the carboxy-terminal (C-terminal) hypervariable region (Chiu et al., 2002; Gorfe et al., 2007), which contains the –CAAX box and could bear phosphorylation sites as well as sites for additional lipidation (Hancock et al., 1989; Wennerberg and Der, 2004), as will be described in detail below.

In the case of RhoB, upon isoprenylation of its –CAAX box cysteine (C193), two nearby cysteines (C189 and C192) are further modified by palmitate moieties (Wang and Sebti, 2005), whereas RhoA fosters a polybasic sequence.

RhoB therefore presents several distinguishing features that endow it with unique cellular behavior. The specific lipidation sequence at its C-terminus acts as a plasma membrane and endolysosomal anchor. Furthermore, these lipid modifications determine RhoB degradation through a lysosomal pathway distinct from the proteasomal degradation typical of other GTPases of its family (Pérez-Sala et al., 2009; Stamatakis et al., 2002).

2. Posttranslational modifications of GTPases

Posttranslational modifications constitute an essential regulatory mechanism for protein function, activation, localization and half-life. Most of these changes result in conformational shifts that alter activation states, allow modified proteins to interact with effectors or expose otherwise hidden motifs within their sequence. Common posttranslational modifications include processes such as phosphorylation, hydroxylation and nitrosylation (inorganic residue addition), ubiquitination and glutathionylation (peptide addition), or isoprenylation, myristoylation and palmitoylation (lipid addition), among many others, as reviewed in (Walsh et al., 2005). The resulting functional outcomes range from marking proteins to be degraded, as in ubiquitination, to direct activation for effector interaction, i.e. phosphorylation.

Ras superfamily proteins undergo several posttranslational modifications, including irreversible alteration of their carboxy-terminal sequence by isoprenylation and proteolysis, as well as methylation and further lipidation by palmitate moieties in some instances. Other residues within these proteins can undergo other modifications such as peptidyl-prolyl isomerization, phosphorylation, ubiquitination, glycosylation,

nitrosylation, and ADP ribosylation, as reviewed in (Ahearn et al., 2012). As will be discussed below, some of these modifications alter Ras protein localization, in turn determining the effectors with which they can interact and ultimately their activation patterns.

2.1 Lipidation at C-terminal ends

Lipidation involves covalent attachment of lipids to protein residues and can take place spontaneously or through enzymatic mechanisms. Isoprenylation and myristoylation are irreversible enzymatic modifications that significantly increase protein hydrophobicity, thus elevating the probability of their interaction with membranes. Whereas myristoylation takes place at a glycine residue located in the first position of the protein sequence (after methionine removal), isoprenylation occurs at cysteines in the C-terminal segment. Palmitoylation usually takes place at cysteines that are in the vicinity of isoprenylated or myristoylated residues and confers a more flexible, reversible mode of regulation of protein localization, as reviewed in (Aicart-Ramos et al., 2011). Several Ras proteins become palmitoylated following isoprenylation to better anchor them to membranes, as will be discussed below in further detail. Protein modification by lipids is therefore a crucial tool to modulate subcellular localization and hence site-specific activation and recruitment of proteins, affecting a myriad of signaling platforms.

2.1.1 Isoprenylation

Isoprenylation is an enzymatic process affecting more than 300 proteins in humans by which isoprenoid lipids bind to cysteines through a thio-ether bond, as reviewed in (McTaggart, 2006). Specific prenyl transferases recognize particular sequences to catalyze farnesylation, in the case of farnesyl transferase (FT) or geranylgeranylation, in the case of geranylgeranyl transferases (GGT) I and II. Many Ras proteins contain a "-CAAX box" at their C-terminus, where "C" is the cysteine amenable to isoprenylation, "A" stands for aliphatic residues and "X" can be any amino

acid (Hancock et al., 1989). As depicted in Figure 4, -CAAX boxes undergo modifications including isoprenylation, proteolysis and methylation.

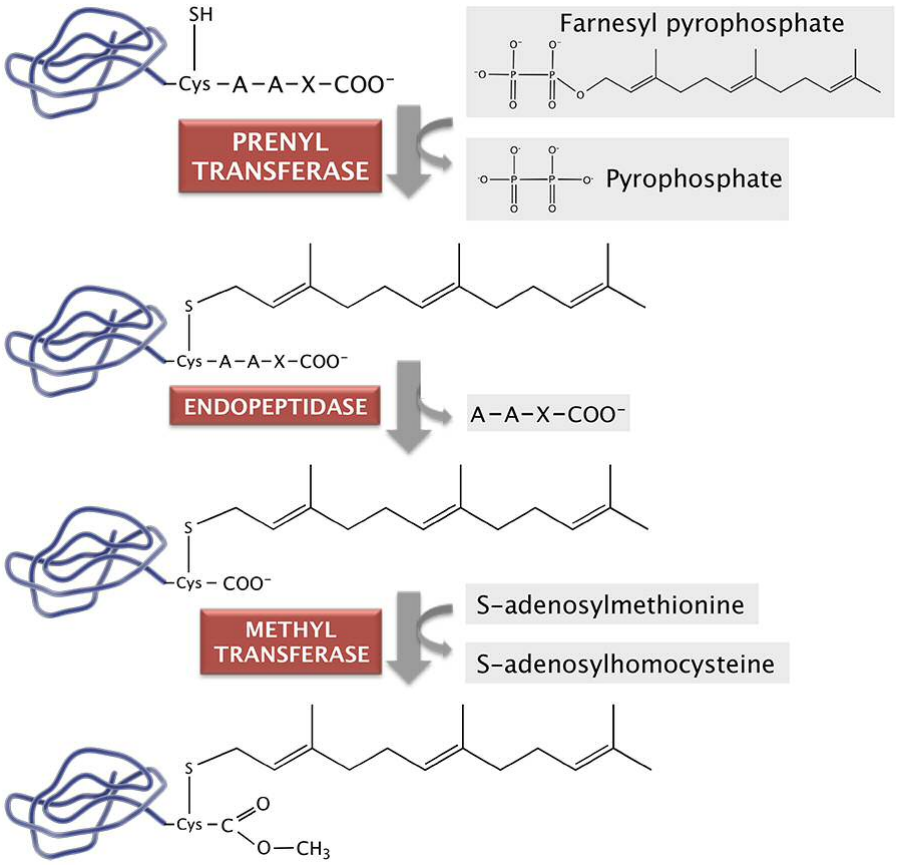

Figure 4. Protein isoprenylation and CAAX box processing.

Proteins containing a CAAX box undergo posttranslational processing, beginning with isoprenylation by prenyl transferases. An endopeptidase cleaves the last three amino acids (-AAX), and methylation of the C-terminal end is brought about by a methyl transferase. Shown here is farnesyl pyrophosphate (C15), though some proteins become geranylgeranylated by GGT using a geranylgeranyl pyrophosphate moiety (C20) as a substrate. See text for details.

In the case of FT- and GGT I-mediated isoprenylation, the X residue in –CAAX boxes of target proteins determines whether the cysteine will be modified by a farnesyl or geranylgeranyl isoprenoid. FT modifies proteins in which the X residue is methionine, serine, alanine or glutamine, whereas GGT I acts on proteins bearing a leucine residue. However, certain proteins can be modified by either FT or GGT I depending on other biochemical features of the –CAAX box surroundings (Hartman et al., 2005) or on isoprenoid availability (Whyte et al., 1997). FT and GGT-I share an α subunit and possess specific β subunits that recognize CAAX motifs and transfer either

farnesyl pyrophosphate or geranylgeranyl pyrophosphate, respectively. In contrast, GGT II requires an accessory protein, Rab escort protein (Rep) that recognizes whole Rab proteins and presents them to the catalytic subunit (Nguyen et al., 2010). GGT II is responsible for single or double geranylgeranylation of Rab proteins at their C-terminal –CAC, -CC, -CCX, -CCXX, -CCXXX or –CXXX motif cysteines (Desnoyers et al., 1996; Leung et al., 2006; Maurer-Stroh et al., 2003). Once isoprenylation has taken place, the amino acids that remain at the carboxy end of the isoprenylated cysteine are cleaved by a specific endoprotease and the carboxyl group of the cysteine is methylated by a specific methyltransferase for isoprenylated proteins (Pérez-Sala et al., 1991; Sinensky, 2000; Tan et al., 1991).

2.1.2 Palmitoylation

Palmitoylation is the addition of a palmitate moiety (C16:0) to a cysteine residue through a thioester bond, as reviewed in (Dietrich and Ungermann, 2004). As shown in Figure 5, the cysteine sulfhydryl group needs to be in its thiolate form, i.e. unprotonated, in order to carry out a nucleophilic attack on the α carbon of palmitoyl-CoA. This reaction can occur spontaneously depending on the cysteine pK_a, which is determined by the intra- and intermolecular surroundings, but is greatly enhanced when catalyzed by palmitoyl transferases (PAT), a.k.a. protein acyl transferases, which contain a conserved aspartate-histidine-histidine-cysteine (DHHC) active site rich in cysteine residues, as reviewed in (Aicart-Ramos et al., 2011). These enzymes and the substrate palmitoyl-CoA are present on membranes, so that proteins that are to be palmitoylated need to come in close contact with PAT-containing membranes (Dunphy et al., 1996). Isoprenylation increases the probability of a protein to bind to membranes, and palmitoylation presents a further structural determinant that stabilizes membrane association, as reviewed in (Smotrys and Linder, 2004; Smotrys et al., 2005). Depalmitoylation is mediated by palmitoyl-protein thioesterases (Verkruyse and Hofmann, 1996), allowing proteins to undergo repeated cycles of palmitoylation/depalmitoylation (Aicart-Ramos et al., 2011).

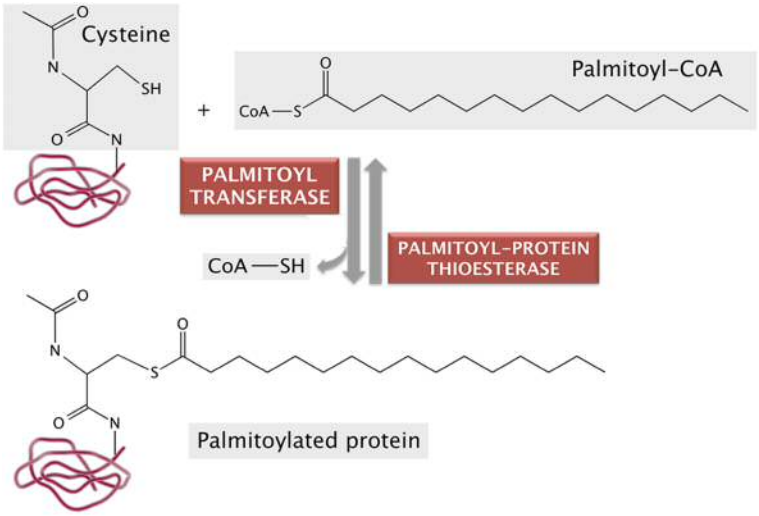

Figure 5. Protein palmitoylation.

In red, a random protein structure with its palmitoylation cysteine depicted chemically. The cysteine thiolate group produces a nucleophilic attack on the electrophilic carbon on the palmitoyl-CoA chain to yield a palmitoylated protein and free CoA. This reaction can take place spontaneously or be catalyzed by palmitoyl transferases. Depalmitoylation is catalyzed by palmitoyl-protein thioesterases. Adapted from (www.lipidlibrary.aocs.org).

Many protein families provide examples of palmitoylation-mediated membrane association. Such is the case of a multitude of integral membrane proteins such as heterotrimeric G-proteins, tetraspanins, the mannose 6-phosphate (M6P) receptor, or synaptotagmins, all involved in general endocytic trafficking processes (Schweizer et al., 1996; Stipp et al., 2003; Veit et al., 1996). These proteins, though already spanning the membrane, are able to associate at specific microdomains such as lipid rafts and hence form signaling platforms, as is the case for transmembrane adaptor proteins, e.g. LAT (Linker of Activation for T cells) (Stepanek et al., 2014). Furthermore, membrane anchors of peripheral membrane proteins often consist in palmitoylation either close to myristoylated residues, as for Src tyrosine kinases, or in the vicinity of previously isoprenylated cysteines, as is the case for the Ras protein superfamily (Aicart-Ramos et al., 2011), and is described as follows.

Within the Ras family of proteins, H-Ras is palmitoylated at two cysteine residues present in the hypervariable domain (C181 and C184), N-Ras contains a single palmitoylation site (C181) and K-Ras4B possesses no cysteine residues but its interaction with cellular membranes is favored by the presence of a polybasic domain that is attracted to negatively charged polar head groups of membrane phospholipids, much like RhoA. In the case of H-Ras, localization is mainly at the plasma membrane

and various intracellular structures, including the endoplasmic reticulum (ER), the Golgi complex, recycling endosomes (Gómez and Daniotti, 2005; Hancock and Parton, 2005) and to randomly moving nanoparticles known as rasosomes (Rotblat et al., 2006). These differences are critical to determine the specific trafficking and site of action of the different Ras proteins, as reviewed in (Omerovic et al., 2007; Pérez-Sala, 2007). Other proteins that also contain additional cysteines close to the isoprenylation site that are amenable to palmitoylation include TC10, Rap2, or RhoB (Aicart-Ramos et al., 2011; Michaelson et al., 2001; Uechi et al., 2009). TC10 has been detected at the plasma and perinuclear membranes, identified as components of secretory or endosomal compartments (Michaelson et al., 2001; Watson et al., 2003), whereas Rap2 has been detected in secretory granules (Mollinedo et al., 1993) and recycling endosomes (Uechi et al., 2009). Fully lipidated RhoB is both isoprenylated and bipalmitoylated (Wang and Sebti, 2005), which is required for its association with endolysosomes (Pérez-Sala et al., 2009).

2.2 Cyclopentenone prostaglandins

In addition to lipidation by isoprenoid or palmitate moieties, proteins may suffer modification by reactive lipid species of varied structure. Cell metabolism under both basal and pathological conditions gives rise to products derived from lipid peroxidation that can form stable adducts with particular protein residues (Bogatcheva et al., 2005). Oxidative and nitrosative stress produce many of these products, which play a role in numerous pathologies such as neurodegenerative diseases (Dianzani, 2003), vascular alterations (Lee and Park, 2013), and cancer (Garzón et al., 2011). Amongst the many electrophilic lipids that are produced in cells, cyclopentenone prostaglandins (cyPG) are a family of reactive lipid species with anti-inflammatory, anti-viral and anti-tumoral effects, which makes them a forthcoming option as exogenous therapeutic compounds (Sánchez-Gómez et al., 2004; Straus and Glass, 2001). cyPG generation is increased in cells undergoing oxidative stress, whereas cyPG production in homeostatic cells is low (Ceaser et al., 2004; Koenitzer and Freeman, 2010). The electrophilic nature of cyPG allows them to react with nucleophilic residues including cysteines, in turn eliciting

structural changes within the whole protein that provide new reactivity and electrophilicity. cyPG of different structural characteristics present specificity towards particular cysteine residues, so that different cyPG enter distinctive intramolecular binding pockets even within the same protein. Moreover, cyPG bind to proteins involved in a multitude of different cellular tasks (Garzón et al., 2011; Renedo et al., 2007). These features account for dual actions: cyPG modification of proteins involved in redox regulation can modulate oxidative stress pathways, whereas binding and subsequent inhibition of NF-κB (nuclear factor kappa-light-chain-enhancer of activated B cells) pathway proteins contributes to cyPG anti-inflammatory effects (Díez-Dacal and Pérez-Sala, 2010; Kim and Surh, 2006). The pleiotropic behavior of these electrophilic lipids is therefore a reflection of the variety of intracellular targets, many of which have been discovered in the past decade through proteomic studies, as reviewed in (Garzón et al., 2011; Oeste and Pérez-Sala, 2014). Interestingly, Ras proteins are included in this expanding list of cyPG targets (Oeste et al., 2011; Stamatakis and Pérez-Sala, 2006), as discussed below in further detail.

As shown in Figure 6, cyPG are derived from peroxidation of membrane fatty acids, in particular arachidonic acid, through the action of cyclooxygenases (COX) or non-enzymatically through the isoprostane pathway (Funk, 2001; Gao et al., 2003). In the case of the COX pathway, prostaglandin synthases act on the precursor PGH_2 to give rise to PGD_2 and PGE_2 (Funk, 2001). The latter two PG can also be formed by non-enzymatic epimerization of isoprostanes through the isoprostane pathway (Gao et al., 2003), which gives rise to *trans* isomers of PG, i.e. isoprostanes such as iso-PGJ_2 and iso-PGA_2. J series cyPG arise from dehydration of PGD_2 to PGJ_2, which can be further dehydrated to form 15d-PGJ_2 (15-deoxy-^{12,14}-Prostaglandin J_2) or give rise to Δ^{12}-PGJ_2 through an albumin-dependent mechanism (Narumiya and Fukushima, 1985; Shibata et al., 2002). cyPG of the A series are produced upon dehydration of PGE_1 or PGE_2 (Ohno et al., 1986).

cyPG synthesized in this manner contain an α, β-unsaturated carbonyl group within their cyclopentane ring, which renders highly electrophilic -β carbons. Therefore, they are amenable to forming Michael adducts through nucleophilic attack by thiol moieties from cysteines, as seen at the bottom of Figure 6. The cysteine residues to which cyPG bind present structural characteristics allowing for the entry and

positioning of specific cyPG to form the stable, covalent Michael adducts with consequences on biological functions.

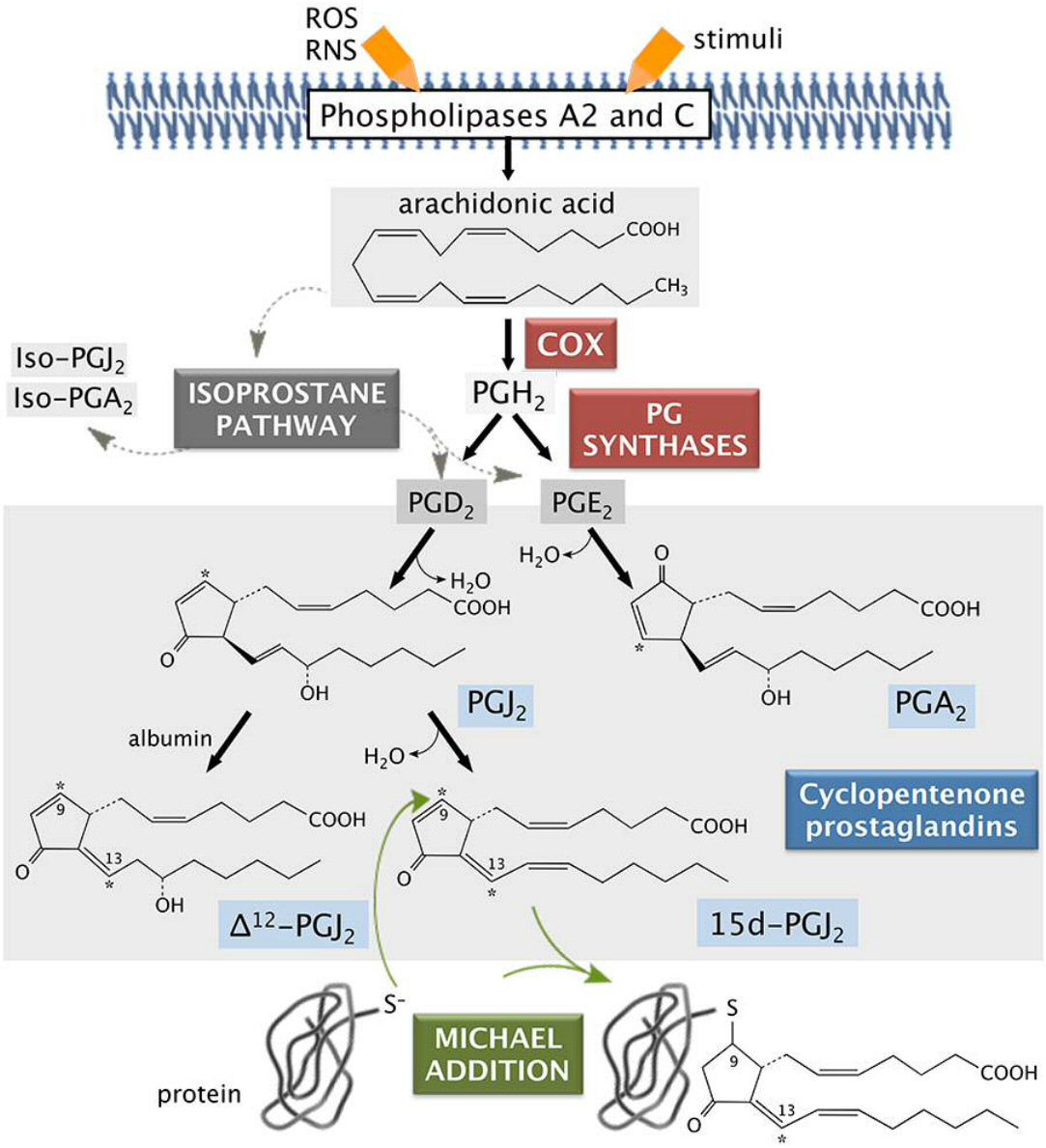

Figure 6. Cyclopentenone prostaglandin formation and covalent binding to proteins through Michael addition.

cyPG (blue shaded boxes) are formed by spontaneous dehydration of their PG precursors (gray shaded boxes). These precursors are generated in turn from unsaturated fatty acids such as arachidonic acid by the action of cyclooxygenases (COX) or through non-enzymatic processes, i.e. the isoprostane pathway (dashed arrows). Arachidonic acid is formed as a product of phospholipase A2 or C cleavage of membrane-bound phospholipids. cyPG contain electrophilic carbons (asterisks) that can undergo attack by nucleophilic groups such as cysteine thiolates and form Michael adducts (green arrows), as shown at the bottom for 15d-PGJ_2. See text for details.

2.2.1 Cyclopentenone prostaglandin modification of Ras proteins

cyPG containing either one or two electrophilic carbons, i.e. single enones or dienones, can bind to different subsets of proteins depending on the steric attributes of the cysteines in the protein to be modified. Several studies have shown that the dienone cyPG 15d-PGJ_2 can establish Michael adducts with cysteine residues of proteins as structurally and functionally different as actin, vimentin (Stamatakis et al., 2006), NF-κB, PPARγ (Peroxisome proliferator-activated receptor gamma) (Cernuda-Morollón et al., 2001; Shiraki et al., 2005), Keap1 or GSTP1-1 (Glutathione S-transferase P) (Levonen et al., 2004; Sánchez-Gómez et al., 2007). The fact that electrophilic carbon count is particularly important for selectivity is reflected by cyPG binding to Ras proteins. Various cyPG have been found to modify and activate Ras proteins in an isoform- and site-selective manner (Oliva et al., 2003). Specifically, single enone cyPG, e.g. PGA_1 or PGJ_2 bind preferentially to C118, which is present in the GTP binding site in all three Ras proteins, namely H-Ras, K-Ras and N-Ras. However, the dienone 15d-PGJ_2 can bind two cysteine residues simultaneously (C181 and C184), located at the H-Ras C-terminus (Renedo et al., 2007). Since other Ras proteins such as N- or K-Ras do not contain this sequence, they are not preferential targets for dienone cyPG binding. Interestingly, modification of the H-Ras C-terminal sequence by cyPG or other small reactive molecules elicits changes in its membrane partitioning and distribution along the endocytic pathway (Oeste et al., 2011). It is thus apparent that cyPG selectivity can fine-tune intracellular pathways by modifying not only specific proteins, but also particular cysteine residues within the same protein, which can have consequences on its subcellular sorting and localization.

3. Endolysosomal sorting and degradation

Endocytosis is the means by which cells internalize extracellular material as well as plasma membrane proteins and lipids, among many other substances. As summarized in Figure 7, this material is engulfed by plasma membrane and pinched off to produce endocytic vesicles, which undergo multiple maturation processes on their way towards lysosomes, recycling compartments, autophagosomes, or other intracellular destinations. Trafficking of these endocytic vesicles involves signaling through membrane receptors from the outside-in and recycling these components for further receptor-effector cascades or producing metabolic building blocks, hence contributing to overall cell functions, as reviewed in (Huotari and Helenius, 2011). During their maturation process, these vesicles evolve through dynamic interaction of non-discrete compartments that are in constant flow from one to another. However, distinct proteins and lipids attach to vesicles at different points in the endocytic route, aiding in their categorization into specific types of endosomes. Interestingly, accumulating evidence points at site-selective signaling within the cell, for certain signaling molecules bind to different effectors depending on their subcellular localization (Schmidt-Glenewinkel et al., 2008), and some signaling processes require previous endocytosis of their components to regulate the specificity, duration and magnitude of the signal, as reviewed in (Sadowski et al., 2009). The components that attach to vesicles during their internalization will hence define their ultimate subcellular destination and function, such as traveling back to the plasma membrane for recycling or inclusion into multivesicular bodies (MVB) for secretion or degradation (Huotari and Helenius, 2011; Platta and Stenmark, 2011).

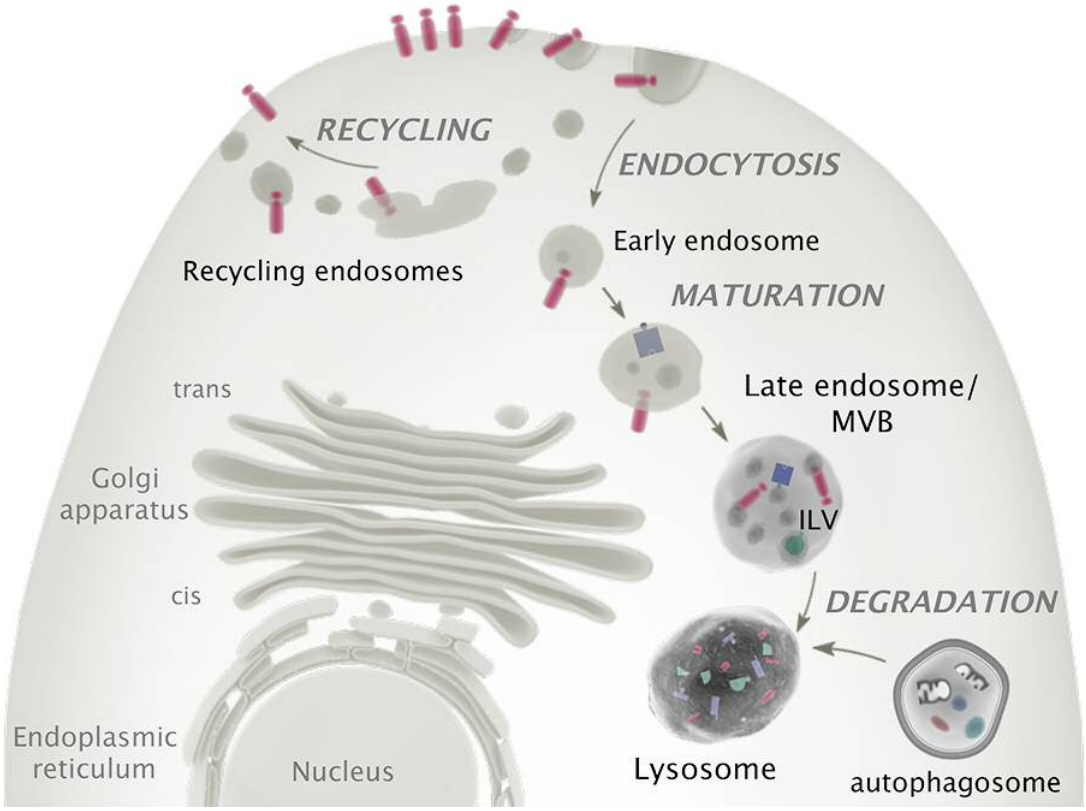

Figure 7. The endocytic pathway.

Cellular components residing at the plasma membrane such as signaling receptors (red rods) are internalized along with extracellular material during endocytosis. The vesicles that pinch off can be sent along recycling endosomes back to the plasma membrane in a process that recycles receptors for a new round of outside-in signaling at the cell surface. Alternatively, endocytic vesicles undergo a series of maturation steps from early endosomes to late endosomes/MVB, including membrane invagination to form intraluminal vesicles (ILV). Fusion with lysosomes elicits macromolecule degradation by specific enzymes working at low pH levels within these compartments, resulting in receptor down-regulation and signaling termination. Autophagosomes containing damaged organelles and cellular material for degradation also fuse to lysosomes to produce simpler components that can be reused by the cell. See text for details.

Degradation of endocytosed material implies macromolecule breakdown into its constituent parts, e.g. proteins into amino acids to use in protein synthesis. It is therefore essential for cells to be endowed with several degradation machineries. The first protein-specific degradation mechanism described within the cell was the proteasome, which is a cytosolic protease that degrades misfolded and short-lived regulatory proteins in the cytoplasm (Schwartz and Ciechanover, 2009). Proteins that are destined towards this degradation machinery are modified by several ubiquitin moieties forming a chain that is recognized by the proteasome. Ubiquitination can also mark proteins for other subcellular outcomes and is a complex, target-specific process

involving several enzymes (Sadowski et al., 2012). In the case of transmembrane proteins, a single ubiquitin molecule marks them for degradation, though this process must necessarily occur *via* vesicular transport, in particular through endosomes to the lysosome or vacuole, where degradation takes place. Lysosomes are acidic organelles containing hydrolytic enzymes and are at the crossroads of several degradation processes, for they degrade proteins with long half-lives arriving in endosomes or aid in clearing away larger elements packaged in phagosomes or autophagosomes (de Duve, 1969; Fader and Colombo, 2009; Saftig and Klumperman, 2009). It is indeed vital for cell homeostasis to tightly coordinate the complex processes encompassing vesicular biogenesis, membrane trafficking and the degradation of cellular components by means of precise macromolecular machineries.

3.1 Protein machineries involved in sorting

Intense research in the past decades on the proteins involved in endosomal sorting has uncovered a plethora of interaction networks and transport systems to shuttle cargo to and fro within the cell, as reviewed in (Bishop, 2003). Vesicle biogenesis is a topologically complicated process in which the membrane must curve forcefully and still accommodate transmembrane or peripheral membrane proteins and their effectors (McMahon and Gallop, 2005). Proteins responsible for inducing curvature, coating of developing omegas and membrane scission at the plasma membrane are key players in the initial steps of vesicle generation (Stachowiak et al., 2013). However, once endosomes are formed, their destination is tightly regulated by other sets of proteins such as Rab proteins that assemble onto the newly formed vesicles and help in their uncoating, trafficking (i.e. along microtubules), tethering, and fusion with one another (Stenmark, 2009). Furthermore, extensive maturation gives rise to vesicles that suffer internal processes of their own, such as the production of intraluminal vesicles (ILV) from the membrane of MVB mediated by the ESCRT (endosomal sorting complex required for transport) protein machinery (Raiborg and Stenmark, 2009) or acquisition of acidic pH values. The relatively recent discoveries of tethering protein complexes, namely, HOPS (homotypic fusion and vacuole protein sorting complex) (Seals et al., 2000) and CORVET (class C core vacuole/endosome tethering complex) (Peplowska et

al., 2007) unveil the role of these multi-protein machineries in homotypic fusion of endocytic compartments prior to SNARE (Soluble NSF (*N*-ethylmaleimide-sensitive factor) Attachment Protein Receptor) participation, as reviewed extensively in (Solinger and Spang, 2013). Furthermore, anterograde transport from the Golgi to late endosomes or lysosomes and vacuoles is mediated by carboxypeptidase Y and AP-3 (heterotetrameric adaptor protein complex 3) pathways, whereas retromer governs retrograde trafficking within these compartments with the help of other proteins such as sorting nexins (Cullen and Korswagen, 2012; Epp et al., 2011). However, these complexes are beyond the scope of this dissertation, in which attention will be focused on the Rab and ESCRT protein machineries involved in endolysosomal trafficking and MVB biogenesis, to contextualize the localization of the endosomal GTPases under study.

3.1.1 Rab proteins

As described above and seen in Figure 1, Rab proteins constitute the largest of the Ras subfamilies. Membrane tethering is determined by their two C-terminal geranylgeranyl moieties and the immediate upstream protein sequence (Chavrier et al., 1991), as well as binding to specific GDI or GDI recycling factors (Dirac-Svejstrup et al., 1997; Ullrich et al., 1994; Ullrich et al., 1993). The multitude of Rab proteins contained in human cells and the processes in which they are involved are reflected in Table 1.

Rab functions that are basic to cell homeostasis include trafficking between the ER, plasma membrane or endosomes and the Golgi apparatus, as well as intra-Golgi trafficking. Distinct Rab proteins also mediate early and late endosome biogenesis, maturation and fusion with lysosomes, as shown in Table 1. Endocytic recycling, exocytosis or phagosome dynamics also involve members of this protein family. Furthermore, Rab proteins also mediate other more specific, cell-type dependent transport mechanisms, such as melanosome biogenesis and transport, ciliogenesis, or tight junction assembly in epithelial cells (Stenmark, 2009). Many of these Rab proteins mediate trafficking steps, which are controlled by feedback mechanisms involving their effectors: sorting adaptors, motor adaptors for vesicle transport on actin or tubulin,

tethering factors or simply their respective GAP, GDI or GEF. These interactions are at the core of Rab protein involvement in vesicle budding, motility or fusion (Stenmark, 2009).

Rab GTPases	Function
Rab1	ER–Golgi trafficking
Rab2	Golgi–ER trafficking
Rab6, Rab33, Rab40	Intra–Golgi trafficking
Rab8	Golgi–Plasma membrane trafficking
Rab22	Golgi–early endosome transport, both directions
Rab5	Early endosome biogenesis and maturation
Rab7	Late endosome and phagosome maturation Fusion with lysosomes
Rab9	Late endosome–Golgi transport
Rab4	Fast endocytic recycling
Rab11, Rab35	Slow endocytic recycling
Rab3, Rab26, Rab27, Rab37	Regulated exocytosis
Rab33, Rab24	Autophagosome formation
Rab18	Lipid droplet formation
Rab32, Rab38	Melanosome biogenesis and transport
Rab8, Rab17, Rab23	Ciliogenesis
Rab13	Tight junction assembly

Table 1. Functions of Rab GTPases.

Rab GTPases are crucial for a wide variety of intracellular tasks, which they perform at specific subcellular localizations. Where indicated, several Rab proteins act in concert to regulate a particular trafficking or biogenesis event. See text for details.

Amongst the trafficking routes mediated by Rab proteins, the most important step in endosome biogenesis is the exchange of Rab5 for Rab7 on early endosomes maturing to late endosomes. In this process, early endosomes derived from internalization the plasma membrane are covered by Rab5, which is replaced by Rab7 following an exchange of their GEF (Poteryaev et al., 2010; Rink et al., 2005). Switching Rab5 for Rab7 implies that recycling Rabs such as Rab4 and Rab11 are lost, whereas late

endosomal Rab9 is recruited. Other concomitant endosomal maturation steps include phosphatidylinositol species turnover, acquisition of hydrolases and other proteins from the trans-Golgi network, lumen acidification by V-ATPases, and morphological or size variations (Huotari and Helenius, 2011).

Due to the importance of Rab proteins in intracellular trafficking, mutations in several of these proteins give rise to pathological scenarios including congenital disorders such as Griscelli Syndrome 2, in which Rab27a is mutated (Menasche et al., 2003; Mitra et al., 2011), or X-linked choroideremia, arising from Rep-1 mutation and subsequent deficits in Rab27a geranylgeranylation (D'Adamo et al., 1998; Seabra et al., 1993; Seabra et al., 1995). In addition, Rabs can mediate tumorigenesis (Recchi and Seabra, 2012) and are involved in infectious processes, since many pathogens hijack Rab pathways either during endocytosis while entering the cell, e.g. *Salmonella enterica* serovar Typhimurium or coxsackie virus (Coyne et al., 2007; Smith et al., 2007), or interfering with endosome maturation steps once inside the cell, e.g. *Lysteria monocytogenes* and *Helicobacter pylori* (Prada-Delgado et al., 2005; Terebiznik et al., 2006).

The concerted action of Rab proteins with other machineries adds further complexity to endosomal sorting. For example, late endosomes that have acquired Rab7 undergo internal rearrangements such as acquisition of material from the Golgi, homotypic fusion instead of fusion with early endosomes, or ILV formation giving rise to MVB (Huotari and Helenius, 2011). This latter process is catalyzed by yet another multi-protein sorting machinery, the ESCRT proteins.

3.1.2 ESCRT proteins in MVB biogenesis

There is a multitude of proteins involved in the formation of MVB that function sequentially from cargo recognition, deformation of the membrane, to internalization of cargo into ILV of MVB (Raiborg and Stenmark, 2009). The components involved in recognizing ubiquitin on cargo to be degraded were studied in yeast and termed Class E Vacuolar protein sorting (Vps) proteins (Raymond et al., 1992). It was soon determined that Vps proteins combine at MVB membranes to form the multi-subunit ESCRT machinery represented in Figure 8 to mediate ILV biogenesis.

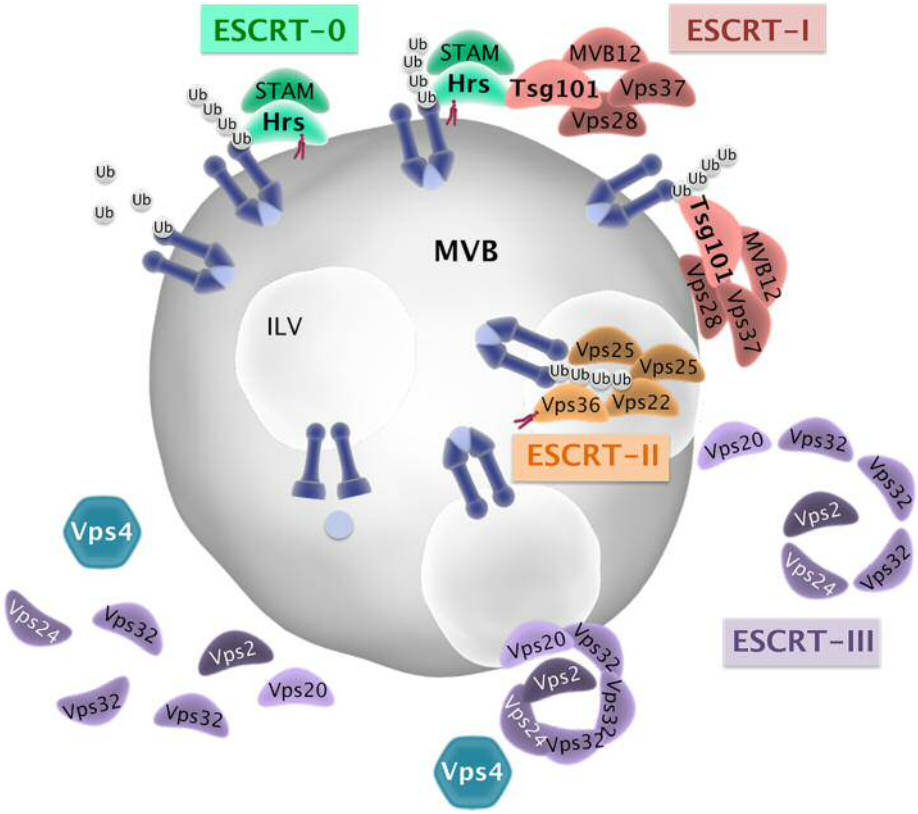

Figure 8. Schematic of the ESCRT protein machinery.

The ESCRT machinery aids in sorting endosomal cargo and MVB biogenesis through ILV production. Dark blue rods bound to light blue circles represent receptors bound to their ligand that have been internalized from the plasma membrane and arrive at the MVB limiting membrane during endocytosis. Ubiquitin binds to these receptors and is recognized by ESCRT-0 (green components) through binding of Hrs to PI(3)P (red phospholipid). ESCRT-I (red shapes) is recruited by this machinery and cargo is transferred along the pathway such that ESCRT-I together with ESCRT-II (orange shapes) gives rise to MVB membrane invagination. ESCRT-III (purple spiral) binds to ESCRT-II along with other associated proteins responsible for deubiquitinating cargo. ESCRT-III forms spiral filaments surrounding the forming vesicle neck to induce its pinching off from the limiting membrane to form an ILV. Ultimately, the ATPase Vps4 (teal hexagon) is recruited by ESCRT-III and promotes its disassembly to recycle components. The nomenclature used here refers mostly to yeast proteins, though alternative nomenclatures have developed for mammalian orthologues. Adapted from (Rusten et al., 2012).

As addressed above, protein complexes aid vesicles in diverse maturation steps along the endocytic route (see Figure 7), including membrane budding events that elicit multivesicular compartment formation. The ESCRT –I, -II and –III complexes were described as assemblies of Vps proteins, each involved in a specific step of MVB biogenesis (Babst et al., 2002a; Babst et al., 2002b; Katzmann et al., 2001). A fourth complex, ESCRT-0, was defined later on, though it is the first to act by recognizing ubiquitinated cargo such as monoubiquitinated cytosolic domains of membrane receptors and forming a protein mesh on endosomes (Raiborg et al., 2001; Raiborg and

Stenmark, 2009). The fundamental ESCRT-0 protein is Vps27p, or Hrs (Hepatocyte growth factor-regulated tyrosine kinase substrate) in humans (Figure 8, green). Hrs recognizes ubiquitinated cargo and also contains a phosphoinositol-3-phosphate (PI(3)P) binding domain termed FYVE. ESCRT-I is responsible for binding to ubiquitinated cargo and ESCRT-0 simultaneously (Katzmann et al., 2001). Vps23p or its homolog in humans, Tsg101 (Figure 8, red), is at the core of ESCRT-I, for it directly binds to cargo and Hrs. Once ESCRT-0 is recycled, ESCRT-I can interact with ESCRT-II (Figure 8, orange), which aids in early steps of membrane curvature and in assembling the next complex (Babst et al., 2002b). ESCRT-III function is one of the most important steps in MVB biogenesis, since a subset of its subunits is in charge of generating membrane curvature to accommodate ILV production, while other proteins in this complex aid in vesicle abscission (Babst et al., 2002a; Hanson et al., 2008). Currently, there is still debate as to how ESCRT-III subunits (in humans, charged multivesicular proteins, or CHMP) assemble to deform membranes, with two main hypotheses still standing, i.e. the helical and dome models, represented by purple spirals in Figure 8, as reviewed in (Henne et al., 2013). In turn, several ESCRT-associated proteins perform crucial tasks such as deubiquitinating cargo or aiding in membrane deformation (Clague and Urbe, 2006). Vps4 is an ATPase that is in charge of terminating ILV formation by providing energy for membrane scission at the vesicle neck and promoting ESCRT-III dissociation from the MVB (Shim et al., 2008). Interestingly, ESCRT machineries do not accompany cargo into ILV, but rather are all recycled for subsequent rounds of endolysosomal sorting (Babst et al., 1998; Williams and Urbe, 2007).

Though the canonical ESCRT sorting pathway begins with cargo ubiquitination, several studies have shown that this route can also be responsible for ubiquitin-independent sorting. In yeast, acid trehalase is targeted to lysosomes via MVB in an ubiquitin-independent manner (Huang et al., 2007a). In mammalian cells, several cytokine receptors and the G-protein coupled receptors (GPCR) DOR (delta opioid receptor) and PAR1 (protease-activated receptor 1) are similarly sorted into MVB through ubiquitin-independent mechanisms involving at least part of the ESCRT machinery (Amano et al., 2011; Dores et al., 2012; Hislop et al., 2004). A recent study further suggests that binding to any ESCRT protein can mediate ubiquitin-independent

sorting, such that weak affinity for ESCRT and strong membrane association will mediate internalization into MVB, whereas a strong interaction with ESCRT but weaker membrane binding will send proteins along the recycling pathway to the plasma membrane, regardless of their ubiquitination state (Mageswaran et al., 2014). Therefore, some MVB cargo contains structural determinants that allow for ESCRT-dependent sorting into ILV in the absence of ubiquitin.

The ILV inside MVB can have different fates. If retained in the endosomal route, they will be taken to the lysosome to be degraded (Futter et al., 1996). Alternatively, ILV can be liberated to the extracellular space after fusion of MVB with the plasma membrane, hence becoming exosomes, as reviewed in (Simons and Raposo, 2009). Whether degradative and exocytic ILV are contained within distinct MVB or can be found in the same MVB has been the subject of much debate. Recently, two subpopulations of ILV have been shown to coexist within the same MVB (Edgar et al., 2014), as depicted in Figure 9.

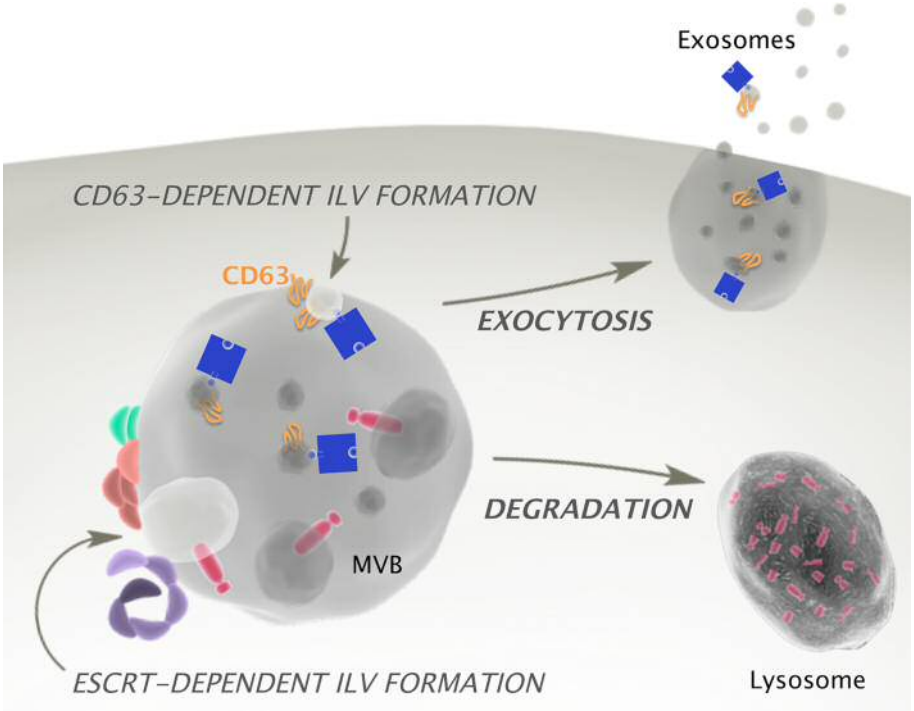

Figure 9. ILV biogenesis and destination.

The limiting membrane of MVB invaginates to form either large ILV through ESCRT-dependent mechanisms (machinery shown in green, red and purple) or to form small ILV in a process involving CD63 (shown in orange). In this model, the same MVB holds both types of ILV, as described recently (Edgar et al., 2014); however, it is not yet clear whether this is the case or if specific MVB exist for each type of ILV. Small ILV containing CD63 and material to be secreted (blue squares) are released into the extracellular milieu upon fusion of the MVB with the plasma membrane during exocytosis. On the other hand, large ILV containing cargo such as signaling receptors (red rods) fuse with lysosomes to elicit degradation of ILV content.

The two types of ILV differ in size, biogenesis and cellular fate. Large, sorting ILV are formed Hrs-dependently, whereas small, exocytic ILV appear due to sorting mediated by the tetraspanin CD63, as will be explained below. It is therefore possible that both ESCRT-dependent and -independent ILV generation occur simultaneously within the cell, giving rise to specific types of vesicles with unique destinations. This point is further substantiated by the fact that CD63-positive ILV still appear in the absence of members of all ESCRT complexes, suggesting that ESCRT-independent mechanisms of MVB biogenesis are still operative in this setting (Stuffers et al., 2009). Indeed, the major histocompatibility complex-II (MHC-II) in dendritic cells can be sorted to lysosomal ILV when ubiquitinated under resting conditions *via* an ESCRT-dependent process, whereas cell activation abolishes MHC-II ubiquitination and promotes its internalization into exosomal ILV that are liberated towards the T cells with which they interact (Buschow et al., 2009).

Though represented as distinct processes in Figure 9, crosstalk most likely exists between degradative or exocytic ILV biogenesis pathways, as reflected in a recent report presenting an RNA interference screen of 23 ESCRT proteins. Several ESCRT proteins, e.g. Hrs or Tsg101, were found necessary not only for degradative ILV formation but also for exosome biogenesis, suggesting that exosomes can be formed by the ESCRT machinery as well as by ESCRT–independent pathways (Colombo et al., 2013).

3.1.3 CD63-mediated sorting

The role of CD63 in formation of exosomal ILV highlights the fact that this tetraspanin is inextricably involved in late endosomal trafficking, as reviewed in (Pols and Klumperman, 2009). Tetraspanins are a family of proteins containing four transmembrane domains, glycosylated residues and most contain cysteines amenable to palmitoylation, as is the case for CD63, as reviewed in (Hemler, 2005). These posttranslational modifications aid in homo- and heteroligomerization to produce tetraspanin-enriched microdomains (TEM) in which tetraspanins of several types along with receptors, integrins, metalloproteinases and cholesterol occupy a tightly packed area of membrane, particularly on the plasma membrane (Yang et al., 2002). In fact, as

shown in Figure 10, a cholesterol-palmitoyl interaction is also established by the palmitates bound to tetraspanins, further stabilizing these TEM (Charrin et al., 2003).

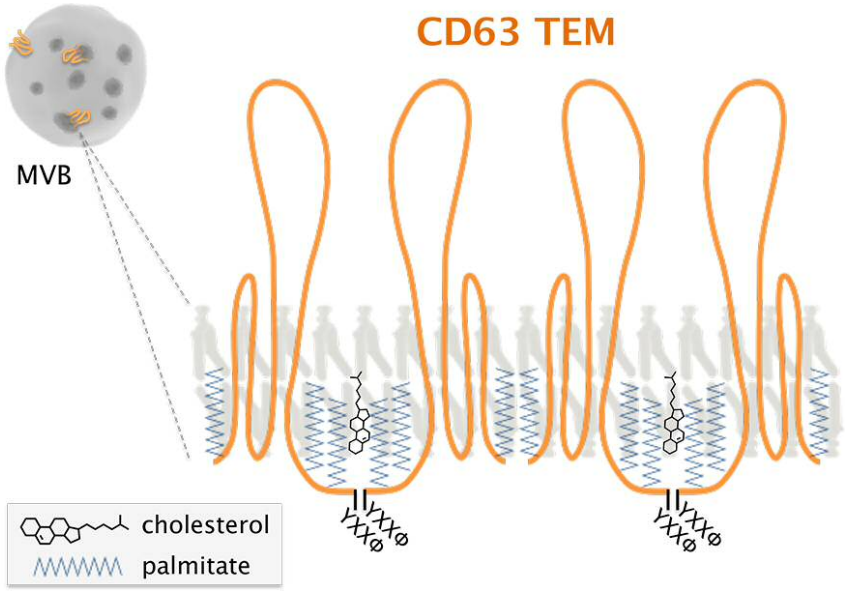

Figure 10. CD63 tetraspanin-enriched microdomains.

Zoom-in of a membrane from an ILV destined for exosomal release. CD63 molecules are shown in orange, containing four transmembrane domains and two loop domains. Cysteine residues at their N- and C-termini become palmitoylated (blue zigzags), which allows for interaction with membrane-embedded cholesterol (black structures). The C-terminal YXXΦ motifs that interact with AP complexes for intracellular shuttling are also depicted. Tetraspanins associate with each other to form oligomers, as shown here for four CD63 molecules, to form tetraspanin-enriched microdomains (TEM).

In the case of CD63, its association with late endosomes and ILV usually predominates over plasma membrane localization. Specifically, ILV destined for exosome formation are enriched in several tetraspanins including CD63 (Escola et al., 1998). This tetraspanin contains the lysosomal targeting sequence "YEVM", which follows a "YXXΦ" pattern recognized by adaptor protein complexes, in which a crucial tyrosine residue is followed by any two amino acids (X) and an aliphatic, bulky residue (Φ), as reviewed in (Bonifacino and Traub, 2003). Therefore, CD63 contains several structural determinants that direct it to the late endocytic pathway.

A newly synthesized CD63 polypeptide chain undergoes glycosylation and palmitoylation at the Golgi prior to export to the plasma membrane, cycling back inward when its sorting signal is recognized by AP-2 and traveling further from recycling endosomes to late endosomes/MVB and lysosomes via AP-3 binding, as reviewed in (Pols and Klumperman, 2009). Following these pathways, it has been

reported that CD63 could be involved in trafficking of MHC-II in dendritic cells (Vogt et al., 2002) or recycling of the H^+/K^+ ATPase pump in gastric parietal cells (Duffield et al., 2003). Additionally, a truncated form of CD63 was shown to down-regulate chemokine receptor CXCR4 plasma membrane levels due to receptor internalization in T lymphocytes (Yoshida et al., 2008). Once localized at late endosomes/MVB, CD63 can mediate ESCRT-independent sorting of certain proteins, as is the case for specific domains of the melanosomal protein Pmel17 (Theos et al., 2006; van Niel et al., 2011). Furthermore, CD63 plays a central role in ESCRT-independent exosome biogenesis, as described above, which is also reflected by its use as an exosomal marker, as reviewed in (Andreu and Yáñez-Mo, 2014). Recently, the direct role of TEM in exosome formation has been set forth by a comprehensive high-throughput proteomic analysis that highlights their importance in selecting receptors and signaling proteins for exosomal packaging (Pérez-Hernández et al., 2013). It is interesting to note that though CD63 is involved in sorting proteins of various origins, its knock-out (KO) mouse model is viable and displays normal lysosomal function, though these mice suffer kidney pathologies. However, considering the amount of tetraspanins expressed in cells, there could be redundancies such that other members of this protein family could compensate for CD63 loss (Schröder et al., 2009).

Though MVB biogenesis and cargo sorting require proteins such as CD63 or ESCRT components, it also depends on the lipid composition in which membrane proteins are embedded. It has been proposed that specific membrane domains and the lipids contained therein can play a part in the invagination of the MVB limiting membrane to form ILV (Matsuo et al., 2004). Moreover, it has been described that certain lipid compositions favor the formation of MVB in the absence of protein components, both in liposome models and in cells (Matsuo et al., 2004; Trajkovic et al., 2008), as will be described in the following section.

3.2 Lipid involvement in endosomal sorting

Lipids are distributed unevenly among cellular membranes and hence play a significant role in the distribution of membrane proteins in different organelles. As schematized in Figure 11, intracellular membranes have been proposed to be divided

into two distinct environments according to lipid properties: the biosynthetic, pre-Golgi system that includes the ER, and the secretory-endocytic, post-Golgi system that includes the plasma membrane and endocytic vesicles (Lippincott-Schwartz and Phair, 2010). Following this model, ER/cis-Golgi membranes contain monounsaturated lipids usually with neutral head groups that favor interactions with cytosolic proteins preferring lipid-packing defects. On the other hand, the trans-Golgi, plasma membrane and endocytic compartments include more negatively charged lipids packed tightly (i.e. phospholipids with more saturated acyl chains) to favor electrostatic interactions (Figure 11). Other specialized lipids appear at specific subcellular locations. For instance, cholesterol and glycosphingolipids reside on both leaflets of the plasma membrane, while phosphatidylethanolamine (PE) and phosphatidylserine (PS) remain at its inner leaflet, as reviewed in (Bigay and Antonny, 2012). Furthermore, scarce but highly specialized phosphoinositides appear at different membrane sites throughout the cell. The plasma membrane contains PI(4,5)P_2 and PI(3,4,5)P_3 whereas PI(3)P appears at early endosomes and controls many endocytic processes through proteins with PI(3)P binding domains (Gillooly et al., 2000; Schink et al., 2013). The specialized phospholipid, 2,2'-dioleoyl lysobisphosphatidic acid (LBPA, a.k.a. BMP) (Kolter and Sandhoff, 2005) is exclusively localized to late endosomes, particularly ILV of MVB (Kobayashi et al., 1999), and has the ability to deform membranes *in vitro*, thus possibly playing a role in MVB invagination, as discussed below (Matsuo et al., 2004). Therefore, the dynamic nature of membrane trafficking depends not only on protein-based sorting complexes, but also on organelle identity conferred to specific endomembranes by lipids of varied acyl composition, head group charge and overall physicochemical structure.

Lipid gradients exist along the biosynthetic pathway, so that there is more cholesterol density and sphingolipids from the ER towards the PM (Maxfield and van Meer, 2010), as depicted in Figure 11. Cholesterol and sphingolipids are responsible for thickening the membrane bilayer, which is reflected by the transmembrane span of proteins (Sharpe et al., 2010). In particular, cholesterol is enriched in recycling endosomes, as well as in ILV of MVB (Möbius et al., 2003). Cholesterol has been found to appear at particularly high curvature regions (Wang et al., 2007), which could explain its concentration in ILV. This sterol also stabilizes fluid phosphoinositide domains, which could be involved in forming signaling platforms that require concentrating these

scarce phospholipids into an area that accommodates interactions between signaling proteins (Jiang et al., 2014). Furthermore, in the context of signaling receptors, several GPCR have been shown to directly interact with cholesterol through their palmitoyl moieties (Cherezov et al., 2007; Zheng et al., 2012), similarly to tetraspanins (Charrin et al., 2003).

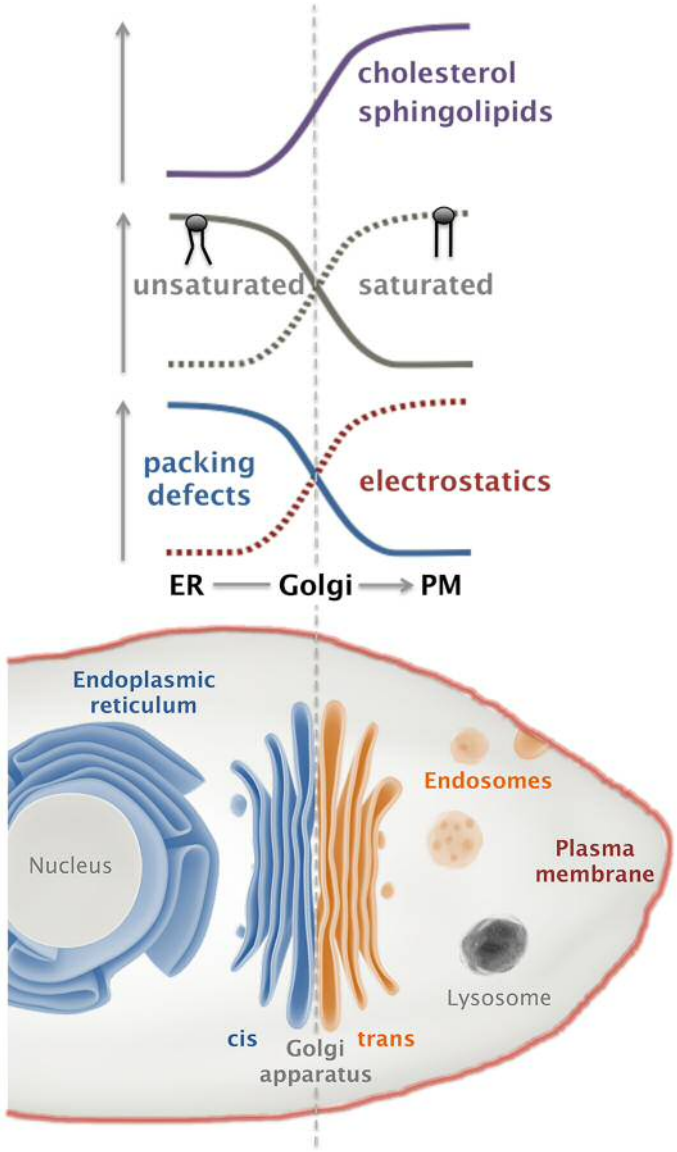

Figure 11. Lipid properties defining membrane environments within the cell.

Studies based on lipidomics and probe detection point to two distinct membrane environments within the cell. As shown to the left of the dashed line (blue structures), the ER and cis-Golgi membranes are characterized by lipid-packing defects due to the unsaturated chains that their phospholipids contain, whose head groups are weakly charged. Furthermore, they present low levels of cholesterol and sphingolipids, producing thin membranes. In contrast, trans-Golgi, endosomal and plasma membranes (orange and red components to the right of the dashed line) are characterized by inner leaflet phospholipids with negatively charged polar groups (high electrostatics) and saturated chains, as well as elevated cholesterol and sphingolipid levels, rendering them thicker and more tightly packed. Adapted from (Bigay and Antonny, 2012).

Regarding the formation of ILV of MVB, several *in vitro* studies have shown that lipids alone can mediate membrane invagination on liposomes with particular compositions (Matsuo et al., 2004; Trajkovic et al., 2008). The specialized lipid LBPA could be involved in the ESCRT-dependent formation of degradative ILV (Matsuo et al., 2004), whereas the sphingolipid ceramide induces the formation of ILV destined to become exosomes (Trajkovic et al., 2008) (see Figure 9). These findings are in line with studies describing high levels of LBPA in ILV of MVB within the cell, whereas exosomes are not enriched in this lipid (Laulagnier et al., 2004; Wubbolts et al., 2003). Another report suggests that cholesterol-rich MVB are destined for exosome formation and cholesterol-poor vesicle populations are sent to the lysosome to be degraded (Möbius et al., 2003). Furthermore, ILV have been shown to undergo back-fusion and blend back into the MVB limiting membrane via an LBPA-mediated process employed by certain pathogens to escape their degradation, as reviewed in (Falguières et al., 2009). However, there is still debate regarding whether exosome biogenesis is dependent on ESCRT and its associated proteins, e.g. Hrs, Alix (Baietti et al., 2012; Colombo et al., 2013; Gibbings et al., 2009) or mostly lipid-based and perhaps involving CD63 (Trajkovic et al., 2008). It is therefore probable that ILV themselves or even specific microdomains of the MVB limiting membrane, though thoroughly dependent on their lipid composition, are regulated by tight interplay with complex protein machineries owing to their highly dynamic nature (Bissig and Gruenberg, 2013).

Lipid composition also has its effects on peripheral membrane proteins such as Ras and Rho proteins, since their trafficking depends on lipid modifications, as described above. In the case of proteins that are both isoprenylated and palmitoylated, isoprenylation could be responsible for a weak interaction with the membrane, whereas single or double palmitoylation would aid in its binding to membranes with a particular composition (Rocks et al., 2005). These palmitate moieties are saturated chains that occupy a small space and can therefore force their way into tightly packed membranes containing saturated phospholipids, such as the plasma membrane and late endocytic vesicles. An elegant *in silico* model suggests that H-Ras forms clusters at the interface of lipid domains with its palmitate chains preferentially oriented towards liquid ordered domains (L_o, cholesterol-rich, with saturated phospholipids), whereas its polyunsaturated farnesyl moiety is directed towards the liquid disordered membrane

domain (L_d), hence increasing membrane curvature (Janosi et al., 2012). H-Ras was indeed found to cycle between L_d and L_o domains in its GTP- or GDP-bound form, respectively, underscoring the importance of lateral segregation of peripheral proteins on their function (Prior et al., 2001). Lipid packing, electrostatics or curvature could play a further role in membrane selectivity, as is the case for members of the Rho family (Rac1 and Rac2) or the Ras protein, K-Ras4B, which contain basic residues at their C-terminus that allow electrostatic interactions with PS on membranes (Ahearn et al., 2012; Bigay and Antonny, 2012). It is therefore apparent that lipid composition is crucial for peripheral membrane proteins to accomplish their biological roles at distinct subcellular locations.

3.3 Other sorting and degradation pathways

Early stages of protein sorting within the cell involve bulk flow of many proteins towards the *cis* Golgi upon translation at the ER. However, post-Golgi trafficking events become increasingly specialized for the proteins to be sorted, so that more cargo-specific sorting machineries appear further along the endocytic route towards lysosomes, secretion or recycling. Along with the pivotal Rab and ESCRT protein sorting machineries described above, other mechanisms act in parallel to coordinate the busy flow of material in later stages of protein shuttling within the cell. Many proteins contain sequences that are recognized by sorting entities (Bonifacino and Traub, 2003), as exemplified by soluble acid hydrolases, which are modified by M6P and recognized by M6P receptors in the Golgi apparatus that will accompany them to the lysosome, as reviewed in (Ghosh et al., 2003). However, other M6P-independent mechanisms involving the sorting proteins sortilin or lysosomal integral membrane protein 2 (LIMP-2) also work in the cell to transfer soluble proteins into lysosomes (Coutinho et al., 2012; Ghosh et al., 2003). As for lysosomal transmembrane proteins, their targeting sequences contain tyrosines (such as the "YXXΦ" motif in CD63 mentioned above) or dileucine motifs that are recognized by specific AP complexes, as extensively reviewed in (Bonifacino and Traub, 2003). Distinct AP complexes are present on membranes such as the plasma membrane, Golgi, endosomes and others, from which they recognize motifs in cargo proteins and mediate their transport (Bonifacino and Traub, 2003).

Additionally to protein-specific sorting, cell type-dependent processes are responsible for the formation and transport of certain specialized vesicles, such as lysosome-related organelles (LRO), e.g. melanosomes for pigmentation; basophil, azurophil and lytic granules or MHC class II compartments for immune responses; and platelet-dense granules for coagulation, as reviewed in (Dell'Angelica et al., 2000). Their biogenesis is mediated by yet another protein machinery termed BLOC 1-3 (biogenesis of lysosome-related organelles complex), containing proteins that are mutated in the lysosomal disorder Hermansky-Pudlak syndrome (HPS), which will be considered below, as reviewed in (Dell'Angelica, 2004).

3.3.1 Autophagy

The term “autophagy”, literally “self-eating”, originally was designated for a process in which proteins and even organelles are surrounded by double membranes of varied origin called phagophores, which mature to autophagosomes and fuse with lysosomes to degrade these large amounts of cellular material (Mizushima et al., 2008). The explosion of research in this field has led to the discovery of numerous autophagic pathways, so that the original term is now referred to as macroautophagy, to differentiate it from the other two main forms of autophagy, i.e. microautophagy, implying direct lysosomal internalization, and chaperone-mediated autophagy, in which the chaperone Hsc70 unfolds proteins prior to their internalization into the lysosome to be degraded (Cuervo and Dice, 1996; Lee et al., 2012). Cells undergo these degradation processes to redeliver the necessary biosynthetic building blocks to the cytosol when they detect a nutrient or energetic shortage, or under stress conditions including pathogen invasion and excessive protein aggregation, as reviewed in (Yang and Klionsky, 2010). The autophagy-related proteins (Atg) are the core molecular machinery of canonical autophagy and work together in sequential complexes during phagophore maturation towards autophagosomes, as reviewed in (Mizushima et al., 2011). Though autophagy was first regarded as a degradation and cell death mechanism, numerous reports now corroborate its role in survival, bioenergetics, cell differentiation, immunity, and tumor suppression, as reviewed in (Boya et al., 2013).

Interaction between autophagy and endolysosomal sorting is obvious at the point of autophagosome-lysosome fusion, but some instances of autophagosome fusion to early and late endosomes have been documented (Berg et al., 1998; Dunn, 1994; Liou et al., 1997). In fact, the fusion of endocytic vesicles such as MVB and autophagosomes gives rise to structures called amphisomes, which further fuse to lysosomes for degradation (Eskelinen, 2005). Moreover, some studies suggest that Rab11 could play a role in MVB-autophagosome fusion to form amphisomes, whereas Rab7 would mediate the next step of fusing to lysosomes, as reviewed in (Fader and Colombo, 2009). Other members of the Rab family also appear at the crossroads of endolysosomal and phagocytic pathways, such as Rab1 at the initial formation of the phagophore and Rab9 during non-canonical Atg5/Atg7-independent autophagy, among others, as reviewed in (Chua et al., 2011). Studies both in mammalian cells and *Drosophila* lacking certain ESCRT proteins showed impaired autophagy and accumulation of ubiquitin-positive aggregates, again revealing that correct MVB function is necessary for autophagy progression (Rusten and Simonsen, 2008). It has also recently come to light that it is common for autophagic cargo to become ubiquitinated and sorted by autophagy receptors containing ubiquitin-binding domains (Boya et al., 2013). Furthermore, connections between autophagy and exosomal MVB have been established, since autophagy induction by several methods inhibits exosome release and points to a selective MVB fate depending on cellular energy needs (Baixauli et al., 2014). Once again, the boundaries between distinct organelles are often blurred during crosstalk between intracellular trafficking pathways.

4. Lysosomal storage diseases

Lysosomal storage diseases are quite a numerous group of rare inherited metabolic disorders resulting from mutations in specific lysosome-related genes (Ballabio and Gieselmann, 2009; Fuller et al., 2006). Though initially attributed to acid hydrolases of the lysosomal lumen, it has become evident that both lysosomal integral membrane and luminal proteins, among others, are involved in certain lysosomal storage disorders (Saftig and Klumperman, 2009). There are as many as 60 lysosomal protein deficiencies that give rise to accumulation of material from incomplete degradation or trafficking in degradative compartments (Sagne and Gasnier, 2008). Some of these disorders arise from problems in LRO biogenesis, mediated by transporters and tethering or sorting factors (Huizing et al., 2008). In most cases, manifestations appear during childhood and often include varying degrees of neurodegeneration and immune deficiencies that can cause death at a relatively early age unless palliated by bone marrow transplantation or recently developed treatments such as enzyme replacement therapy, as reviewed in (Platt et al., 2012). Table 2 summarizes several lysosomal storage diseases and the proteins altered by mutations in their respective genes.

There are many pathological scenarios involving malfunction of lipid transport routes, but here the focus will be on alterations of late endosome lipids. In Niemann-Pick type C (NPC) disease, a set of lysosomal integral membrane proteins that act as cholesterol transporters at late endosomes (NPC1/NPC2) are deficient (Table 2). Late endosomes and lysosomes in NPC patients accumulate massive amounts of cholesterol and glycosphingolipids due to abnormal low-density lipoprotein processing within the endocytic pathway (Mukherjee and Maxfield, 2004). Furthermore, this cholesterol buildup induces Rab9 sequestration, possibly in its inactive form, which disrupts M6P

receptor trafficking (Ganley and Pfeffer, 2006). It has been described that NPC1 cells could be inducing the release of exosomes loaded with cholesterol, perhaps as a means of circumventing the cytotoxic effects of generalized cholesterol buildup within the cell (Strauss et al., 2010). Alterations of lipid homeostasis are quite severe due to cholesterol and LBPA accumulation in late endosomes and subsequent endolysosomal dilation in several cell types (Carstea et al., 1997; Kobayashi et al., 1999). In fact, this phenotype can be mimicked by treatment with the hydrophobic amine U18666A that has therefore been used to generate NPC-like cells (Mukherjee and Maxfield, 2004; Sobo et al., 2007).

Lysosomal storage disease	Mutated proteins
Niemann–Pick Type C (NPC)	NPC1 or NPC2
Hermansky–Pudlak Syndrome (HPS)	
• HPS–1, HPS–4	BLOC–3
• HPS–2	AP–3
• HPS–3, HPS–5, HPS–6	BLOC–2
• HPS–7, HPS–8	BLOC–1
Chediak–Higashi Syndrome (CHS)	LYST

Table 2. Lysosomal storage diseases and mutated proteins.

Lysosomal storage diseases are caused by point mutations in genes that code for proteins involved in late endocytic trafficking. NPC proteins are involved in cholesterol transport, whereas proteins responsible for the various forms of HPS mediate vesicular transport of lysosome-related organelles (BLOC) or general late endosomal trafficking (AP-3). Many point mutations have been described for the Lyst gene, all of which give rise to CHS of varying degrees of severity.

Mutations in several LRO biogenesis-related proteins give rise to recognizable hypopigmentation disorders due to malfunction of melanosome biogenesis or trafficking, as reviewed in (Dessinioti et al., 2009). Such is the case for Hermansky-Pudlak syndrome (HPS), in which mutation of several specific proteins can elicit similar phenotypes, and Chediak-Higashi syndrome (CHS), resulting from mutations in the Lysosomal trafficking regulator (Lyst) protein, as will be discussed in detail below. There are eight human HPS subtypes (Table 2), which arise from mutations in key LRO trafficking and maturation machinery proteins, i.e. BLOC-3 mutations in HPS-1 and HPS-4, AP-3 in HPS-2, BLOC-2 in HPS-3, HPS-5 and HPS-6, and BLOC-1 in HPS-7 and HPS-8, as reviewed in (Wei, 2006). Apart from LRO machineries, certain Rab

family proteins have been shown to play a role in HPS mouse models and perhaps in human pathology, for BLOC-3 acts as a Rab-GEF for Rab38 and Rab32 to recruit these proteins to premelanosomal membranes. Furthermore, Rab38 co-localizes with BLOC-2 and AP-3 at endosomal membranes, suggesting a role for this Rab in cargo trafficking during LRO biogenesis, as reviewed in (Krzewski and Cullinane, 2013).

4.1 Chediak-Higashi Syndrome

CHS is a rare autosomal recessive lysosomal storage disorder characterized by enlarged granules in many cell types, including melanocytes, neutrophils, leukocytes and neurons, among others. The large, dense granules are either lysosomes or LRO destined for secretion and involved in diverse cellular functions such as immune responses, pigmentation or coagulation. These functions are compromised in CHS patients, as reflected by their clinical manifestations which include partial oculocutaneous albinism, bleeding disorders, neutropenia, recurrent infection and neurological dysfunction, that can lead to death associated to a severe phase due to uncontrolled proliferation of cytotoxic T lymphocytes (Ward et al., 2000).

The genetic defects that underlie CHS consist of mutations in the CHS1/LYST gene, homologous to the *beige* gene in mice. This gene codifies a cytosolic protein of 3801 amino acids (approximately 429 kDa) with still unclear functions (Huizing et al., 2001). The LYST protein is a member of the BEACH (BEige And Chediak–Higashi) protein family and mutations that are phenotypically similar to CHS have been found in numerous mammalian species (Ward et al., 2000). Enlarged lysosomes and LRO are found mainly at the perinuclear region of CHS cells, pointing to a disruption in vesicle trafficking (Burkhardt et al., 1993).

There are several functional studies on CHS cells or murine *beige* models that describe alterations in late vesicular traffic and their cellular impact. Similarly to HPS, deficiency in CHS melanosome secretion underlies oculocutaneous albinism in these patients (Stinchcombe et al., 2004). Under physiological conditions, it has been established that cells are able to use their lysosomes as Ca^{2+}-regulated secretory compartments to "parch" the plasma membrane after wounding, making them crucial in membrane resealing (Reddy et al., 2001). In CHS and *beige* cells, lysosomal exocytosis

and consequent plasma membrane repair are defective (Huynh et al., 2004). Also in line with these findings, other exocytic organelles seem to be responsible for CHS immune deficiencies. CHS patients suffer from a loss of secretion at the immunological synapse, where CTL normally discharge proteins such as perforin *via* secretory lysosomes (Stinchcombe et al., 2000). Furthermore, CHS B lymphocytes present deficient peptide loading onto MHC class II as well as delayed antigen presentation as a result of defects in MHC-II transport from the TGN into MVB (Faigle et al., 1998). It has been proposed that LYST could act as a scaffold for complexes involved in LRO biogenesis that are defective in HPS pathogenesis as well, such as AP-3 or BLOC-1 (Callahan et al., 2009). Yeast two-hybrid screens using truncated forms of LYST revealed direct interaction with several proteins involved in late endosomal dynamics such as Hrs and several SNARE proteins (Tchernev et al., 2002). Rab14 interaction with a LYST homolog (LsvB) has been observed in the amoeba *Dictyostelium discoideum,* proposing that LsvB regulates lysosomal size and maturation through Rab14, though these studies are yet to be replicated in human cells (Kypri et al., 2013). Recent findings using small interfering RNA-depletion of LYST in cancer cells also point to a role for this protein in lysosome size and quantity, which could be regulated by fission or fusion events, instead of being directly responsible for LRO biogenesis or general degradation pathways (Holland et al., 2014). Indeed, in *Dictyostelium*, LsvB has been found to have an inhibitory role in vacuole fusion (Falkenstein and De Lozanne, 2014), whereas previous studies in *beige* mouse cells suggested that LYST promotes lysosomal fission (Durchfort et al., 2012). Clearly, the exact function of this remarkably large protein in endolysosomal biogenesis or sorting still warrants further studies.

AIMS AND OBJECTIVES

Small GTPases control crucial cellular functions from specific membrane localizations. Among the factors involved in their regulation, modifications at C-terminal sequences play key roles, though the involvement of lipidation and its interplay with other structural determinants in subcellular targeting of GTPases has not been fully elucidated. Therefore, the work presented in this dissertation is focused on analyzing the role of lipid modifications of RhoB cysteine residues on its intracellular sorting and determining whether its lipidation motif *per se* is able to reproduce the behavior of the full-length protein. Furthermore, the possibility that lipidation sequences could be targeted by other structurally diverse modifications, including reactive species arising in pathological scenarios, has not been explored. Therefore, the following objectives were projected:

- To study endosomal GTPase C-terminal sorting signals involved in subcellular localization.
- To evaluate the importance of C-terminal isoprenylation and palmitoylation in attachment to intracellular vesicles.
- To determine the subcellular localization of chimeras bearing the RhoB C-terminal lipidation motif.
- To assess whether the latent sorting mechanisms for the RhoB C-terminus are conserved in cells from different species.
- To explore the potential role of key molecular machineries, i.e. ESCRT complexes, CD63 or lipid dynamics, in sorting of RhoB and related chimeras.
- To set the basis for studying the potential alteration of endosomal GTPase localization and modification in experimental models of disease.

MATERIALS AND METHODS

1. Materials

1.1 General reagents

1.1.1 Cell culture reagents

Cell culture medium including DMEM, RPMI 1640, and TC100 as well as Newborn calf serum, penicillin/streptomycin, glutamine and trypsin-EDTA were from Gibco Life Technologies. NCTC 109 medium was from Sigma. Fetal bovine serum (FBS) was from Lonza Inc. Sterile plastic material for cell culture was obtained from Falcon (Beckton Dickinson). For cell imaging of live cells, 35-mm glass bottom dishes (p35) from MatTek Corp. were used.

1.1.2 Electrophoresis and Western Blotting reagents

For protein separation through polyacrylamide gel electrophoresis (PAGE), electrophoresis purity acrylamide, N,N'-methylenebisacrylamide, ammonium persulfate, N,N,N',N'-tetramethylethylenediamine (TEMED), sodium dodecyl sulfate (SDS), glycine and Tris were acquired from Bio-Rad. For DNA separation, molecular biology grade agarose from Pronadisa was used for gels. Polyvinylidene fluoride (PVDF) Immobilon-P membranes were from Millipore, the bicinchoninic acid (BCA) Protein Assay Kit for measuring protein concentration in cell lysates was from Pierce and the enhanced chemiluminescence (ECL) detection system was from Amersham Biosciences.

1.1.3 Other reagents

High purity salts, buffers and other reagents used for preparing solutions were mainly from Sigma and Merck. Milli-Q distilled water was from Millipore. Lipofectamine 2000, Lipofectamine RNAiMax, Lysotracker Red (LTR), 7-amino-4-chloromethylcoumarin (CMAC, a.k.a. CellTracker Blue), scrambled siRNA and siRNA against Hrs or Tsg101 were from Life Technologies. Chloroquine, 2-bromopalmitate, phenylarsine oxide (PAO), dibromobimane (DBB), leupeptin, filipin, carbobenzoxy-L-

leucyl-L-leucyl-L-leucinal (Z-LLL, a.k.a. MG-132), C6 ceramide, dihydroceramide C6, and ethidium bromide were from Sigma. U18666A, simvastatin and zaragozic acid (ZGA) were from Merck. Cyto-ID Green Detection Reagent for autophagy monitoring and Lyso-ID Red Detection Reagent were from Enzo Life Sciences. All prostanoids were from Cayman Chemical. Human recombinant proteins were from Calbiochem-Novabiochem (H-Ras), Jena Bioscience (RhoB and K-Ras4B) or Abcam (N-terminal His-tagged Rap2B). GFP-Trap agarose beads were from ChromoTek.

1.2 Antibodies

Antibodies for immunoblotting were: Anti-RhoB (mainly sc-180 but also sc-8048), anti-RhoGDI (sc-360), anti-Rab7 (sc-10767), anti-ubiquitin (sc-8017), anti-Hsp90 (sc-7947), and anti-LAMP1 (sc-20011) from Santa Cruz Biotechnology; anti-Tsg101 from Abcam; antiserum against Hrs, as described in (Raiborg et al., 2001); anti-pan Ras (Ab-3) from Merck; anti-Rap2 form BD Biosciences; anti-GFP from Clontech or Roche; secondary anti-mouse and anti-rabbit Immunoglobulins (Ig) conjugated with horseradish peroxidase (HRP) from Dako. Streptavidin-HRP was from GE Healthcare Life Sciences. For immunofluorescence, anti-giantin from Covance and anti-rabbit 568 from Invitrogen were used.

1.3 Primers

The primers used for sequencing or to generate plasmids by mutagenesis or PCR were synthesized automatically at the Protein Chemistry Facility at CIB-CSIC in an Applied Biosystems 3400 synthesizer and purified in Sephadex G25, NAPTM columns from Amersham.

1.4 Plasmids

Small-scale plasmid DNA preparation was carried out using the High Pure Plasmid Isolation Kit from Roche whereas large-scale plasmid isolation was performed with the EndoFree Plasmid Maxi Kit from Qiagen. All restriction enzymes are from

Promega. Digestion products were separated by electrophoresis on 1% agarose gels with 5 ng/ml ethidium bromide in Tris-acetate-EDTA (TAE) buffer prior to visualization under UV light on a Gel-Doc XR Imaging System (Bio-Rad). DNA fragment purification from agarose gels was performed with the Geneclean Turbo Kit from MP Biomedicals. The LigaFast Rapid DNA Ligation System from Promega was used for plasmid ligation. In the case of point mutations, primer pairs were designed and used with the QuikChange II XL Site-Directed Mutagenesis Kit from Agilent Technologies. All plasmids were sequence verified at the DNA Sequencing Service, Secugen S.A. at CIB-CSIC.

1.4.1 Donated and commercial plasmids

The following plasmids were kindly provided by various colleagues:

- pcDNA3-HA-RhoB (Prof. G.C. Prendergast, Lankenau Institute for Medical Research, Wynnewood, PA)
- Lamp1-GFP (Prof. J. Lippincott-Schwartz, NIH, MD)
- GFP-Rab7 (Prof. C. Bucci, University of Copenhagen, Denmark)
- GFP-Vps4 WT and E334Q (Prof. P. Woodman, University of Manchester, UK)
- GFP-Rab5 (Prof. J. Bonifacino, NIH, MD)
- GFP-2xFYVE and mCherry-2xFYVE (Prof. H. Stenmark, Radium Hospital, Oslo, Norway)
- GFP-H-Ras (Dr. J.M. Rojas, ISCIII, Majadahonda, Spain)
- RFP-LC3 (Prof. T. Yoshimori, Research Institute for Microbial Diseases, Osaka, Japan)

Other plasmids were obtained from commercial sources:

- GFP-Rab11, GFP-Rab9A, GFP-Rap2A, GFP-Rap2B, GFP-CD63 (all in a pEZ-M29 backbone for N-terminal GFP fusion) and mCherry-CD63 (pEZ-M55 backbone) were from Genecopoeia.
- pEGFP-C1, pmCherry-C1 and pDendra2-C were from Clontech.
- pTagRFP-C was from Evrogen.

The following constructs were generated by Genewiz Inc. (South Plainfield, NJ) by oligonucleotide synthesis and cloning into parent vectors:

- GFP-CINCSKVL (GFP-8-C244S, isoprenylation defective GFP-8 mutant)
- GFP-SINSCKVL (GFP-8-C240,243S, palmitoylation defective GFP-8 mutant)
- tRFP-T-CINCSKVL (tRFP-T-8-C242S)
- tRFP-T-SINSCKVL (tRFP-T-8-C238,241S)
- GFP-HA-RhoB X (expressing RhoB from *Xenopus laevis*)
- tRFP-T-HA-RhoB X
- GFP-CINCCKVL Asp (GFP-8 for *Aspergillus nidulans* transformation using p1902 as template) (Pantazopoulou and Peñalva, 2009)
- GFP-SINSCKVL Asp (GFP-8-C239,242S, palmitoylation defective GFP-8 for *A. nidulans* transformation)

1.4.2 Previously generated plasmids

Using some of the plasmids above, several constructs were previously generated and described in publications from the Pérez-Sala laboratory and colleagues:

- pEGFP-C1-HA-RhoB WT (GFP-RhoB) (Stamatakis et al., 2002)
- pcDNA3.0-GFP-CINCCKVL (GFP-8), GFP plus the last 22 amino acids of RhoB (GFP-22), and GFP-CINCCLIT (GFP-8-TC10, from the TC10 C-terminus) (Pérez-Sala et al., 2009)
- pTagRFP-RhoB (tRFP-RhoB) and pTagRFP-CINCCKVL (tRFP-8), tRFP plasmids containing a S162T mutation to improve photostability (Shaner et al., 2008): tRFP-T-RhoB and tRFP-T-8, as well as the triple mutants of GFP-HA-TC10 (K194N, K195Q, H196N; GFP-TC10-NQN) and GFP-HA-RhoB (insertion of KKH after L179, GFP-RhoB-KKH) (Valero et al., 2010)

1.4.3 Plasmids generated for this work

1.4.3.1 mCherry-8

Analogously to GFP-8, pmCherry-CINCCKVL was generated as described (Pérez-Sala 2009) using pmCherry-C1 as a template, by attaching the last eight amino acids of RhoB, a stop codon, and an EcoRI site to the C-terminus of mCherry cDNA by PCR with the following forward and reverse primers, respectively:
5'-GAGTAGAAGCTTATGGTGAGCAAGGGCGAGGAG-3'
5'-CCGAATTCTAGAGGACCTTGCAACAGTTGATACACTTGTACAGCTCGTC-CATGC-3'
PCR products were digested with HindIII and EcoRI and cloned into pcDNA3.0.

1.4.3.2 pDendra2-CINCCKVL (Dendra-8)

Analogously to mCherry-8, pDendra2-8 was generated using pDendra2-C as a template, by attaching the last eight amino acids of RhoB and an EcoRI site to the C-terminus of Dendra2 cDNA by PCR with the following forward and reverse primers, respectively:
5'-GCGCTAGCTCGAGGTACCGC-3'
5'-CCGAGCTCTAGAGGACCTTGCAACAGTTGATACACCACACCTGGCTGG-3'
PCR products were digested with HindIII and EcoRI and cloned into pDendra2-C.

1.4.3.3 mCherry-HA-RhoB

The cDNA of HA-RhoB was obtained from pEGFP-HA-RhoB by digestion with BglII and EcoRI. The fragment was purified and ligated with pmCherry-C1 previously digested with the same restriction enzymes.

1.4.3.4 Plasmids generated by site-directed mutagenesis

- *pEZ-mCh-CD63 Y235A and pEZ-GFP-CD63 Y235A:* Mutation of the YXXΦ motif tyrosine in CD63 was performed in both pEZ-mCherry-CD63 and pEZ-GFP-CD63 WT plasmids using the following oligonucleotides:
  5'-CTCGAGCTACATCACCTCGGC**GC**CACTTCTGATACTCTTC-3'
  5'-GAAGAGTATCAGAAGTG**GC**GCCGAGGTGATGTAGCTCGAG-3'

2. Methods

2.1 Cell culture

The following cell lines were used throughout this work and cultured as described:

- HeLa adenocarcinoma cells from the American Type Culture Collection (ATCC) were cultured in DMEM supplemented with 10% FBS, 100 U/ml penicillin and 100 µg/ml streptomycin at 37°C in an atmosphere with 5% CO_2.
- Bovine aortic endothelial cells (BAEC) were obtained from Lonza and cultured in RPMI1640 medium supplemented with penicillin/streptomycin and 10% calf serum at 37°C, 5% CO_2. BAEC were used between passages 5 and 12 and were grown to near confluence for experiments.
- Human primary fibroblasts from healthy subjects (AG09309 and AG10803), CHS patients (GM02075), NPC1 patients (GM03123) and HPS-2 patients (GM17890) were obtained from the NIGMS Human Genetic Cell Repository at the Coriell Institute for Medical Research, cultured in DMEM supplemented with 10% FBS and penicillin/ streptomycin at 37°C, 5% CO_2 and used up to passage 20.
- *Xenopus laevis* A6 cells were obtained from Sigma and cultured at 28°C in NCTC 109 medium supplemented with 15% distilled H_2O, 2 mM glutamine, 10% FBS and penicillin/ streptomycin.

- High Five cells, derived from ovarian cells of the cabbage looper *Trichoplusia ni*, were from Invitrogen. These cells were cultured at 28ºC in TC100 medium supplemented with 10% FBS, penicillin/ streptomycin and 10 μg/ml gentamycin.

All cell lines were passaged by trypsin-EDTA detachment, complete medium wash and centrifugation at 1000xg for 5 min, suspension in fresh medium, and plating at the desired dilution.

2.1.1 *Aspergillus nidulans* culture

Aspergillus nidulans was cultured in complete medium (MCA) or synthetic complete medium (SC) containing 1% glucose and 5 mM ammonium tartrate (i.e. 10 mM NH^{4+}) as carbon and nitrogen sources, respectively. GFP-8 and GFP-8-C239S,C242S were expressed under the control of the gpdAmini promoter, using a single-copy integration construct targeted to pyroA, as described previously (Pantazopoulou and Peñalva, 2009).

Strains used in this work:

- MAD690: yA2; argB2::[argB*-alcA^{p}::GFP]; pantoB100
- MAD4689: wA2; pyroA4::[pyroA*-gpdAmini::GFP-8]; pantoB100
- MAD4688: wA2; pyroA4::[pyroA*-gpdAmini::GFP-8-C239S,C242S]; pantoB100

2.2 Cell treatments

Treatments with the various agents described in each section were performed in the absence of serum, unless otherwise stated. As has been described for BAEC, this situation induces a near-quiescent state and does not reduce cell viability (Hernández-Perera et al. 1998). Control cells received an equivalent amount of vehicle as required.

- Inhibition of GTPase isoprenylation was elicited by treatment with 10 μM simvastatin for 24 h.

- Palmitoylation was inhibited using 2-bromopalmitate (2-BP) at 20 μM for 6 h.
- In order to disrupt the endolysosomal pathway, cells were treated with 10 μM chloroquine or U18666A for 20 h.
- For proteasome blockage, Z-LLL at 5 μM was used for 24 h.
- For cholesterol depletion, ZGA was added at 50 or 100 μM for 24 h, as indicated.
- Secretion was induced by treatment with C6 ceramide at 10 μM for 24h, using dihydroceramide C6 at the same concentration as control.
- For induction of autophagy, cells were incubated in amino acid-free medium (EBSS) for the times indicated. All further treatments and staining procedures were performed also in this medium to avoid autophagy reversion.

2.3 Transient transfections

Transient cell transfection was carried out at 80% confluence with Lipofectamine 2000 following the instructions of the manufacturer, i.e. using 1 μg of DNA and 3 μl (single transfections) or 4.5 μl (double transfections) of Lipofectamine per p35 dish. Unless otherwise indicated, after transfection, cells were allowed to recover for 24 h in complete medium before treatment with the indicated agents in the absence of serum. Imaging of live cells or biochemical analysis was performed 48 h after transfection to minimize its effects.

2.4 Cell lysis

2.4.1 Lysis of mammalian cells

In preparation for SDS-PAGE, cells were homogenized by forced passes through a 26½-gauge needle in lysis buffer containing 50 mM Tris, pH 7.5, 0.1 mM EDTA, 0.1 mM EGTA, 0.5% SDS, 0.1 mM β-mercaptoethanol, 50 mM sodium fluoride and 0.1 mM sodium orthovanadate with 2 μg/ml of the protease inhibitors leupeptin and aprotinin as well as 1.3 mM Pefabloc prior to boiling at 95°C for 5 min. Lysates for subcellular fractionation were obtained in the same buffer, without SDS. Alternatively, cells were scraped with a rubber scraper and directly lysed in Laemmli sample buffer

containing the protease and phosphatase inhibitors mentioned above by boiling at 95ºC for 5 min prior to gel loading.

For immunoprecipitation procedures, cells were lysed in radioimmunoprecipitation assay (RIPA) buffer, i.e. 10 mM Tris/Cl pH 7.5, 150 mM NaCl, 0.5 mM EDTA, 0.1% SDS, 1% NP-40, 0.5% deoxycholate plus protease and phosphatase inhibitors.

2.4.2 *Aspergillus nidulans* lysis

Total protein extracts of the *A. nidulans* strains used in this work were obtained from 200-250 mg of mycelium filtered through Miracloth (22-25 μm pore), drained, frozen in dry ice and lyophilized. The lyophilized mycelium was ruptured by a 10 second pulse in the FP120 Fast Prep Cell Disruptor (BIO101/Savant) at 4ºC using a 0.55 cm ceramic sphere. Pulverized mycelium was resuspended in alkaline lysis buffer containing 0.2 M NaOH and 0.2% β-mercaptoethanol. Proteins were precipitated by adding trichloroacetic acid to 7.5% and incubation on ice for 10 min. Samples were centrifuged at 14000 rpm for 5 min at 4 ºC and the resulting pellet was neutralized with Tris Base at 1 M. Laemmli sample buffer with protease inhibitors was added to samples, which were vortexed and boiled at 100ºC for 2 min prior to loading on 12.5% polyacrylamide gels containing 0.1% SDS.

2.5 Western blotting (WB)

Protein concentration was estimated by the BCA method. Volumes equivalent to 20 μg of protein were run on 12.5 or 15% SDS-polyacrylamide electrophoresis gels and transferred to Immobilon-P membranes using a semi-dry, Whatman filter-based method. The proteins of interest were visualized using an ECL detection system. Protein levels were estimated by image scanning of the ECL exposures and their values were corrected by the band intensities of the signal given by an antibody against a non-related protein, where indicated. Blots were quantified using ImageJ software (US National Institutes of Health, Bethesda, MD, USA).

Direct binding of DBB to recombinant proteins was assessed by visualization of the gel under UV light on a Gel-Doc XR Imaging System (Bio-Rad), as described (Sinz and Wang, 2001). Unbound DBB, which is essentially non-fluorescent, becomes fluorescent upon cysteine cross-linking (excitation maximum=385 nm, emission=477 nm).

2.6 Subcellular fractionation

For S100/P100 fractionation, total cell lysates were obtained by disrupting cells in the detergent-free buffer described above. Lysates were centrifuged at 1000xg for 5 min at 4 °C. Post-nuclear supernatants were further subjected to ultracentrifugation at 100,000xg for 1 h at 4 °C to obtain soluble and membrane cellular fractions. Supernatants (S100) were collected and pellets (P100) were resuspended in lysis buffer containing 1% NP-40 and 0.1% SDS. These fractions were loaded onto gels for WB, as described above.

2.7 Gene knock-down using siRNA

HeLa cells were depleted of ESCRT components the day after plating by transfection with 75 nM Hrs siRNA or 25 nM Tsg101 siRNA, and control cells were transfected with 50 nM scrambled (scr) siRNA using Lipofectamine RNAiMax according to the manufacturer's instructions. Cells were re-plated after 3 days, transfected with fluorescent constructs and grown for an additional 2 days before either live microscopy visualization or cell lysis and WB.

The following siRNA sequences were used:

Hrs: 5'-CGACAAGAACCCACACGUC-3'
Tsg101: 5'-CCGUUUAGAUCAAGAAGUAUU-3'

Scrambled siRNA was a double-stranded 21-mer RNA that does not correspond to any sequence encoded in the human genome.

2.8 Pull-down assays

GFP fusion proteins were immunoprecipitated using GFP-Trap agarose beads. After the described lysis, incubation with GFP-Trap took place for 1 h at 4°C. Beads were washed three times with detergent-free lysis buffer and eluted with Laemmli sample buffer for 10 min at 95°C. WB was performed on non-bound (not shown) and eluates as well as total lysates to assess protein retention.

2.9 Live cell microscopy

2.9.1 Confocal microscopy

For live visualization, cells were cultured on glass-bottom dishes, transfected with fluorescent constructs, treated with the indicated agents and visualized directly on a confocal microscope, either Leica DMRE2, Leica SP5 or Zeiss LSM 810 equipped with 405, 488, 568 and 642 nm diode lasers. Unless otherwise stated, images shown are single channels or overlays of single Z-sections for co-localization visualization. All experiments were repeated at least three times and representative results are shown. Scale bars represent 20 μm.

For live lysosome tracking, cells were stained with 25 nM LTR for 15 min at 37°C. When staining with other lysosomal or autophagosomal probes such as Lyso-ID or Cyto-ID, images were obtained shortly after staining to minimize loss of fluorescence. Care was taken to briefly observe cells under the UV lamp before imaging to minimize fading of the probes. Lyso-ID and Cyto-ID were diluted in the total volume of serum-free culture medium to be used for staining at 37 °C for 30 min to maintain endothelial cell morphology and viability during cell imaging. In experiments in which autophagy was induced by incubation of cells in EBSS, staining and washing (for autophagy reversion experiments) was also performed in this medium. In the case of Cyto-ID/LTR co-staining, LTR was added to the medium of cells that had been incubated with Cyto-ID for 15 min, left for an additional 15 min to co-stain and visualized immediately afterwards.

2.9.2 Super-resolution microscopy

In vivo super-resolution 3D structured illumination microscopy (SIM) imaging was performed on a Deltavision OMX V4 system (Applied Precision, GE Healthcare) equipped with an Olympus 60x NA 1.42 objective, cooled sCMOS cameras and 405, 488, 568 and 642 nm diode lasers. Z-stacks covering the whole cell were recorded with a Z-spacing of 125 nm. A total of 15 raw images (5 phases, 3 rotations) per plane were collected. Reconstruction and alignment of these raw images was performed using Softworx software (Applied Precision, GE Healthcare company).

2.9.3 Photoswitchable fluorescent protein tracking

Dendra-8 photoswitching and isoprenylation inhibition-and-release experiments were performed on transfected BAEC on glass-bottom dishes. The transfection medium was removed after 5 hours and replaced with serum-free medium with or without 10 μM simvastatin. Cells were observed 24 hours post-treatment on the Leica SP2 confocal microscope and photoswitching was performed by exposure to 405 nm UV light. The resulting green-to-red conversion was recorded in both channels. Simvastatin was either added or removed to the corresponding dishes in serum-free medium and photoconverted, red Dendra-8 was tracked 24 hours later by confocal microscopy.

2.9.4 *Aspergillus nidulans* microscopy

For microscopy experiments in *Aspergillus*, hyphae were cultured in Lab-Tek chambers (Thermo Fischer Scientific, 115411; 0.3 ml of medium per well) at 25–28°C in pH 6.5 'watch minimal medium' (WMM) containing 100 mM sodium acetate and 5 mM ammonium tartrate as carbon and nitrogen sources, respectively. Hyphae were visualized on an inverted fluorescence microscope (Leica DMI6000B) equipped with an EL6000 external light source with metal halide lamp epifluorescence excitation, driven by Metamorph® software (Molecular Dynamics) and coupled to a CCD camera (ORCA ER-II; Hamamatsu). Vacuoles were detected with CMAC.

2.9.5 Image analysis

Co-localization analysis was performed with LAS-AF software from Leica on single z-sections of images to obtain co-localization rates (expressed as percentages) and Pearson coefficients (coefficient r x 100). Alternatively, ImageJ (Fiji) software was used to obtain Pearson coefficients. At least 30 cells were analyzed per experimental condition. For stained cells, whole-field images were analyzed, whereas in the case of transfected cells, regions of interest (ROI) including transfected cells and excluding non-transfected cells were delimited prior to image analysis. Results are presented as mean co-localization rates or Pearson coefficients ± standard error of mean (SEM).

2.10 Immunofluorescence

For immunofluorescence with anti-giantin antibody, cells grown on glass bottom p35 were fixed in 4% paraformaldehyde for 20 min at room temperature (r.t.), washed twice in PBS and permeabilized with 0.05% saponin in PEM buffer (80 mM PIPES, 5 mM EGTA, 1 mM $MgCl_2$ pH 6.8) for 5 min. Incubation with anti-giantin at 1:500 dilution was carried out in PBS containing 0.05% saponin for 1h. After PBS washes, cells were incubated with anti-rabbit-Alexa 568 at 1:200 in 1% BSA in PBS for a further hour.

For filipin staining, fixed cells were washed 3× with PBS, incubated with 1.5 mg/mL glycine in PBS for 10 min at room temperature and subsequently with 0.05 mg/mL filipin in 10% normal goat serum in PBS for 2 h.

2.11 Mass spectrometry

Full-length H-Ras or RhoB protein or the H-Ras K170-K185 peptide were incubated at 5 μM in the presence of prostanoids, DBB or PAO at 50 μM or vehicle (DMSO) for 1 h. For some experiments, full-length protein incubation mixtures were then subjected to digestion with trypsin for 4 h at 37°C. Purification on ZipTip C18 (Millipore) was carried out prior to MALDI-TOF MS analysis on an AUTOFLEX III MALDI-TOF-TOF instrument (Bruker-Franzen Analytik) operated in the positive

mode, as reported in detail (Renedo et al., 2007). Selected peptides were further analyzed by MALDI-TOF-TOF MS-MS.

2.12 Statistical analysis

Data for WB quantification or co-localization analysis is shown as mean ± SEM of at least three independent experiments. Statistical significance was calculated by Student's *t* test for unpaired observations. A p value of less than 0.05 was considered significant and marked by asterisks, where indicated.

RESULTS

1. Structural determinants involved in RhoB endolysosomal localization

1.1 Subcellular localization of endosomal GTPases

Previous studies from the laboratory explored the subcellular localization of the small GTPase RhoB, as well as the pathways responsible for its degradation. In endothelial cells, RhoB is degraded through a lysosomal pathway, as discerned by treating cells with selective inhibitors of the major degradation pathways prior to protein analysis and microscopy studies (Pérez-Sala et al., 2009). Experiments with specific organelle markers using fluorescent RhoB fusion constructs showed RhoB association with late endosomal compartments, though their precise nature elicited further studies that are included within this section.

1.1.1 RhoB localization at endolysosomes

Several reports have shown that RhoB has a varied cell-type, activation- and lipidation-state dependent subcellular localization that comprises the plasma membrane, Golgi apparatus, early or late endosomes, MVB and lysosomes (Michaelson et al., 2001; Pérez-Sala et al., 2009; Rondanino et al., 2007; Wherlock et al., 2004). Therefore, studies were performed to define the basal subcellular localization of this GTPase under varying conditions in different cell types, as well as the structural determinants that elicit this pleiotropic distribution (Pérez-Sala et al., 2009; Valero et al., 2010). In order to do so, several fluorescent constructs of wild-type RhoB, i.e. GFP-RhoB, tRFP-T-RhoB, and mCherry-RhoB were transiently transfected into cells such as BAEC, human primary fibroblasts, HeLa cells, and others.

In BAEC, GFP-RhoB as well as a variety of specific organelle markers was employed to outline the subcellular fate of this GTPase, as shown in Figure 12. Cells were treated with the amphiphilic amino-steroid, U18666A, as a pharmacological tool to alter late endocytic lipid dynamics and induce membrane invagination into MVB, which results in enlarged endolysosomes (Marchetti et al., 2004; Sobo et al., 2007).

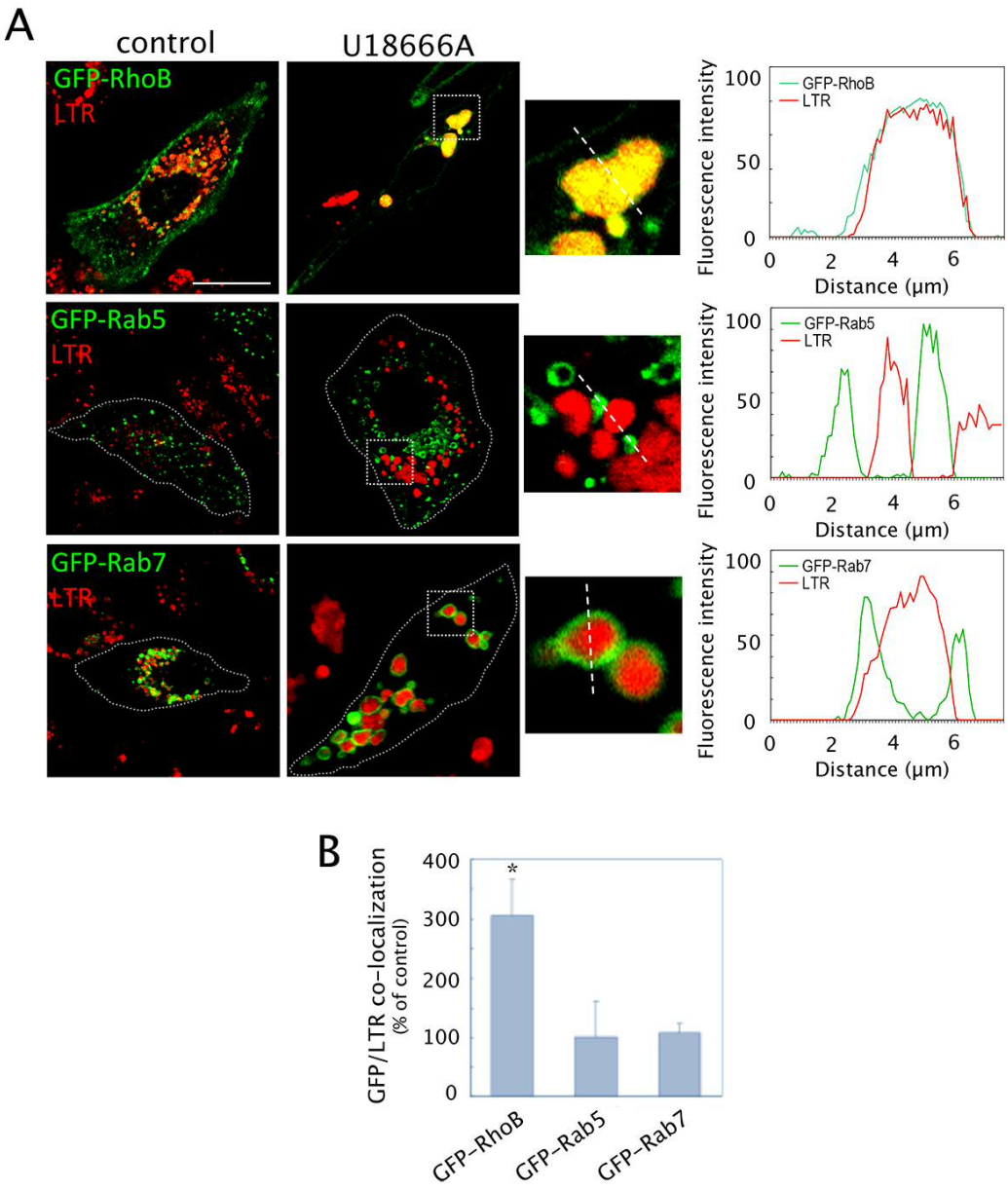

Figure 12. Subcellular distribution of GTPases following U18666A treatment.

(A) BAEC transfected with the indicated constructs were treated with U18666A as described in Methods, stained with LTR and observed live by confocal microscopy. Insets show zoom-ins of areas with dashed lines, from which profiles are derived (right panels). (B) GFP and LTR co-localization in U18666A-treated cells is used as an indicator of internalization into acidic compartments, expressed as percentage of the values compared to untreated cells. *p < 0.05 versus the same condition in the absence of U18666A.

Staining of the endolysosomal lumen is commonly performed using LysoTracker® Red (LTR), which is a widely used cationic amphiphilic drug that marks acidic compartments (Chazotte, 2011). GFP-RhoB amply co-localizes with this probe in many cell types including BAEC (Figure 12), particularly after treatment with U18666A.

In sharp contrast, a fusion protein of the early endosomal Rab5 (Bucci et al., 1992), used to mark membranes of early endosomes, does not appear at dilated endolysosomes induced by U18666A, as shown in Figure 12 by its lack of co-localization with LTR. In line with the above results, GFP-Rab5 does not co-localize with RhoB constructs (Pérez-Sala et al., 2009). However, fluorescently tagged Rab7, which has been shown to accumulate at late endocytic vesicles (Bucci et al., 2000), is present on endolysosomes, though retained at their limiting edge (Figure 12A, see profiles). As summarized from several works in Figure 13, endolysosomes containing RhoB constructs are also marked by late endocytic markers such as GFP-Rab9, Lamp1-GFP, LBPA, or cholesterol, but not considerably by the recycling endosome component, GFP-Rab11 (Patterson and Lippincott-Schwartz, 2002; Pérez-Sala et al., 2009; Ullrich et al., 1996; Valero et al., 2010).

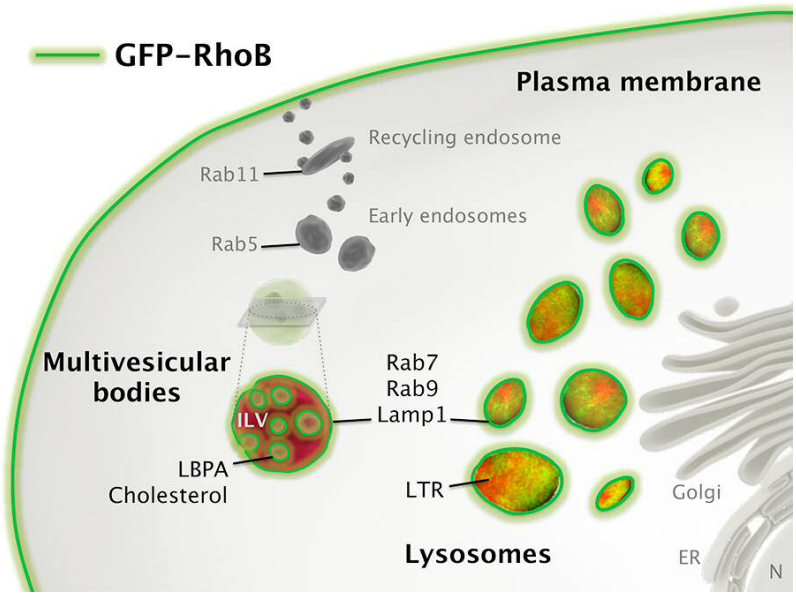

Figure 13. Schematic summary of GFP-RhoB subcellular localization.

A summary of previous work is shown here for conciseness. Full-length RhoB tagged with GFP is present at localizations depicted in green but not at those in gray. An orthogonal section of a model MVB shows its luminal content, where GFP-RhoB co-localizes with LBPA antibodies and cholesterol (stained by filipin). Likewise, the limiting membranes of both MVB and lysosomes have been found to be marked by fluorescent constructs of Rab7, Rab9 and Lamp1 that coincide with the presence of GFP-RhoB. In the lumen of MVB and lysosomes, LTR is found to co-localize with GFP-RhoB, eliciting a patchy, yellowish, red-to-green varied coloration. However, RhoB constructs tend not to overlap with the early endosomal component Rab5 or with Rab11 residing at recycling endosomes. See text for further details. ER, endoplasmic reticulum; N, nucleus.

Making use of these varied protein and lipid markers, it becomes evident that RhoB constructs appear at very specific subcellular sites, namely late endocytic vesicles such as MVB, as well as the lysosomal lumen, with varying degrees of plasma membrane localization (Figure 13).

1.1.2 Small GTPase C-terminal sequences in subcellular localization

Previous studies from our group established that RhoB degradation *via* the endolysosomal pathway is dependent on the full lipidation of its hypervariable C-terminus, i.e. isoprenylation and bipalmitoylation (Pérez-Sala et al., 2009; Stamatakis et al., 2002). However, several other small GTPases are similarly modified by these three lipids at their C-terminal sequences, as shown in Table 3, namely TC10, H-Ras, Rap2A or Rap2B.

Ras GTPase	C-terminal sequence
RhoB	-VREVF-ETATRAAL--------QKRYGSQNGCINCCKVL
TC10	-LKTVFDEAIIAILTP-KKH---TVKKRIGSRCINCCLIT
H-Ras	-VEDAFYTLV-REIRQHKLRKLNPPDESGPGCMSCKCVLS
Rap2A	-VDELFAEIV-RQMNY-------AAQPDKDDPCCSACNIQ
Rap2B	-VDELFAEIV-RQMNY-------AAQPNGDEGCCSACVIL

Table 3. C-terminal sequences of isoprenylated and bipalmitoylated GTPases.

Hypervariable regions of several small GTPases that are isoprenylated at their CAAX cysteine, shown in green, and palmitoylated at two other cysteines further upstream, shown in red. Residues removed by CAAX box proteolysis are shown in gray and basic residues are depicted in blue.

The spacing of cysteines amenable to lipidation, as well as the nature of the amino acids between them, differs among these proteins (Table 3). To explore the subcellular destination of these GTPases, fluorescent constructs were expressed in BAEC and observed by confocal microscopy. Figure 14 shows the localization of these constructs under basal conditions and upon treatment with U18666A compared to that of GFP-RhoB. An H-Ras construct shows predominant plasma membrane localization instead of accumulation at endolysosomes (Figure 14). This behavior could be due to the fact that the two amino acids between the palmitoylatable cysteines in H-Ras are

different than those of RhoB. In the case of Rap2 proteins, they become palmitoylated at contiguous cysteines, whereas RhoB contains two amino acids that separate these cysteines. As shown in Figure 14, this sequence elicits GFP-Rap2B accumulation at the limiting membrane of dilated endolysosomes, resulting in lower co-localization with LTR compared to GFP-RhoB. Therefore, though these GTPases are all isoprenylated and bipalmitoylated, differences in their lipidation sequences or other determinants could confer differential subcellular localization.

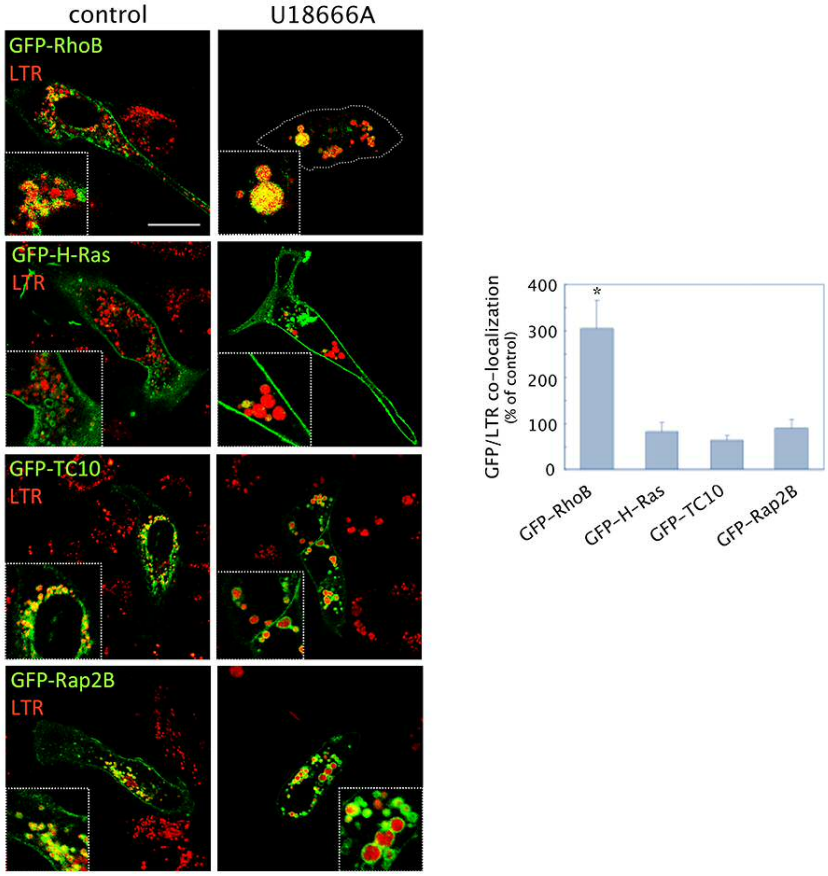

Figure 14. Localization of isoprenylated and bipalmitoylated GTPases.

BAEC transfected with the indicated constructs were treated as in Figure 12. Zoom-ins are shown in the insets. Co-localization of GFP and LTR signals was assessed as in Figure 12. *p < 0.05 versus the same condition in the absence of U18666A by Student's t-test.

RhoB and TC10 are highly homologous proteins (68% homology, 52% identity) with obvious differences in the –AAX amino acids of the CAAX box, as well as in the hypervariable region, with more basic residues present in TC10 but not RhoB. Nevertheless, their lipidation sequences are highly similar. Remarkably, when

comparing these proteins, TC10 is retained at the limiting membrane of late endocytic vesicles, instead of inside their lumen, as seen for RhoB constructs (Figure 14).

In order to study the structural determinants responsible for the differences observed between TC10 and RhoB constructs, protein chimeras of GFP fused to the last eight amino acids of these GTPases at its C-terminus were generated. Taking into account that the last three amino acids of these sequences would be cleaved after isoprenylation, the remaining sequences would be identical, as seen in Table 3. Moreover, since both CAAX boxes can undergo isoprenylation by either farnesyl or geranylgeranyl, the resulting lipidated chimeric proteins could become completely alike. Therefore, the chimeric proteins GFP-CINCCKVL (a.k.a. GFP-8, derived from RhoB, extensively described in the next section) and GFP-CINCCLIT (referred to as GFP-8-TC10) become identical once the cysteines have been lipidated. Indeed, as shown in Figure 15, the localization patterns of GFP-8 and GFP-8-TC10 are indistinguishable both in control cells and after U18666A treatment.

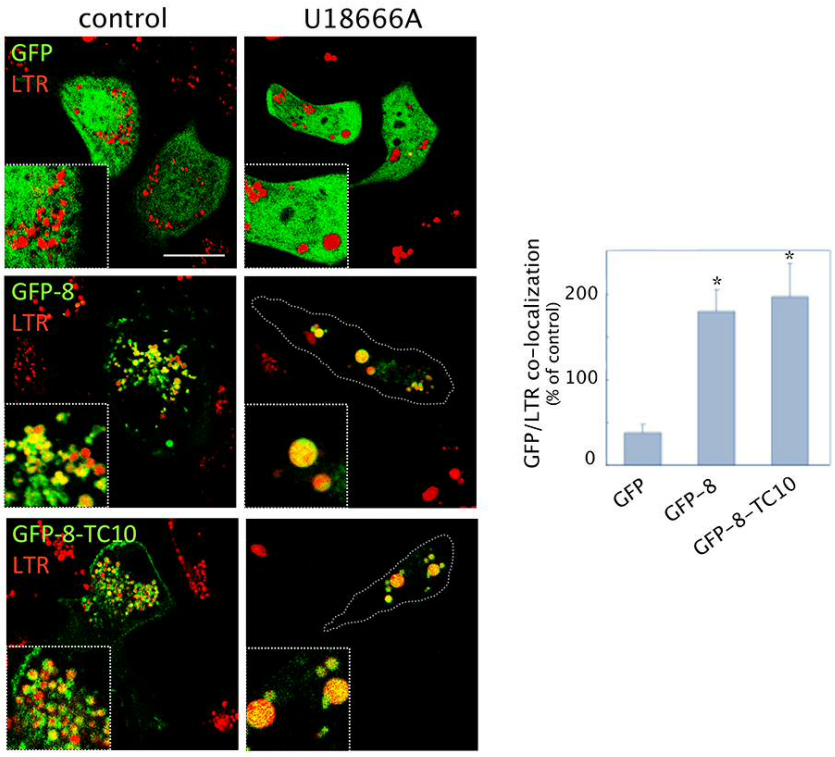

Figure 15. Localization of chimeric proteins derived from the RhoB or TC10 C-terminus.

BAEC were transfected with constructs obtained by fusing the last eight amino acids of RhoB (GFP-8) or TC10 (GFP-8-TC10) to the C-terminus of GFP, treated with U18666A, stained with LTR and visualized live by confocal microscopy. The graph shows GFP and LTR co-localization, as above. *$p < 0.05$ versus the same condition in the absence of U18666A.

In light of the results above, the TC10 sequence must contain a sorting motif upstream of these last amino acids that is responsible for full-length TC10 accumulation at the limiting membrane of MVB, as opposed to GFP-8-TC10 predominant localization inside endolysosomes. Indeed, TC10 contains a basic amino acid patch, "-KKH", that hinders its entry into the lumen of late endocytic compartments (Table 3). As seen in Figure 16, mutation of the basic amino acid patch in TC10 (TC10 NQN, Figure 16A) promotes entry into the endolysosomal lumen, as reflected by a significant increase in co-localization with LTR upon U18666A treatment (Figure 16C). Conversely, insertion of the basic amino acid patch into the RhoB sequence (RhoB KKH, Figure 16A) retains this chimera at the limiting membrane of endolysosomes (Figure 16B).

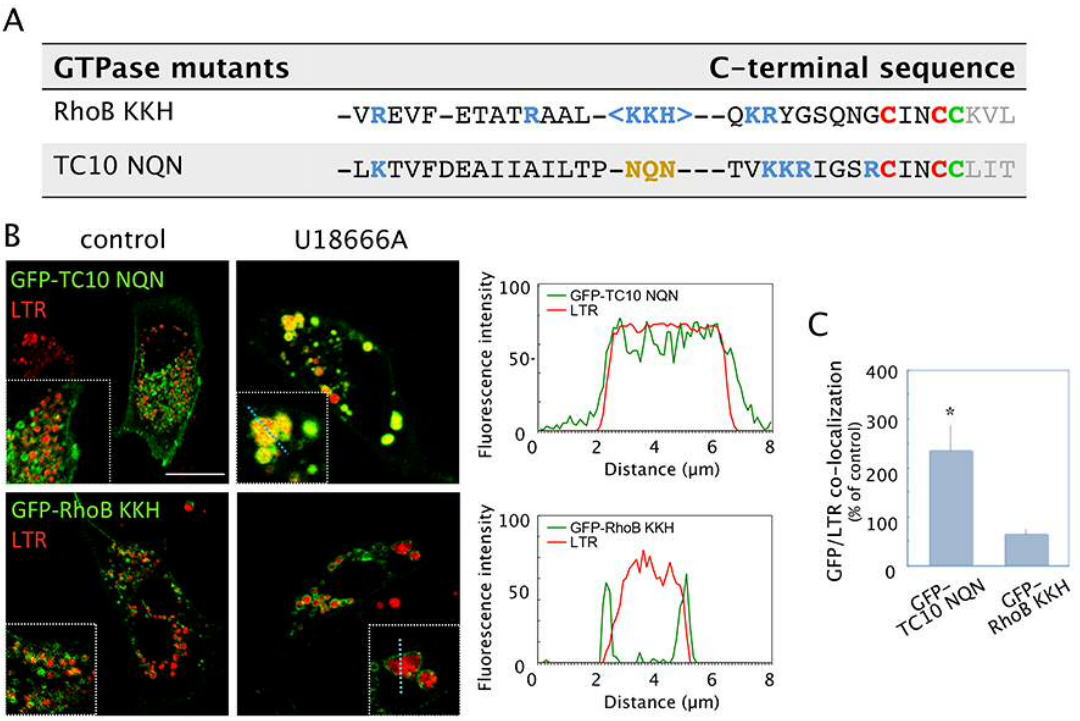

Figure 16. Role of basic residues in the hypervariable regions of TC10 and RhoB in subcellular localization.

(A) Sequences of the GTPase mutants generated by introducing either a basic residue patch (blue, in brackets) into RhoB (RhoB KKH) or a neutral amino acid patch (in yellow) into TC10 (TC10 NQN). Isoprenylation cysteines are shown in green and palmitoylation cysteines in red. (B) BAEC transfected with the indicated constructs were treated as above. Insets show zoom-ins of areas with dashed lines, from which profiles are derived (right panels). (C) GFP and LTR co-localization in U18666A-treated cells was assessed as above. *$p < 0.05$ versus the same condition in the absence of U18666A.

Therefore, fine-tuned regulation of small GTPase subcellular localization is determined by isoprenylation or palmitoylation cysteines and charged or uncharged amino acids positioned at strictly specific positions within their hypervariable C-terminal regions. The basic amino acids in TC10 "rescue" the protein from lysosomal degradation. Since this motif is not present in RhoB, it is constitutively sent towards the lysosome. However, posttranslational modifications altering the charge or the interactions of the hypervariable sequence of RhoB could hinder its entry into the degradative compartments and change its localization and/or degradation patterns.

1.2 RhoB C-terminus: CINCCKVL

1.2.1 Co-localization with endocytic markers

Studies from the laboratory using BAEC and chimeric fluorescent proteins bearing sequentially smaller parts of the RhoB sequence at their C-terminal end, from the last 22, 8 to 4 amino acids, determined that the minimum sequence eliciting endolysosomal localization and degradation corresponds to the motif that includes all three lipidated cysteines and the –CAAX box, namely –CINCCKVL (GFP-8) (Pérez-Sala et al., 2009). Since subcellular localization mechanisms are finely regulated and may be cell type-dependent, localization of GFP-8 was studied in greater detail in several additional cell types.

As shown in Figure 17, in human primary fibroblasts under resting conditions, co-transfection of tRFP-T-CINCCKVL (tRFP-T-8) with the fluorescent constructs of several endocytic components highlighted the appearance of tRFP-T-8 inside vesicles surrounded by GFP-Rab7 and Lamp1-GFP. Only marginal co-localization of tRFP-T-8 was observed with GFP-Rab11, which is used as a recycling endosome marker (Ullrich et al., 1996). Co-localization with the early endosome marker, GFP-Rab5 was negligible. Therefore, as seen for GFP-8 in BAEC, tRFP-T-8 in human fibroblasts displays a predominantly luminal endolysosomal localization, as deduced from the profiles in Figure 17.

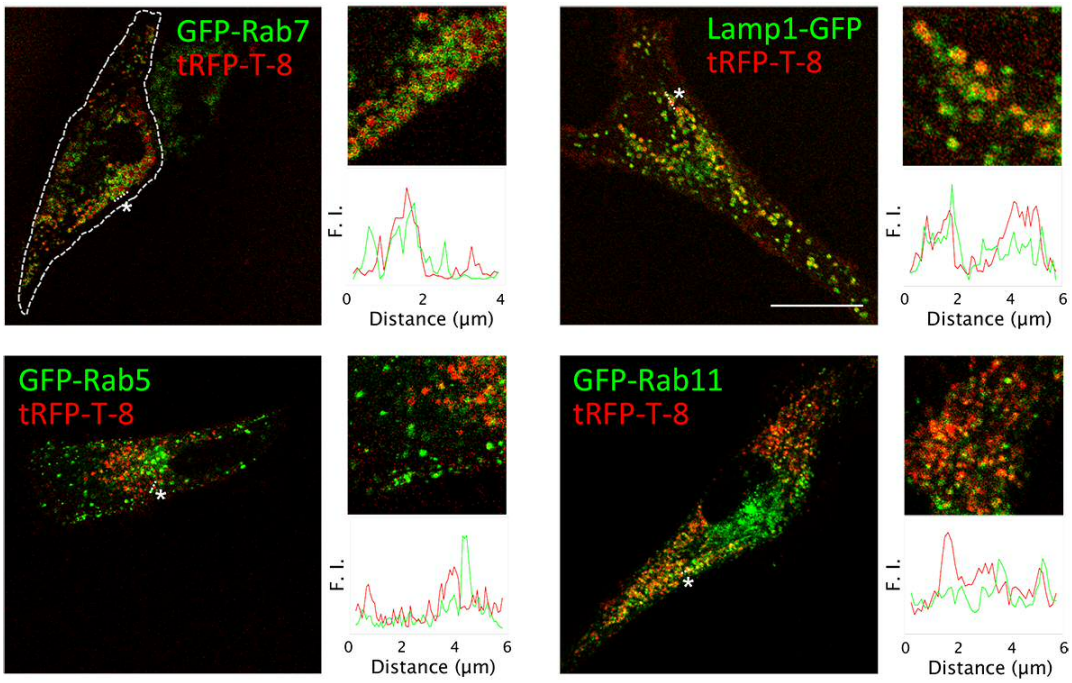

Figure 17. Localization of CINCCKVL chimeras in human primary fibroblasts

Human primary fibroblasts were co-transfected with tRFP-T-8 and the indicated endocytic membrane markers and observed live by confocal microscopy after 16 h in serum-depleted medium. Zoom-ins of original pictures and fluorescence intensity profiles along a section (marked by dotted lines and asterisks) appear to the right of every condition. F.I., fluorescence intensity.

The association of CINCCKVL chimeras with endolysosomal compartments was also confirmed in the widely used human adenocarcinoma cell line, HeLa. Similarly to the results shown in primary fibroblasts, tRFP-T-8 appeared inside Lamp1-GFP-positive vesicles in this cell line (Oeste et al., 2014). The specific localization of CINCCKVL chimeras in the context of endolysosomes was further pinpointed by co-transfecting HeLa with GFP-8 and the mCherry fluorescent construct of CD63, which is used as a marker of ILV of MVB. As described in the Introduction, different populations of ILV could exist within MVB (Edgar et al., 2014). However, the resolution provided by confocal microscopy is not able to discern discrete ILV, so that localization at these small vesicles appears as luminal fluorescence within endolysosomes. As seen in Figure 18, of all the probes and fluorescent proteins used to characterize CINCCKVL chimeras, mCherry-CD63 displayed the highest degree of co-localization (Pearson coefficient = 0.77 ± 0.015).

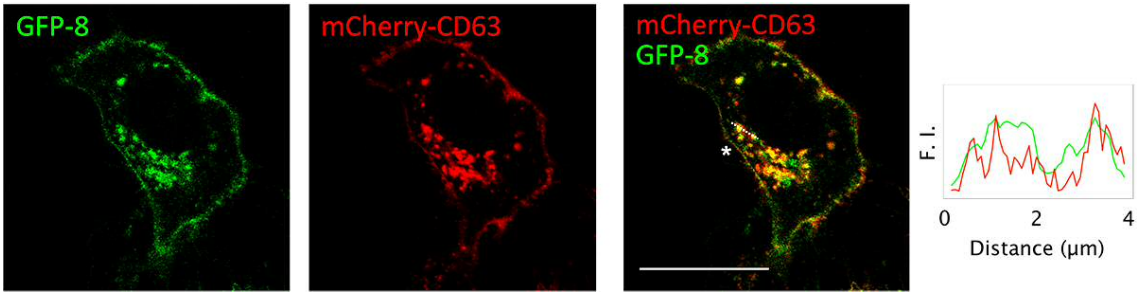

Figure 18. GFP-8 co-localization with the MVB marker, mCherry-CD63.

HeLa cells were co-transfected with GFP-8 and mCherry-CD63 and cultured in serum-depleted medium for 16 h prior to live confocal fluorescence microscopy. Fluorescence intensity profiles along a section (marked by dotted lines and asterisks) appear to the right of the overlay. F.I., fluorescence intensity.

A closer look at these specific structures was obtained using higher resolution *in vivo* three-dimension structured illumination microscopy (SIM), which provides super-resolution imaging, as seen in Figure 19.

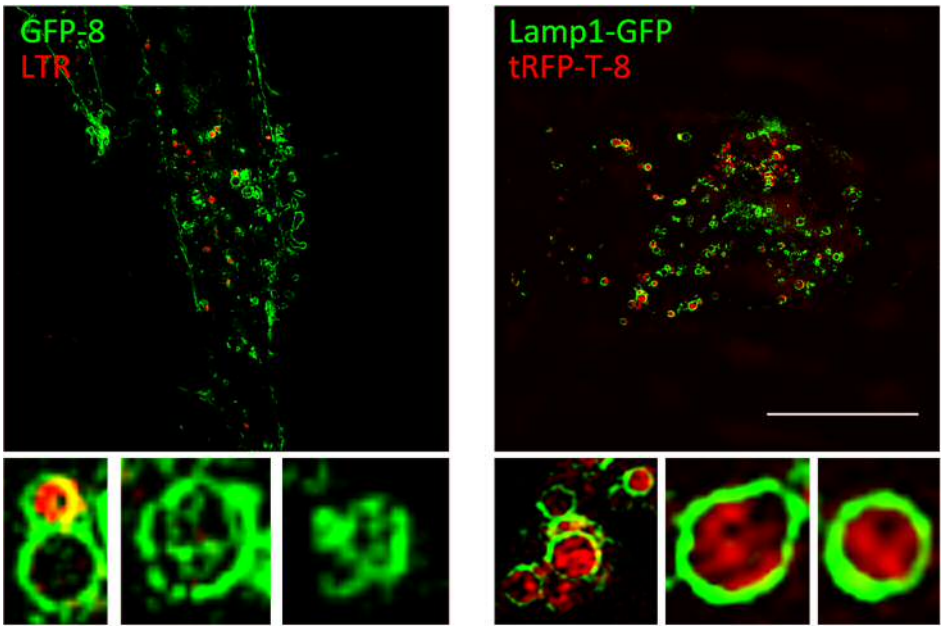

Figure 19. Super-resolution imaging of CINCCKVL chimeras.

HeLa cells were transiently transfected with the indicated constructs and stained with LTR as indicated in the Methods section, prior to live super-resolution microscopy. Lower panels show zoom-ins of compartments with internal vesicles marked by CINCCKVL constructs.

HeLa cells transfected with either GFP-8 or tRFP-T-8 revealed the unequivocal presence of these chimeras in vesicles consistent with ILV of MVB (Figure 19). Inside these compartments, whereas tRFP-T-8 showed a more diffuse pattern, GFP-8 outlined

the inner membranes, which could be due to the decrease in GFP fluorescence resulting from its quenching in acidic pH environments (Kneen et al., 1998). It is thus apparent that the –CINCCKVL sequence can target proteins to specific domains of endolysosomes, some of which are ultimately internalized to form vesicles inside MVB.

1.2.2 Lack of –CINCCKVL chimera co-localization with autophagy markers

As mentioned earlier, -CINCCKVL-mediated RhoB sorting to endolysosomes results in rapid lysosomal degradation, a behavior that also holds for other chimeras with this sequence attached to their C-terminal ends (Pérez-Sala et al., 2009). Considering the lysosomal degradation fate of RhoB and CINCCKVL chimeras as well as the high degree of intracellular crosstalk between endolysosomal and autophagic pathways, autophagy could be involved in breakdown of this GTPase and related constructs. This degradation pathway is often monitored by microscopy in live cells using constructs of the microtubule-associated protein 1 light chain 3 protein, LC3 (Bampton et al., 2005), as shown in Figure 20.

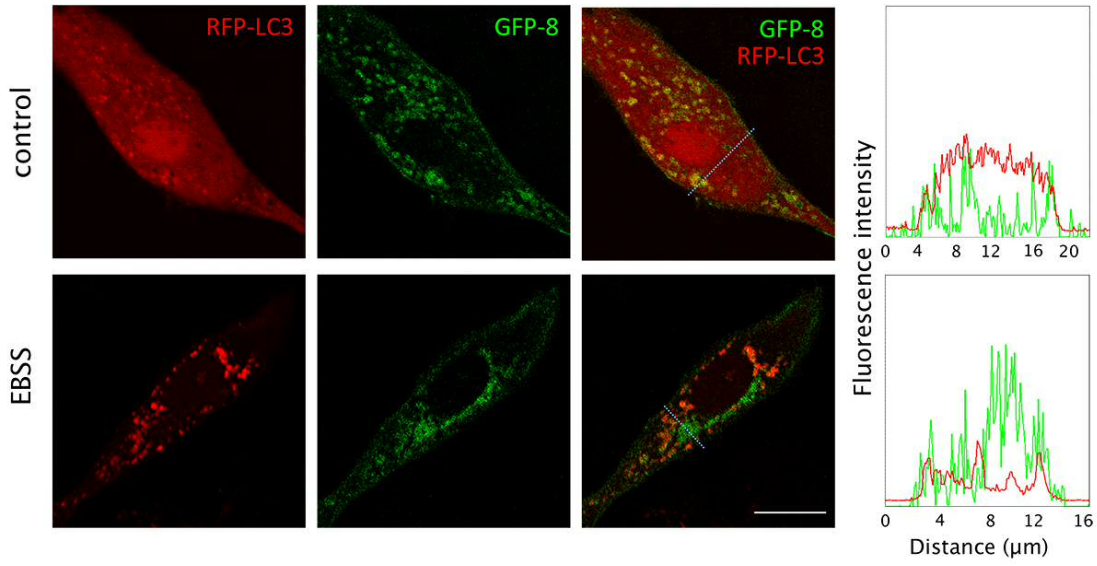

Figure 20. Lack of co-localization between GFP-8 and the autophagic probe, RFP-LC3.

BAEC were co-transfected with GFP-8 and RFP-LC3 and incubated in serum-free medium (control) or amino acid-depleted medium (EBSS) for 20 h prior to live confocal visualization. The right panels show fluorescence intensity of the single channels along the lines pictured in the images.

Upon autophagy induction by e.g. amino acid depletion, LC3 becomes lipidated by a phosphatidylethanolamine moiety, forming LC3-II (Barth et al., 2010; Kabeya et al., 2000; Mizushima and Yoshimori, 2007), which attaches to autophagosomal membranes that can be readily detected by fluorescence microscopy (Barth et al., 2010; Mizushima et al., 2010). Taking advantage of this behavior, RFP-LC3 was co-transfected with GFP-8 in BAEC (Figure 20), in which the autophagic pathway had not yet been described or characterized. We observed that, under normal cell culture conditions, RFP-LC3 showed a diffuse distribution. Following autophagy induction by incubation in the amino-acid free medium, Earle's Balanced Salt Solution (EBSS), RFP-LC3 adopted a punctate pattern characteristic of autophagosome formation. Remarkably, co-localization of GFP-8 with RFP-LC3 was negligible under both conditions, as shown in Figure 20. A similar lack of co-localization with other autophagy markers such as monodansylcadaverine or CytoID was also observed (Oeste et al., 2013). These results indicate that GFP-8 and LC3-positive vesicles are distinct entities, namely endolysosomes and autophagosomes, so that GFP-8 incorporation into the autophagic pathway is unlikely.

1.2.3 CINCCKVL chimera endolysosomal localization depends on lipid modifications

Membrane association of full-length, endogenous RhoB depends on a series of modifications at its C-terminus, including irreversible isoprenylation and reversible bipalmitoylation (Adamson et al., 1992). To confirm whether this is the case for CINCCKVL chimeras, mutants corresponding to the cysteine residues amenable to lipid modification were used in fractionation and microscopy studies. Cells transfected with GFP constructs of these mutants were subjected to whole cell lysis (Figure 21, upper panels) or subcellular fractionation (Figure 21, lower panels) into S-100 (soluble) or P-100 (membrane) fractions to assess the extent of membrane attachment. WB analysis showed that untagged GFP was fully soluble, whereas GFP-8 was detectable only in the membrane fraction. Cysteine mutants that cannot be isoprenylated (GFP-8-C244S) or palmitoylated (GFP-8-C241,243S) and therefore have restricted access to membranes appear mostly in the soluble fraction, with minimal membrane association. Of note,

lower levels of GFP-8 than of GFP or the mutated constructs were detected in whole cell lysates (Figure 21, upper panels), consistent with a rapid turnover of this endolysosome-targeted protein.

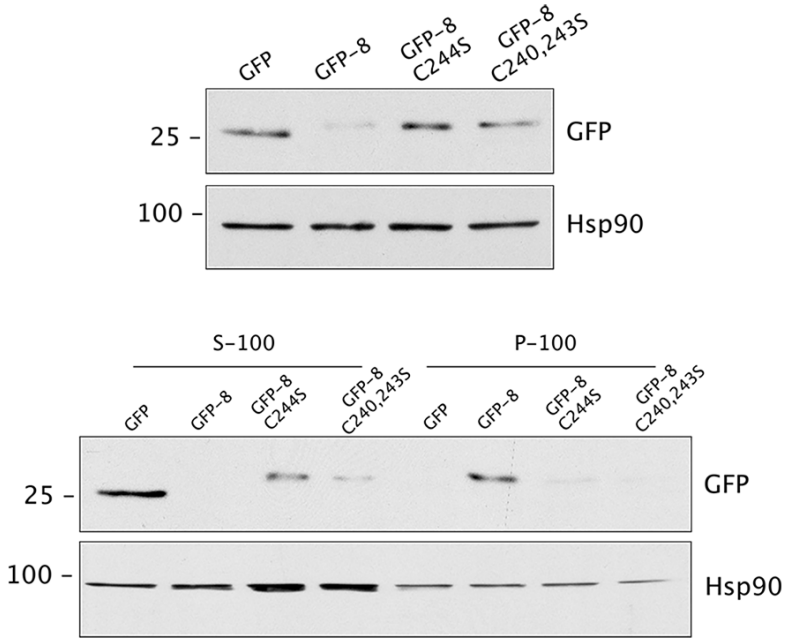

Figure 21. Subcellular fractionation of GFP-8 posttranslational modification mutants.

HeLa cells were transfected with GFP-8 or its indicated lipidation-deficient cysteine mutants. Cell lysis and fractionation were performed as described in the Methods section. Upper panels show total cell lysates whereas lower panels correspond to chimeric protein levels in the soluble (S-100) or particulate (P-100) fraction, assessed by WB with an anti-GFP antibody. Hsp90 was used as a loading control and 25 or 100 kDa markers are shown for electrophoretic mobility reference.

In order to study membrane localization of CINCCKVL cysteine mutants, confocal microscopy studies were carried out. In contrast to the high degree of localization between GFP-8 and LTR (co-localization rate: 62.6±2.5%), the palmitoylation-deficient mutant GFP-8-C241,243S presents a cytosolic distribution that excludes the nucleus (Figure 22), as expected for a mono-prenylated construct bearing only a CAAX box (Pérez-Sala et al., 2009). Furthermore, the isoprenylation mutant (GFP-8-C244S) appears as a cytosolic, non-lipidated protein that excludes some small organelles, thus following a pattern indistinguishable from that of untagged GFP (Figure 22, last two panels). This last construct does indeed contain the palmitoylation cysteines, but the fact that it does not associate with membranes indicates the dependence of palmitoylation on previous isoprenylation and CAAX processing (Wang and Sebti, 2005).

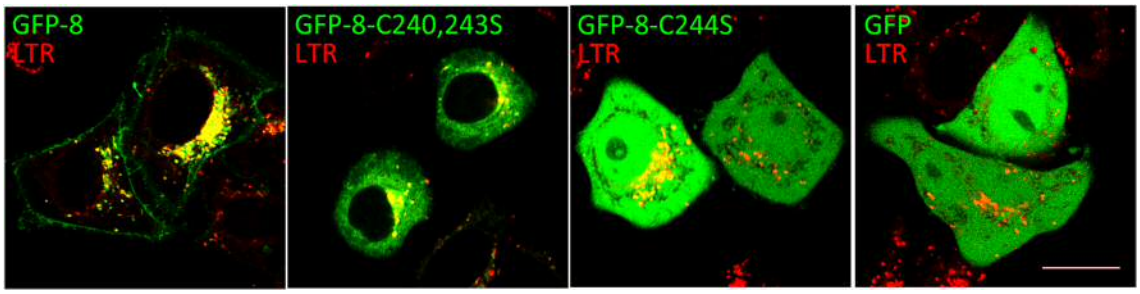

Figure 22. Endolysosomal localization of GFP-8 depends on posttranslational lipidation.

HeLa cells were transfected with GFP-8, its palmitoylation-deficient mutant (GFP-8-C240,243S), the isoprenylation-deficient mutant (GFP-8-C244S), or untagged GFP. Cells were stained with LTR prior to live confocal microscopy observation.

It has been previously described for several Ras family members that they shuttle from the plasma membrane to the Golgi in a palmitoylation-dependent manner (Rocks et al., 2005). Indeed, whereas GFP-8 did not present high co-localization with the Golgi protein giantin (Figure 23, first panel), in the case of the isoprenylated but palmitoylation-deficient mutant GFP-8-C241,243S, cells contained cytoplasmic accumulations that co-localized to a greater extent with the Golgi (Figure 23, second panel). In turn, the isoprenylation mutant as well as untagged GFP showed a similar pattern in which Golgi localization was only partial and collateral to its diffuse distribution (Figure 23, last two panels). Therefore, Golgi localization of GFP-8 probably occurs transiently when its CAAX motif has been isoprenylated and awaits further processing through bipalmitoylation.

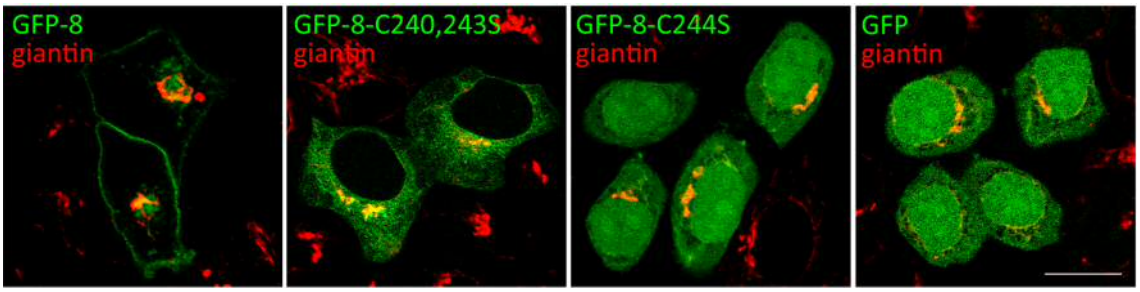

Figure 23. Golgi staining of cells transfected with GFP-8 and its lipidation mutants.

HeLa cells were transfected with the indicated constructs and fixed after 16 h in serum-depleted medium. The Golgi compartment was marked by immunofluorescence using anti-giantin antibodies, as explained in Methods.

As a proof of concept, GFP-8 isoprenylation and palmitoylation inhibition were carried out pharmacologically rather than through cysteine mutation. Treatment with

2-bromopalmitate to block palmitoylation elicited a GFP-8 subcellular localization similar to the corresponding mutant, i.e. diffuse cytosolic and excluding the nucleus (Figure 24A, left panel). Similarly, simvastatin treatment for inhibition of isoprenoid biosynthesis resulted in a totally diffuse pattern, as observed for the equivalent cysteine mutation (Figure 24A, right panel). It is hence possible to pharmacologically modulate the selective localization of CINCCKVL proteins to subcellular membranes by inhibiting lipidation of the C-terminal cysteines.

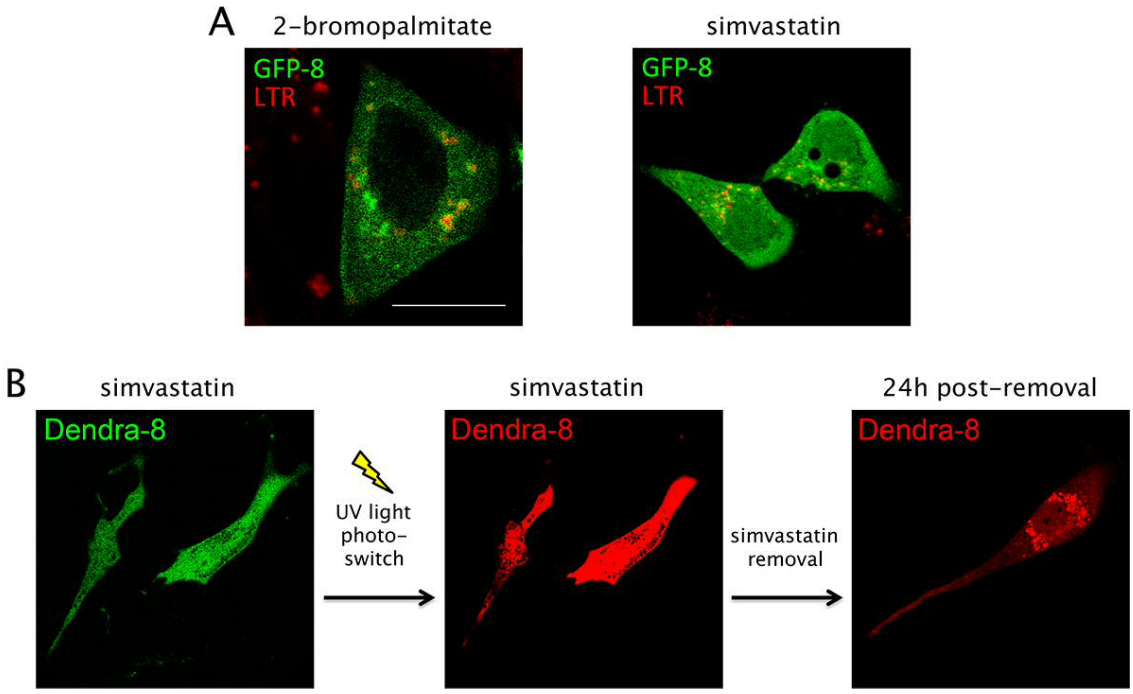

Figure 24. Lipidation inhibition by pharmacological treatment of cells expressing CINCCKVL-chimeras.

(A) HeLa cells were transfected with GFP-8 and treated with 2-bromopalmitate to inhibit palmitoylation or simvastatin to block isoprenylation, as described in Methods, prior to LTR staining and live observation under a confocal microscope. (B) BAEC were transfected with Dendra-8 and treated with simvastatin for 24 h (left panel) prior to UV light exposure to induce green-to-red photoswitching (middle panel). Simvastatin was removed directly after photoswitching and 24 h later subcellular localization of the photoconverted red protein was monitored (right panel).

A question that remains unanswered in this field is whether lipid posttranslational modifications occur only on newly synthesized proteins, or whether a previously existing pool of non-lipidated protein in the cytosol can be processed and subsequently attach to membranes. As seen above, simvastatin treatment elicits a fully cytosolic population of GFP-8 and can therefore be used to address this issue.

Furthermore, the photoswitchable fluorescent protein Dendra2 switches from green to red fluorescence emission after UV light exposure and can be used to track transfected cells before and after photoexcitation. Taking advantage of these tools, BAEC were transfected with a Dendra2-CINCCKVL fusion protein (Dendra-8) and treated with simvastatin to obtain a pool of green, fully cytosolic construct with no lipid modifications (Figure 24B, left). Specific cells were then exposed to UV light on a confocal microscope for photoswitching, providing a pool of red, unprocessed Dendra-8 to be followed (Figure 24B, middle). Simvastatin was removed immediately following green to red conversion to release isoprenylation inhibition, which, as shown in Figure 24, right, allowed endolysosomal targeting of the red protein that had previously been diffuse throughout the cytosol. Therefore, pre-existing cytosolic CINCCKVL proteins may be sorted to endolysosomal localizations upon C-terminal processing, indicating that this process does not need to occur directly on nascent proteins.

1.3 CINCCKVL sorting is conserved from fungi to human cell models

We have shown that RhoB and CINCCKVL-chimeric proteins are targeted to endolysosomal membranes in several mammalian cell types, including human primary fibroblasts, HeLa cells or BAEC. This behavior is consistent with the fact that the C-terminal sequence of RhoB is conserved in mammalian species and birds (Table 4), which must necessarily contain the cellular machinery required for RhoB sorting. However, organisms from other branches of evolution contain either a RhoB protein with a different C-terminal sequence or Ras- or Rho-related proteins with similarities to RhoB that have not been identified as *bona fide* RhoB homologs (Table 4). These proteins contain CAAX boxes and nearby cysteines that could become palmitoylated, but the different spacing between these residues along with other structural determinants could elicit unique subcellular localization patterns, as seen in Section 1.1 for other GTPases. It was therefore uncertain whether non-mammalian organisms that do not present the CINCCKVL sequence in any of their proteins could sort these chimeras to their specific endolysosomal/MVB destinations.

Species	Protein	Accession no.	C-terminal sequence
(synthetic construct)	**GFP-8**	N/A	TAAGITLGMDELYKCINCCKVL
(synthetic construct)	**tRFP-T-8**	N/A	RYCDLPSKLGHKLNCINCCKVL
Homo sapiens	RhoB	NM_004040	TRAALQKRYGSQNGCINCCKVL
Bos taurus	RhoB	NM_001077922	TRAALQKRYGSQNGCINCCKVL
Mus musculus	RhoB	AF481943	TRAALQKRYGSQNGCINCCKVL
Gallus gallus	RhoB	NM_204909.1	TRAALQKRYGTQNGCINCCKVL
Xenopus laevis	RhoB	NM_001096461.1	TRAALQKKHGRSGECMSCCKLL
Drosophila mojavensis	uncharacterized	CH933808.1	TRASLQVKKRKKRSGCWSLSCKLL
Schizosaccharomyces pombe	Rho2	NM_001019998.3	TRAALTVRDSENDKSSTKCCIIS
Aspergillus fumigatus	RasA	XM_748433	TRAPEGKMDVSEPGDNAGCCGKCVIM
Aspergillus nidulans	uncharacterized	AN4953	TRAALLTFDKRKSSCCIVL

Table 4. C-terminal sequences of CINCCKVL chimeras, RhoB homologs and related proteins from diverse species.

On top, the C-terminal sequences of GFP-8 and tRFP-T-8 are shown. Below, several RhoB homologs or related proteins along with their PubMed accession numbers and their C-terminal sequences. In red, potential palmitoylation sites. In green, isoprenylation cysteines.

1.3.1 CINCCKVL sorting in amphibian and insect cells

Within the genome of the amphibian *Xenopus laevis*, an endogenous RhoB protein is encoded with a C-terminal sequence that encloses several distinct structural features (Table 4). Though it presents a very similar CAAX box and two cysteines spaced similarly to human RhoB, the two amino acids between the palmitoylatable cysteines differ. Where human RhoB reads “IN”, *Xenopus* RhoB contains the amino acids “MS”, similarly to the H-Ras sequence that elicits binding to the plasma membrane, primarily. Furthermore, *Xenopus* RhoB contains the basic amino acid patch “KKH” upstream of the lipidated cysteines, reminiscent of the human TC10 protein, which is retained at the limiting membrane of endolysosomes. The effect of these unique structural determinants was assessed by transfection of *Xenopus* epithelial A6 cells with GFP tagged *Xenopus* RhoB (GFP-RhoB X), as seen in Figure 25A, left panel. Compared to the typical endolysosomal localization of GFP-8 (Figure 25A, middle panel) and consistent with its H-Ras- and TC10-like motifs, GFP-RhoB X appears mainly at the plasma membrane and scarcely at endolysosomes, as underscored by its low co-localization with LTR (Figure 25A, right panel). However, human GFP-RhoB and tRFP-T-8 are still sorted to endolysosomes, as gathered from their mutual co-localization as well as overlap of the latter with Lamp1-GFP (Figure 25B).

It is thus apparent that the combination of sorting motifs in *Xenopus* RhoB elicits a localization pattern distinct from both human RhoB and CINCCKVL chimeras. Nevertheless, *Xenopus* cells are able to sort proteins derived from the human RhoB C-terminus though they do not code for this sequence endogenously.

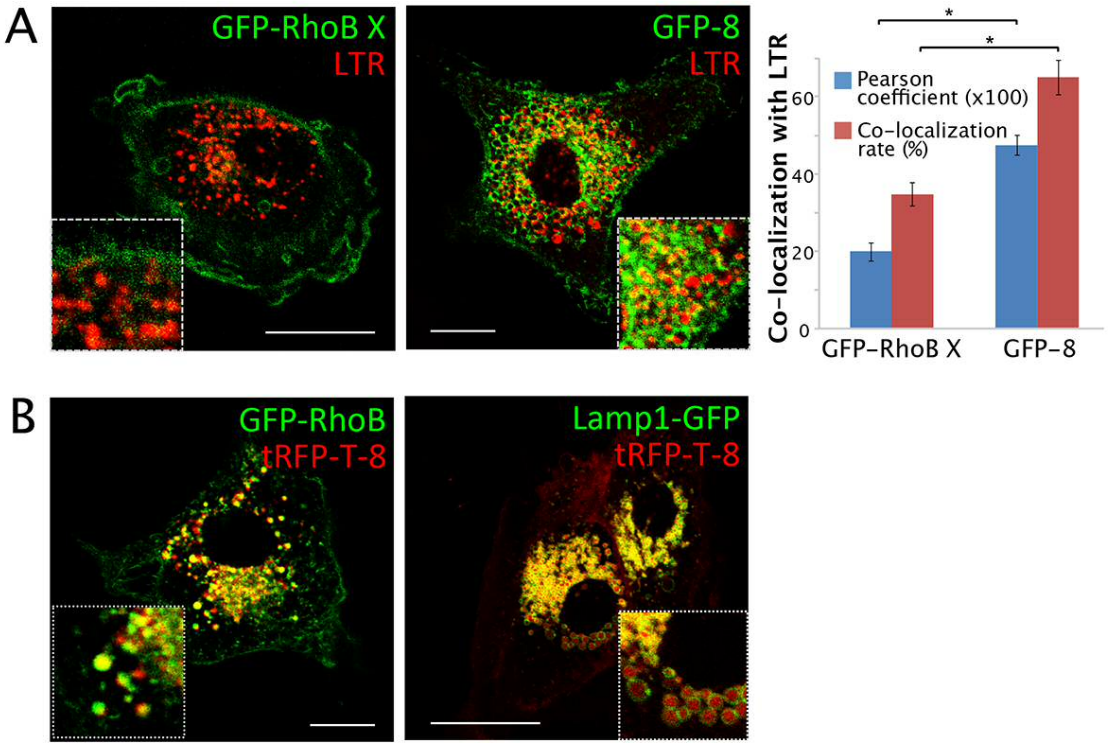

Figure 25. Localization of RhoB-related proteins in amphibian cells.

(A) *Xenopus laevis* A6 cells were transfected with *Xenopus laevis* RhoB (GFP-RhoB X) or GFP-8 and stained with LTR. GFP/LTR co-localization is shown in the right panel as Pearson coefficients (x100) or co-localization rates (in percentages). Asterisks represent $p<1 \times 10^{-6}$ versus GFP-8 (B) A6 cells were co-transfected with human GFP-RhoB or Lamp1-GFP and tRFP-T-8.

Going further down the evolutionary scale to assess the ability of different organisms to sort CINCCKVL chimeras to the late endocytic pathway, cells of the invertebrate *Trichoplusia ni* were transfected with tRFP-T-8. The High Five insect cell line showed tRFP-T-8 sorted into vesicles surrounded by Lamp1-GFP, marking their lysosomal character (Figure 26).

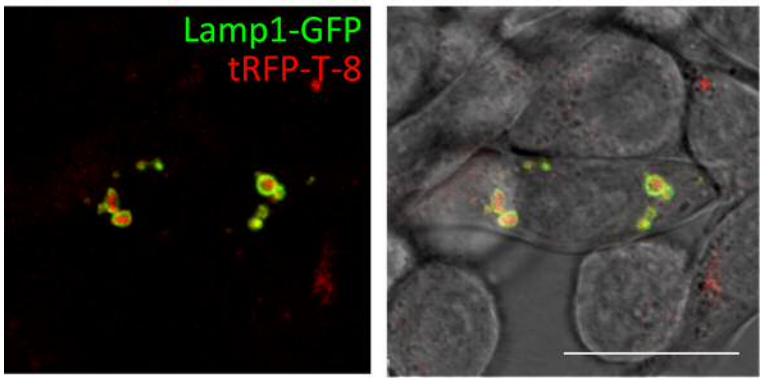

Figure 26. Localization of tRFP-T-8 in High Five insect cells.

High Five cells derived from the cabbage looper *Trichoplusia ni* were co-transfected with Lamp1-GFP and tRFP-T-8 before live observation by confocal microscopy. The left panel shows overlays of single fluorescent channels to which the Differential Interference Contrast (DIC) image has been juxtaposed in the right panel.

In the insect species *Drosophila mojavensis,* an uncharacterized protein containing a CAAX box, an extended basic amino acid patch and only one palmitoylatable cysteine among heterogeneous residues may be found (see Table 4). However, *Trichoplusia ni,* from which High Five cells are derived, does not encode an endogenous RhoB protein. Nonetheless, the structural determinants of the CINCCKVL sequence are robust enough to bestow endolysosomal localization upon its chimeras in this organism, as well.

1.3.2 CINCCKVL localization in *Aspergillus nidulans*

Though palmitoylation occurs on a multitude of proteins and is highly conserved throughout evolution, the mechanisms responsible for this process have remained elusive (Aicart-Ramos et al., 2011). Actually, palmitoyl transferases were discovered roughly a decade ago in yeast (Lobo et al., 2002; Roth et al., 2002), where many crucial proteins undergo this posttranslational modification to regulate their subcellular localization (Roth et al., 2006). A putative Rho-related protein bearing a CAAX box and a possible palmitoylation site is expressed in the fungus *Aspergillus nidulans* (Table 4), but the CINCCKVL motif does not appear in its proteome. To explore whether CINCCKVL sorting can take place in this compelling model organism for vesicular trafficking, *Aspergillus nidulans* strains expressing GFP-8 and its palmitoylation-deficient mutant were established (Figure 27).

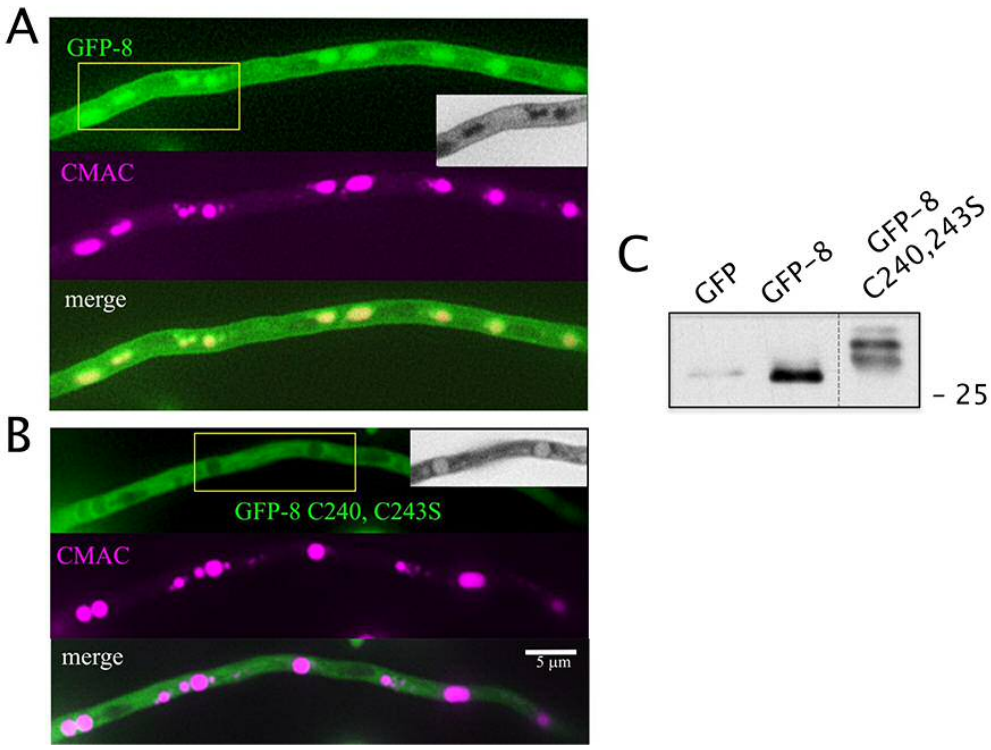

Figure 27. GFP-8 and its palmitoylation mutant in *Aspergillus nidulans*.

Aspergillus nidulans strains established by transformation with GFP-8 (A) or its palmitoylation deficient mutant GFP-8-C240,243S (B) were observed live as described in Methods. Staining with the vacuole marker CMAC is shown in the middle panels and overlays in the bottom panels. Gray scale insets of yellow boxed-in areas are shown for better contrast. (C) *Aspergillus nidulans* strains expressing the indicated constructs were processed for SDS-PAGE and WB using a GFP antibody. Dotted lines indicate a 5-fold shorter exposure time for the last lane than the two preceding ones. The 25 kDa marker is shown for reference.

In the wild-type strain, GFP-8 appears at the plasma membrane as well as in late endosomes and vacuoles stained by the acidic organelle marker CMAC (Figure 27A). In contrast, its palmitoylation-deficient mutant GFP-8-C240,243S is cytosolic and excluded from nuclei, the plasma membrane and CMAC-positive compartments (Figure 27B). Dependence on posttranslational modifications for targeting is similar to that observed in human cells, in which isoprenylation alone is also unable to elicit endolysosomal localization. Lack of GFP-8-C240,243S processing is further evidenced by the appearance of a doublet of slower migrating bands in SDS-PAGE, as described for other Ras superfamily proteins in mammalian cells (Hancock et al., 1989), and shown in Figure 27C. Indeed, levels of the mutant are significantly higher than those of fully lipidated GFP-8, which could be undergoing constitutive vacuolar degradation analogous to its lysosomal degradation in mammalian cells (see Figure 27C, caption).

Moreover, GFP-8 and GFP-8-C240,243S localization patterns are distinct from that of untagged GFP, which appears diffusely throughout the cytoplasm and nucleus, similarly to mammalian cells (not shown).

The filamentous nature of *Aspergillus nidulans* makes it a highly suitable model for tracking the movement of endocytic organelles by time-lapse microscopy (Peñalva et al., 2012). Indeed, GFP-8-positive vesicles could be readily detected travelling within the cell, avoiding nuclei and possibly fusing with large vacuoles also presenting GFP-8 fluorescence (Figure 28A, colored arrows and black arrowhead).

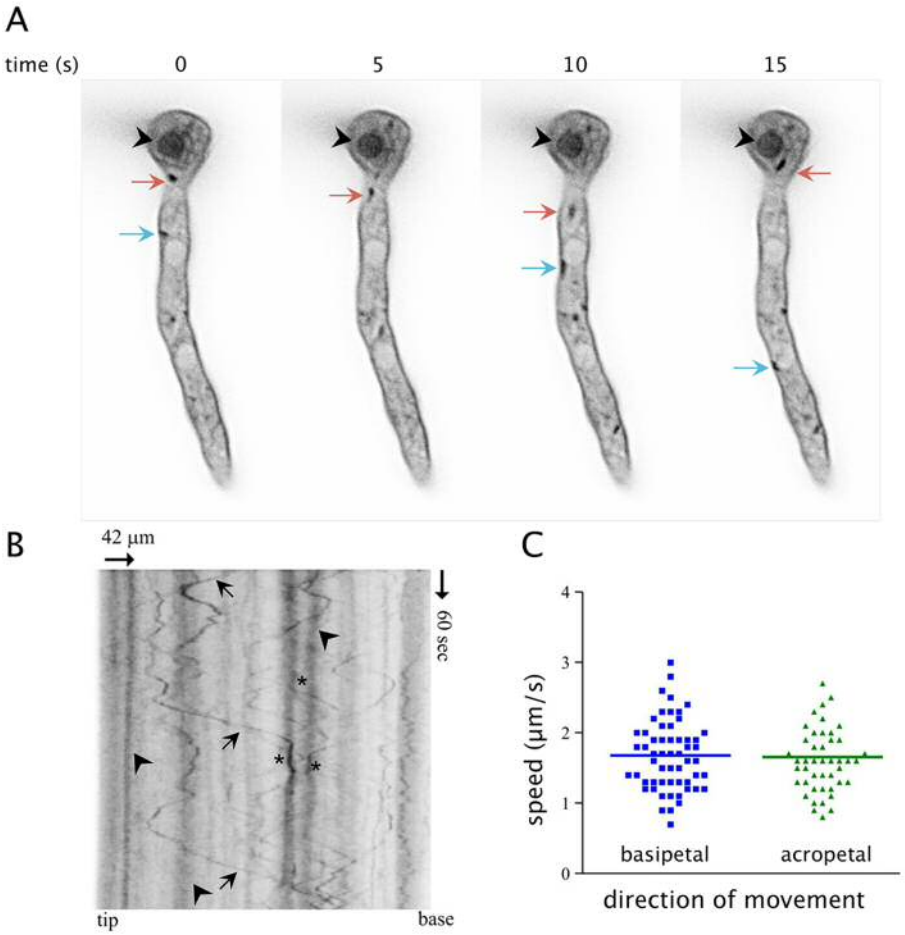

Figure 28. Tracking GFP-8-positive compartments in *Aspergillus nidulans*.

(A) The *Aspergillus nidulans* GFP-8 strain was observed live to follow localization of the construct by time-lapse microscopy. The plasma membrane is marked by GFP-8, as well as a large, sessile vacuole (black arrowhead in all frames). Smaller, motile vesicles also contain GFP-8 (colored arrows). The vesicle marked by a red arrow undergoes both basipetal and acropetal movement, whereas the teal-colored arrow follows a vesicle with acropetal movement only, which is not detectable in the second frame due to movement along the z-axis. (B) Kymograph showing GFP-8-positive compartments in motion from a representative experiment using a GFP-8-expressing strain. Black arrows highlight fast-moving vesicles, whereas black arrowheads mark static vesicles. Asterisks mark possible points of contact or fusion between them. (C) Velocities of individual endosomes travelling in both directions were tracked and are represented in the graph. See text for details.

Fluorescent vesicles can be tracked and their trajectories represented by using kymographs, as shown for GFP-8-positive vesicles of a representative cell in Figure 28B. Thick, straight lines correspond to large, sessile vacuoles (Figure 28B, arrowheads) whereas thin, diagonal lines trace several smaller, fast-moving endosomes (Figure 28B, arrows). Both of these contours come together at certain points that could be indicative of endosome-vacuole fusions (Figure 28B, asterisks). Furthermore, the speed of individual endosomes can be calculated from this type of representation by calculating the slope of their trajectory, be it basipetal or acropetal (Figure 28C). Similar average speeds of approximately 1 to 3 μm per second for GFP-8-containing endosomes in both directions, i.e. fully bidirectional movement, suggests that trafficking of these fast and small vesicles is dependent on microtubules, as has been previously described for other vesicles (Abenza et al., 2012; Abenza et al., 2009). Taken together, these results highlight the presence of GFP-8 along the endocytic pathway in *Aspergillus nidulans* and imply that CINCCKVL sorting occurs through mechanisms conserved in fungi, as well.

2. Mechanisms potentially involved in RhoB sorting

RhoB fluorescent constructs show a very specific subcellular localization at ILV of MVB and lysosomes as well as the plasma membrane, as summarized in Section 1.1.1. This behavior indicates that RhoB follows an endocytic route and accumulates at late compartments to which several sorting machineries escort their cargo, as described in the Introduction (see Figure 9). Therefore, this section comprises studies that attempt to elucidate specific mechanisms involved in driving RhoB constructs and related chimeras to their subcellular destinations, including ILV or the lysosomal lumen, by focusing on protein machineries as well as lipid dynamics.

2.1 Role of the ESCRT machinery in RhoB sorting

The canonical pathway for proteins that enter MVB to be degraded in the lysosome is often represented by ESCRT-mediated internalization of EGFR upon cell stimulation with its agonist. Indeed, RhoB has been shown to be involved in EGFR trafficking in several cell types and its expression is upregulated by EGF stimulation (Canguilhem et al., 2005; Gampel et al., 1999; Lajoie-Mazenc et al., 2008; Tillement et al., 2008). It could be the case that RhoB associates with vesicles on which EGFR travels and therefore follows a similar ESCRT-mediated internalization pathway. Therefore, experiments were carried out in cells in which ESCRT components were altered to study potential ESCRT involvement in sorting of RhoB and its related chimeras.

2.1.1 ESCRT-related processes in sorting of RhoB and related chimeras

ESCRT complexes act sequentially beginning with recognition of ubiquitin by Hrs (the core ESCRT-0 protein) and ending with ESCRT-III disassembly mediated by the ATPase, Vps4. These two major events were approached experimentally in the context of cells expressing RhoB constructs to initially evaluate whether the ESCRT machinery could play a role in their sorting.

There are few studies in which RhoB ubiquitination has been addressed, and those in which RhoB has been found to be ubiquitinated show that this is a cell type- and context-dependent process (Engel et al., 1998; Wang et al., 2014). To establish whether the fluorescent constructs used throughout this study were ubiquitinated, they were expressed in HeLa cells and immunoprecipitated to assay ubiquitin association, as shown in Figure 29. Neither GFP-RhoB nor GFP-8 samples presented signals compatible with ubiquitinated forms of these constructs. Interestingly, the construct GFP-22, which contains a lysine residue potentially susceptible to ubiquitination, was the only sample showing a putative mono-ubiquitinated species, marked by an asterisk in Figure 29A.

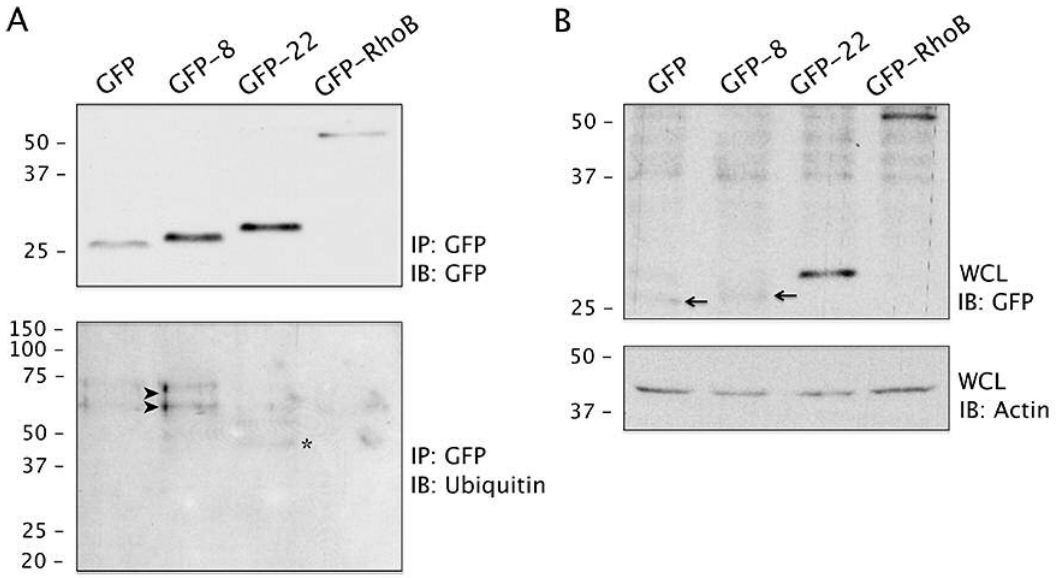

Figure 29. Ubiquitination assays by immunoprecipitation of RhoB constructs.

(A) HeLa cells were transfected with the indicated agents and immunoprecipitated using GFP antibodies conjugated with agarose beads (GFP-Trap) as described in the Methods section. Immunoblots were performed against the indicated proteins. Arrowheads highlight unspecific signals, possibly representing keratin doublets. The asterisk marks faint signals detected consistently in GFP-22 samples. (B) Whole cell lysates (WCL) of samples shown in (A). Arrows mark the GFP and GFP-8 signals.

Therefore, if GFP-RhoB and/or GFP-8 are ubiquitinated, they are so at levels that are undetectable under basal conditions in this type of assay. However, ubiquitin-independent, ESCRT-dependent sorting into ILV of MVB has been previously described (Babst, 2011), as discussed in the Introduction. The ESCRT-associated component, Vps4, was consequently addressed in cells in which the last step of ILV formation was impaired, namely, HeLa cells transfected with a dominant negative form of this protein (Figure 30).

In HeLa cells, transfection of the wild-type GFP-Vps4 construct presents a diffuse pattern throughout the cytosol and does not affect localization at endolysosomes of tRFP-T-RhoB (Figure 30A, top panels) or tRFP-T-8 (not shown), either under control conditions or upon treatment with chloroquine. However, overexpression of dominant negative GFP-Vps4 hinders tRFP-T-RhoB entry into vesicular structures, as shown in the bottom panels of Figure 30A and its profiles. Instead, fluorescent RhoB constructs are mislocalized to the limiting membrane of vesicles formed upon GFP-Vps4 DN expression, defined as aberrant Class E compartments (Bishop and Woodman, 2000), recapitulating the results obtained in BAEC (Pérez-Sala et al., 2009).

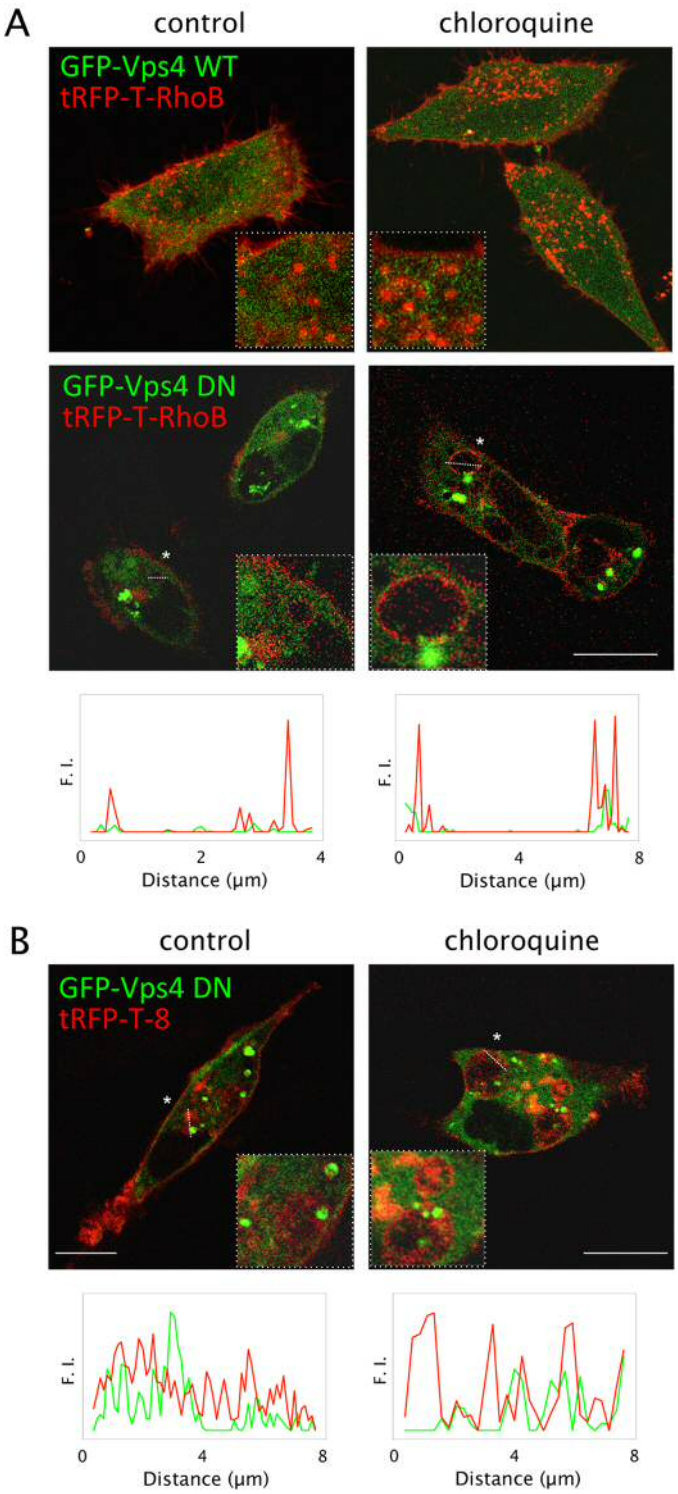

Figure 30. Effect of GFP-Vps4 DN overexpression on RhoB and CINCCKVL chimera localization.

HeLa cells were co-transfected with the indicated constructs and treated with chloroquine for 24 h where specified prior to live confocal microscopy observation. Underneath the panels of cells expressing GFP-Vps4 DN, fluorescence intensity profiles along a section marked by dotted lines and asterisks are shown. F.I., fluorescence intensity.

In contrast, the CINCCKVL construct, tRFP-T-8 is able to enter into the lumen of these compartments in cells expressing the dominant negative mutant of Vps4, as shown in Figure 30B (see profiles). These results point to a possible role for ESCRT proteins in RhoB sorting, so that further studies concerning the ESCRT machinery *per se* were carried out in HeLa cells, as shown below.

2.1.2 ESCRT component depletion in RhoB and –CINCCKVL protein sorting

To further substantiate the role of ESCRT proteins, either control (scr) siRNA or siRNA against either the ESCRT-0 component Hrs or the ESCRT-I protein Tsg101 was transfected into cells to reduce protein levels prior to expression of GFP-RhoB or GFP-8 and chloroquine treatment. The efficiency of ESCRT silencing was analyzed in these cells by SDS-PAGE and WB. As shown in Figure 31A, cells transfected with Hrs-specific siRNA were practically devoid of this ESCRT component as compared to their control (scr). In turn, Tsg101 silencing reduced its protein levels by 72.2 ± 5.3% (Figure 31B).

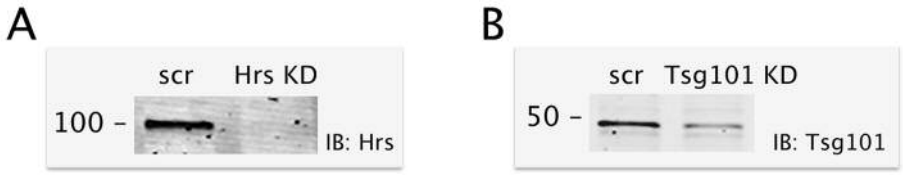

Figure 31. Depletion of ESCRT components by specific siRNA.

(A) HeLa cells were transfected with scrambled (scr) or Hrs-targeted siRNA. Cell lysis was carried out 48 h later and WB against Hrs is shown. (B) Tsg101 levels were assessed similarly to (A). 50 and 100 kDa markers are shown for reference.

As shown by confocal microscopy analysis in Figure 32A, HeLa cells transfected with control siRNA (scr) were able to sort GFP-RhoB to LTR-positive vesicles, as seen above for several cell types. However, knock-down of the ESCRT-0 component, Hrs or the ESCRT-I component, Tsg101 reduced the appearance of GFP-RhoB at acidic vesicles (Figure 32A, see profiles).

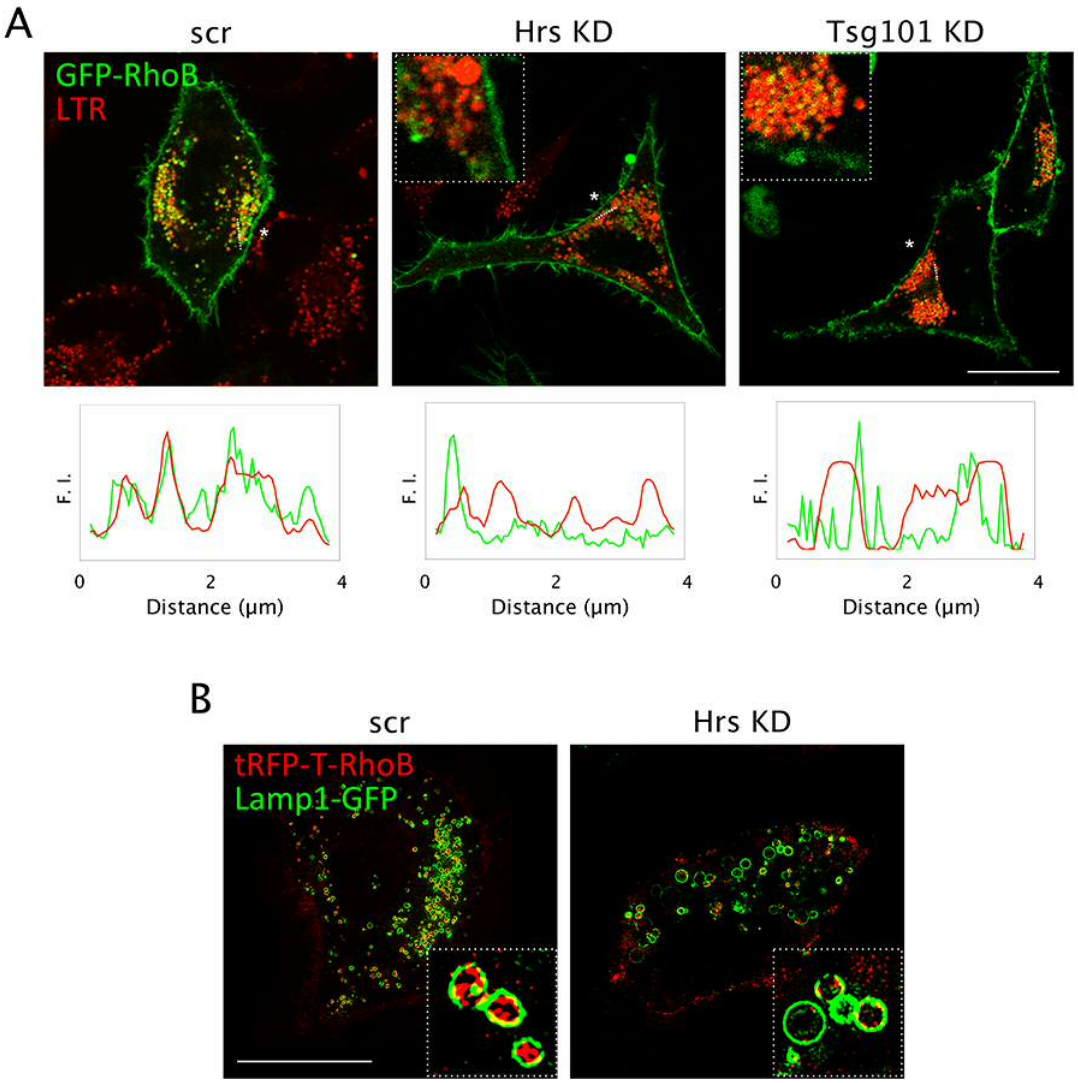

Figure 32. Knock-down of the ESCRT components Hrs or Tsg101 and their effect on localization of RhoB fluorescent constructs.

(A) HeLa cells were transfected with either scrambled siRNA (scr) or siRNA targeting either Hrs or Tsg101 to silence these ESCRT components, replated, and transfected with GFP-RhoB. Cells were treated with chloroquine to induce accumulation at endolysosomes, stained with LTR and observed live by confocal microscopy. Fluorescence intensity profiles along a section (marked by dotted lines and asterisks) appear underneath each condition. KD, knock-down; F.I., fluorescence intensity. (B) HeLa cells transfected with either scrambled siRNA (scr) or siRNA targeting Hrs were further co-transfected with tRFP-T-RhoB and Lamp-GFP. After 24 h of chloroquine treatment, they were visualized live by structured illumination super-resolution microscopy (SIM). Insets show individual MVB and their ILV decorated with RhoB fluorescent protein. The right panel inset highlights the emptier MVB that appear upon Hrs knock-down.

To explore the effect of Hrs knock-down on sorting of RhoB constructs in more detail, the red tRFP-T-RhoB construct was co-transfected with Lamp1-GFP in cells in which Hrs was silenced and observed live under a super-resolution microscope (Figure 32B). Localization of tRFP-T-RhoB at ILV was unmistakably observed in control cells

within MVB surrounded by Lamp1-GFP at their limiting membrane (Figure 32B, left panel). On the other hand, Hrs knock-down cells presented Lamp1-positive structures with a marked reduction of tRFP-T-RhoB inside their lumen, despite treatment with chloroquine that usually causes RhoB construct accumulation inside these vesicles (Figure 32B, right panel inset). Taken together, these results suggest involvement of early ESCRT components in sorting of full-length RhoB constructs.

In order to study the role of the ESCRT machinery on sorting of CINCCKVL constructs, assays analogous to those above were performed on cells transfected with GFP-8. Strikingly, GFP-8 seemed unaffected by either Hrs or Tsg101 knock-down and was still able to enter the lumen of LTR-positive compartments, analogously to its control (Figure 33), in contrast to the marked reduction in endolysosomal localization detected above for GFP-RhoB.

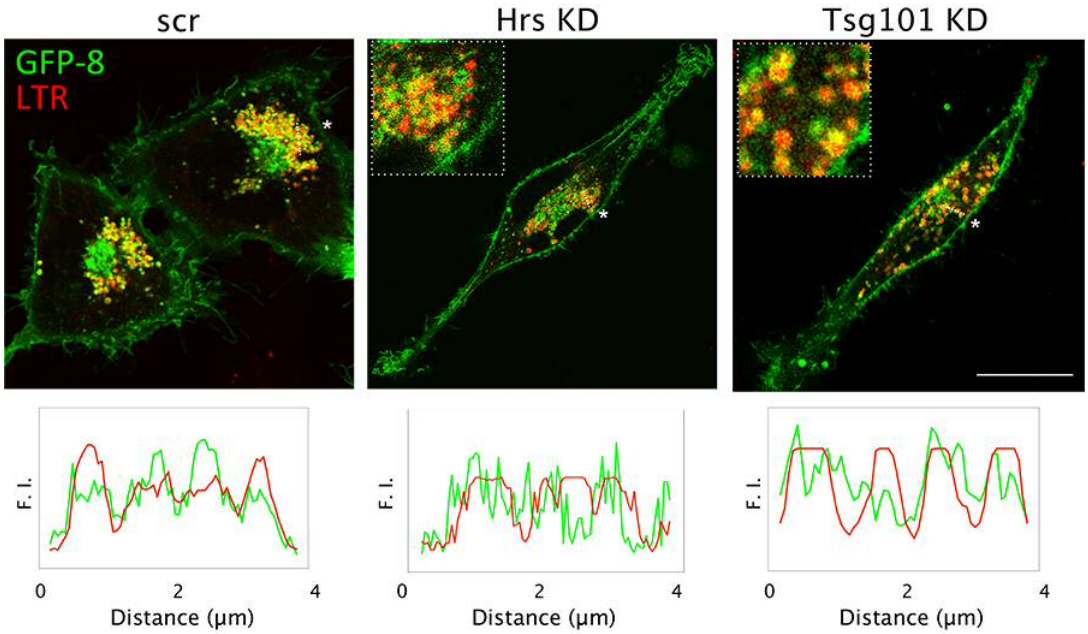

Figure 33. Knock-down of the ESCRT components Hrs or Tsg101 and their effect on GFP-8 localization.

HeLa cells transfected with siRNA targeting ESCRT components, transfected with GFP-8 and treated with chloroquine prior to LTR staining were observed live by confocal microscopy, similarly to Figure 32A. Profiles along a section traced by dotted lines and marked with asterisks show intensity profiles underneath each condition. KD, knock-down. F.I., fluorescence intensity.

In sum, there appears to be a differential effect of ESCRT component knock-down as to the subcellular localization of either full-length RhoB constructs or

CINCCKVL chimeras (compare Figure 32A to Figure 33). These findings are the first studies in which we have encountered dissimilar behavior between full-length RhoB and its sorting motif –CINCCKVL, suggesting that further regulatory determinants in the RhoB protein could be involved in ESCRT interaction, whereas –CINCCKVL bypasses this regulation and enters ILV of MVB independently of ESCRT.

2.2 Lipid-mediated endolysosomal sorting of CINCCKVL

The results above point to ESCRT involvement in full-length RhoB sorting, whereas the C-terminal motif CINCCKVL seems to be targeted to endolysosomes, more specifically ILV of MVB, independently of this protein machinery. Considering that ILV formation can be ESCRT-dependent or –independent (Section 3.2 of the Introduction), other mechanisms possibly involved in CINCCKVL-chimeric protein sorting were assessed. Taking advantage of the fact that inward budding from the limiting membrane of MVB is regulated by its lipid composition (Matsuo et al., 2004; Trajkovic et al., 2008), CINCCKVL chimera subcellular localization was monitored in cells treated with several compounds that modulate late endosomal lipid dynamics.

The precursor mevalonate is used by cells for membrane cholesterol biosynthesis and formation of isoprenoid moieties destined towards protein posttranslational modification, as schematized in Figure 34. The mevalonate pathway can be disrupted at several stages by blocking key enzymes with inhibitors, such as HMG CoA reductase inhibition by statin treatment in cells, which inhibits protein isoprenylation (Figure 34). Furthermore, the lysosomotropic agent U18666A inhibits cholesterol synthesis as well as its trafficking (Figure 34), thus causing its internalization and accumulation into ILV of MVB along with the lipid LBPA, eliciting an NPC-like phenotype (Cenedella, 2009; Kobayashi et al., 1999; Sobo et al., 2007). In turn, the squalene synthase inhibitor zaragozic acid (Figure 34) reduces cellular cholesterol levels and could affect ILV lipid composition significantly, since most of the cholesterol of the endocytic pathway is contained within these vesicles (Möbius et al., 2003).

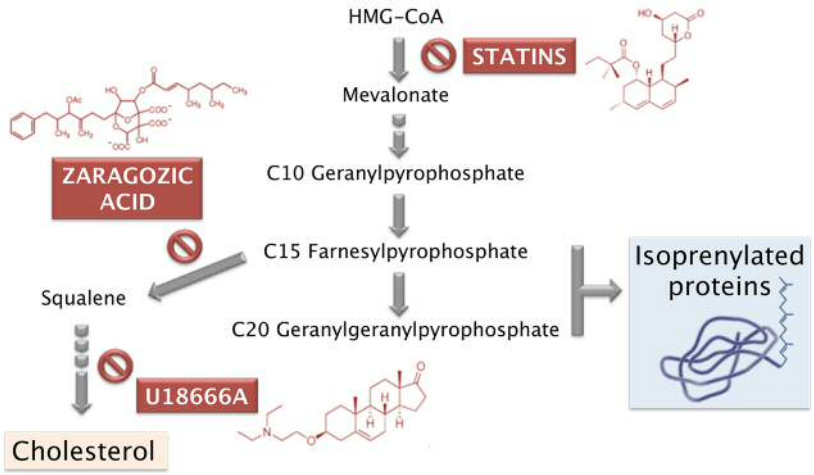

Figure 34. Schematic of the mevalonate pathway and compounds used for its modulation.

Simplified schematic of the mevalonate pathway showing formation of the isoprenylation precursors farnesylpyrophosphate and geranylgeranylpyrophosphate, used in protein modification. The former can be further processed for cholesterol biosynthesis. In red, structures of compounds used in this work to disrupt particular steps of the pathway. Statins such as simvastatin, shown here, inhibit HMG-CoA reductase and therefore halt both protein isoprenylation and cholesterol biosynthesis. In turn, zaragozic acid blocks squalene synthase, blocking subsequent steps of the cholesterol pathway. Similarly, the amphiphilic amino-steroid U18666A hinders cholesterol synthesis and transport. Truncated arrows represent intermediate steps that are not shown here for the sake of clarity.

To assess the effect of lipid alterations in CINCCKVL chimera localization, cells transfected with these constructs were treated with U18666A or ZGA and observed live by confocal microscopy (Figure 35).

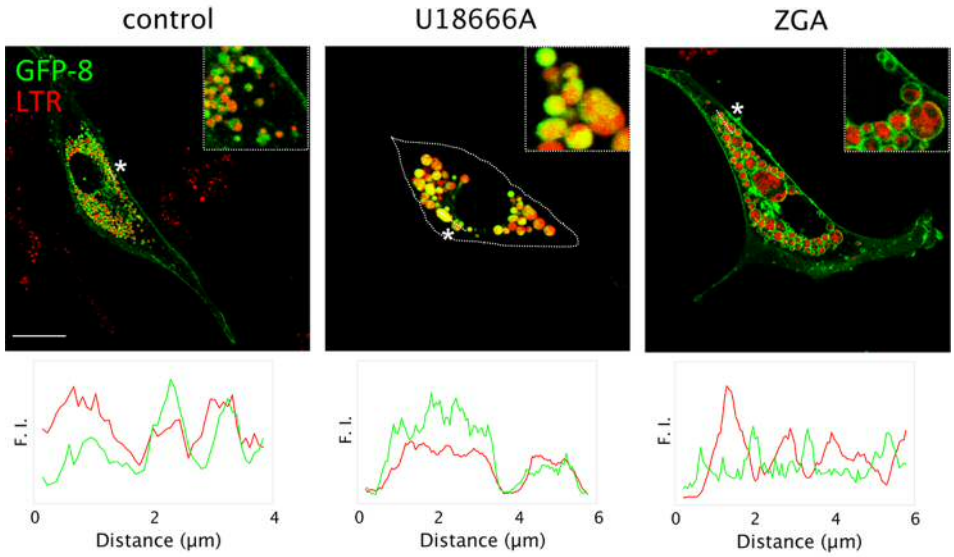

Figure 35. Agents modulating lipid dynamics alter GFP-8 localization.

BAEC transfected with GFP-8 were treated with 10 μM U18666A or 50 μM ZGA for 24 h. Insets show zoom-ins and lower panels represent fluorescence intensity profiles (F.I.) along a section marked by dotted lines and asterisks.

Indeed, these compounds produced drastic phenotypes in several cell types including HeLa cells, BAEC and *Xenopus laevis* cells (Oeste et al., 2014), and the results obtained for BAEC are presented here for clarity. As shown in the middle panel of Figure 35, cells treated with U18666A displayed intensely compact endolysosomes in which GFP-8 accumulated prominently, along with LTR, consistent with results shown in Section 1.1. In sharp contrast, ZGA elicited dilated MVB with either scarce, diffuse staining with GFP-8 or MVB practically devoid of GFP-8, in which GFP-8 was retained at the limiting membranes of MVB and LTR staining was weaker and sometimes patchy (Figure 35, right panel profile). However, ZGA treatment of BAEC transfected with GFP-RhoB showed dilated MVB with patches of LTR in which this construct seemed to enter freely, similarly to its control and conversely to GFP-8, as seen in Figure 36.

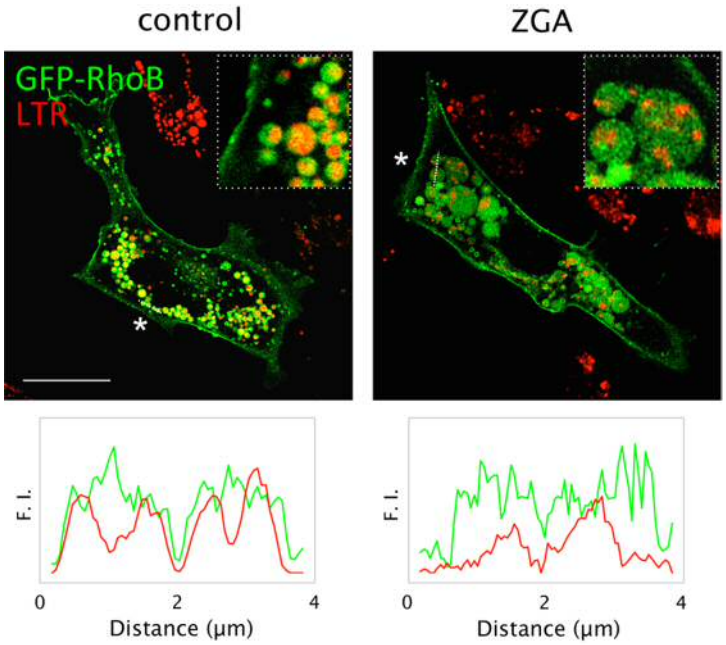

Figure 36. GFP-RhoB appears inside MVB in cells treated with ZGA.

BAEC transfected with GFP-RhoB were treated with ZGA and stained with LTR prior to confocal microscopy observation, as in Figure 35. Insets show details of vesicles and profiles represent fluorescent intensity (F.I.) along sections marked by dotted lines and asterisks.

In order to investigate whether impairment of GFP-8 sorting into the lumen of endolysosomes could be due to a reduction of GFP-8 membrane association, we performed subcellular fractionation studies (Figure 37). For this we used HeLa cells, in which we previously confirmed the inhibitory effect of ZGA on endolysosomal internalization of GFP-8 by confocal microscopy (Oeste et al., 2014). As shown in

Figure 37, cholesterol depletion does not reduce the levels of membrane-associated GFP-8, practically all of which still appears in the particulate (P-100) fraction.

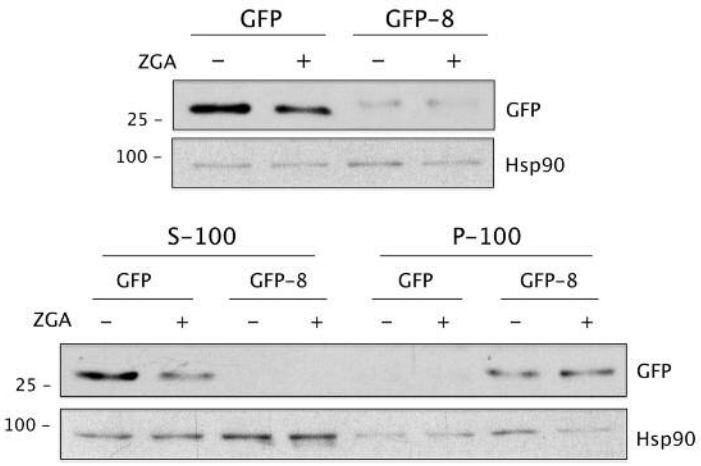

Figure 37. Subcellular fractionation of HeLa cells treated with ZGA.

HeLa cells were transfected with GFP or GFP-8, treated with 100 μM ZGA for 24 h, lysed, and fractionation was performed as described in the Methods section. Upper panels show total cell lysates whereas lower panels correspond to chimeric protein levels in the soluble (S-100) or particulate (P-100) fraction, assessed by WB with an anti-GFP antibody. The 25 kDa marker is shown for electrophoretic reference.

2.3 The tetraspanin CD63 in RhoB and CINCCKVL sorting

The results shown above suggest that sorting of full-length RhoB constructs is mediated partly by the ESCRT machinery, whereas CINCCKVL chimeras seem to enter ILV of MVB regardless of ESCRT disruption. As described in Section 3.1.3 of the Introduction, evidence pointing to ESCRT-independent sorting accumulating in recent years indicates a role for CD63 in trafficking to ILV as well as in biogenesis of ILV destined for release as exosomes (Pols and Klumperman, 2009). Furthermore, the small ILV that still form after Hrs depletion carry CD63 and its cargo (Edgar et al., 2014), so that the internalization of GFP-8 into MVB in cells after Hrs knock-down observed above in Section 2.1.2 could be CD63-mediated. These findings warranted further studies to explore the role of CD63 in sorting of CINCCKVL proteins and full-length RhoB.

2.3.1 Impact of CD63 overexpression on localization of RhoB and CINCCKVL constructs

In HeLa cells, RhoB and CD63 constructs co-localize to a very high degree in their small endolysosomes, as seen in Figure 18. Therefore, co-transfection studies were carried out in BAEC to observe more specific localization inside their larger MVB, particularly after chloroquine treatment (Figure 38). Co-localization was apparent in cells expressing wild-type mCherry-CD63 and GFP-8 (Pearson coefficient = 0.63 ± 0.04), and treatment of these cells with chloroquine further increased co-localization (Pearson coefficient = 0.81 ± 0.03). In contrast, GFP-RhoB and mCherry-CD63 co-localization was significantly lower respect to GFP-8 in control cells (Pearson coefficient = 0.41 ± 0.04). The large vesicles typical of BAEC also presented several GFP-RhoB- or GFP-8-positive structures that did not contain fluorescent CD63 and *vice versa* (Figure 38)..

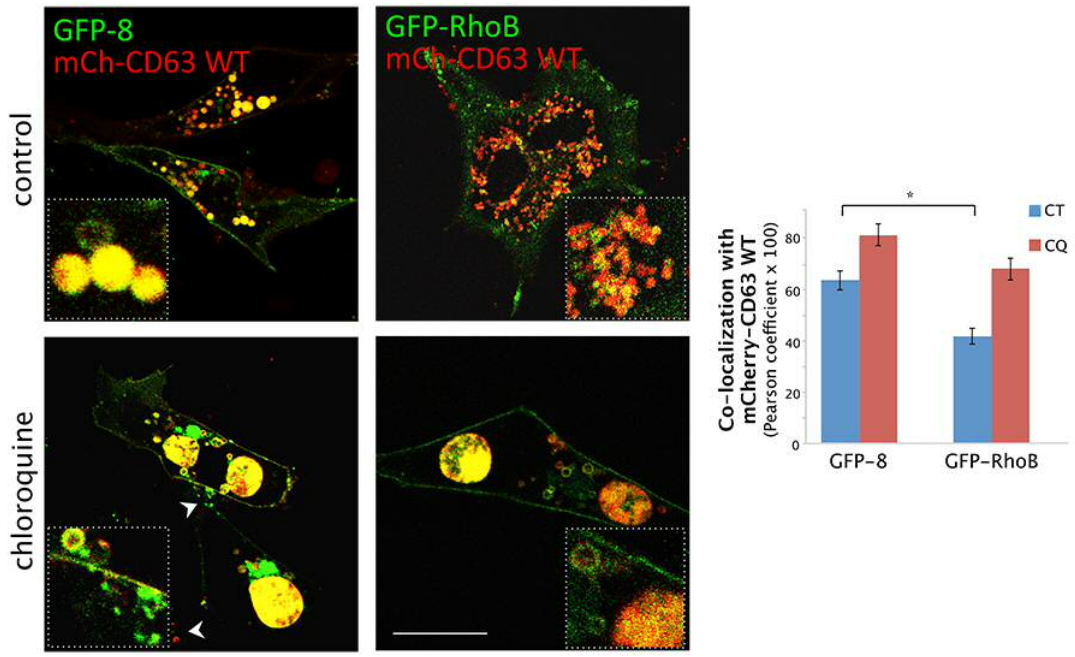

Figure 38. Wild-type mCherry-CD63 co-localization with GFP-8 or GFP-RhoB.

BAEC co-transfected with mCherry-CD63 wild-type (mCh-CD63 WT) and either GFP-RhoB or GFP-8 were visualized by live confocal microscopy after treatment with chloroquine, where indicated. White arrowheads mark the extracellular material in the lower left panel. The graph shows average co-localization between constructs, assessed as described in Methods in the image analysis section. *p < 0.01

In this cell type, whereas co-transfection of CD63 and full-length RhoB constructs was well tolerated under the conditions studied, CD63 in combination with CINCCKVL proteins elicited accumulation of extracellular, vesicular material throughout the culture dish that was positive for GFP-8 and mCherry-CD63 (marked by arrowheads in Figure 38, bottom left panel)

The differential effect of overexpressing CD63 with full-length RhoB constructs versus CINCCKVL proteins could imply that this tetraspanin is involved in sorting, or interacts with, the lipidated RhoB motif. To further explore this possibility, similar studies were carried out with the mCh-CD63 YA construct in which the tyrosine found in the C-terminal lysosomal targeting motif YEVM was mutated to alanine (Figure 39). It has been reported that this mutant is unable to interact with the sorting complex AP-3 and is therefore largely localized to the plasma membrane (Rous et al., 2002).

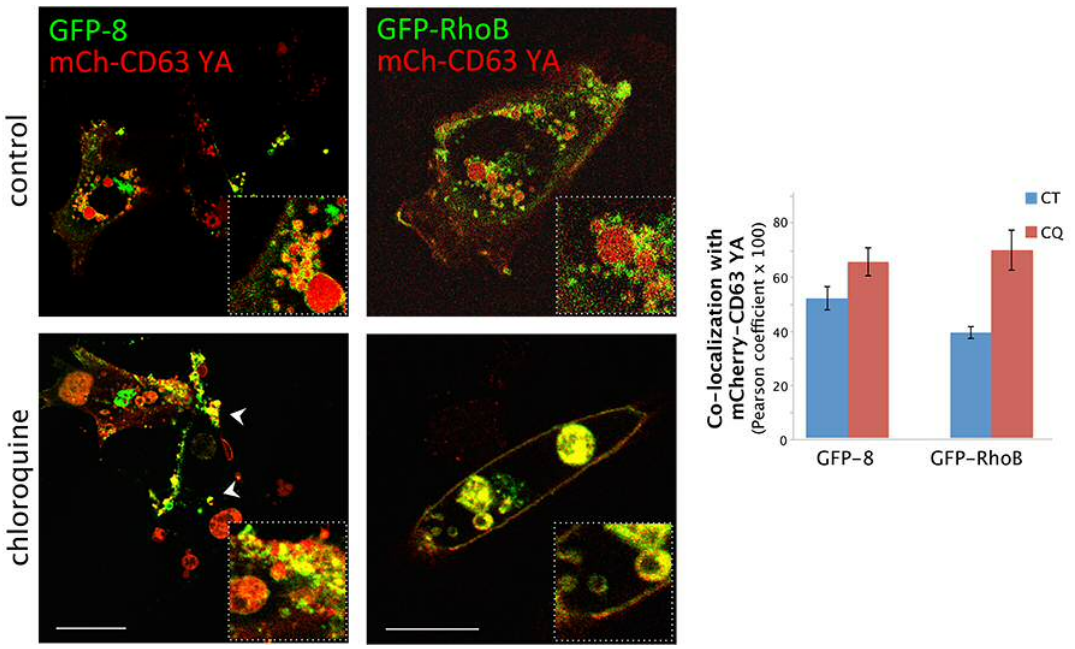

Figure 39. mCherry-CD63 Y235A mutant co-localization with GFP-8 or GFP-RhoB.

BAEC co-transfected with the mCherry-CD63 lysosomal targeting tyrosine mutant (mCh-CD63 YA) and either GFP-RhoB or GFP-8 were visualized by live confocal microscopy after treatment with chloroquine, where indicated. Note the extracellular material marked by arrowheads in the bottom left panel. Co-localization is shown in the graph, as described in Figure 38.

Under the conditions used throughout this work, the proportion of plasma membrane to endolysosomal localization of the CD63 mutant varies in a cell-type dependent manner for, as seen in Figure 39, mCh-CD63 YA is only partially associated

with the plasma membrane in BAEC and is still prominently present at endolysosomes. GFP-8 co-localization with the mCherry-CD63 YA mutant was significantly reduced with respect to the wild-type protein, particularly upon chloroquine treatment (Pearson coefficient = 0.66 ± 0.02 versus 0.81 ± 0.03). Furthermore, large amounts of GFP-8-positive extracellular vesicles were detectable in the medium as well as at the extracellular surface of the plasma membrane in many cells, particularly upon chloroquine treatment (Figure 39, left panels). In contrast, GFP-RhoB co-localization with mCherry-CD63 YA was similar to co-localization with its wild-type form, both for control conditions and after chloroquine treatment (Pearson coefficient = 0.41 ± 0.04 for the YA construct and 0.40 ± 0.05 for the wild-type, control; 0.67 ± 0.04 versus 0.71 ± 0.08, chloroquine treatment). It is therefore possible that the tetraspanin CD63 is involved in CINCCKVL protein sorting, which could potentially result in extracellular localization of the chimera under certain conditions.

2.3.2 Effect of C6 ceramide treatment on RhoB construct localization

Targeting to MVB precedes an important step in protein sorting, for ILV pinched off into the MVB lumen can be sorted to lysosomes for degradation or be secreted into the extracellular milieu by MVB fusion with the plasma membrane, as depicted in Figure 40A. Considering CD63 function in the biogenesis of exosomes and the extracellular destination detected for CINCCKVL proteins in a scenario of aberrant CD63 overexpression, it is possible that this RhoB motif could be preferentially targeted for ILV destined for secretion instead of those destined for degradation in the lysosome, which are usually associated with ESCRT-dependent mechanisms. Furthermore, cell material can be secreted from the cell by direct shedding of microvesicles from the plasma membrane. In fact, a closer look by super-resolution imaging at the plasma membrane of HeLa cells transfected with GFP-8 shows what appear to be discrete compartments possibly corresponding to microvesicles, as well as protruding areas of the plasma membrane budding outwards (Figure 40B). Therefore, it is plausible that CINCCKVL targets its chimeric proteins to be secreted either directly at the plasma membrane or through the late endosomal pathway, into MVB and out of the cell in

exosomes. Nevertheless, it must be taken into account that due to the tight z-sections obtained by super-resolution microscopy, the structures that appear to be vesicles could in fact correspond to undulations still attached to the plasma membrane.

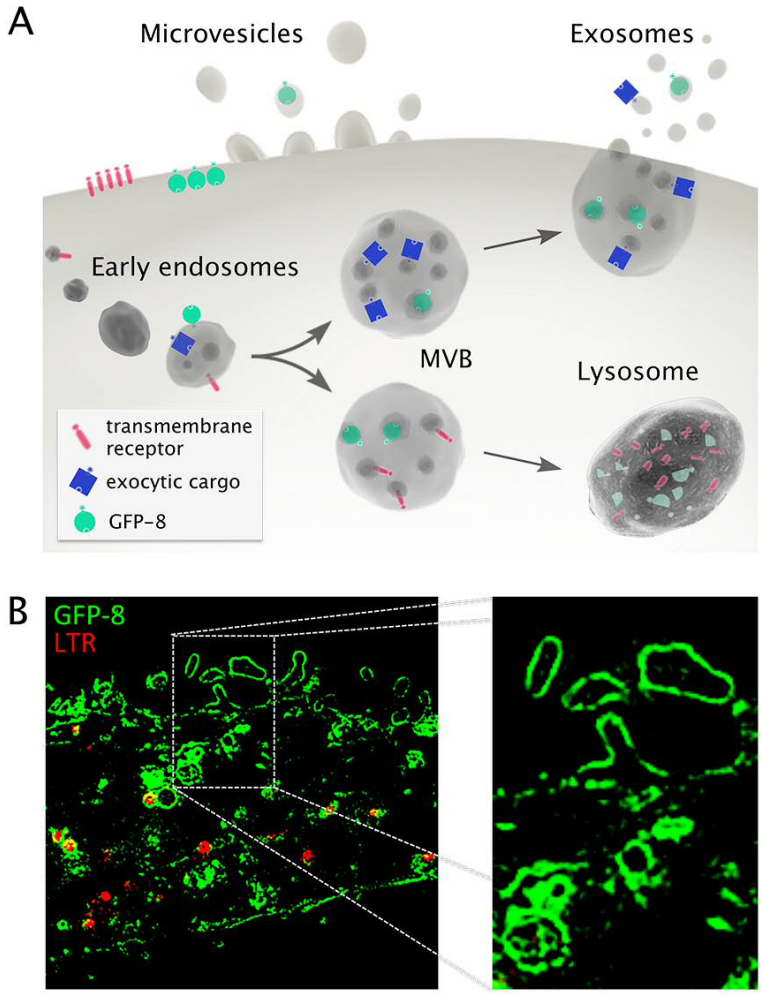

Figure 40. Extracellular vesicle release routes as potential destinations for GFP-8.

(A) Schematic representing pathways for extracellular release of vesicles and their cargo. Whereas microvesicles bud directly from the plasma membrane, exosomes are formed by inward budding of ILV into MVB that can fuse to the plasma membrane, releasing their internal vesicles. MVB can also be destined for fusion with lysosomes for cargo degradation. It has not yet been fully established whether whole MVB are either exocytic or degradative or if ILV destined for either fate can co-exist within the same MVB. Note that budding of small ILV begins at the early endosome stage. Red rods represent transmembrane receptors and blue squares depict proteins destined for secretion. Green circles represent GFP-8 and its possible destinations. Modified from (Raposo and Stoorvogel, 2013). (B) Detailed inspection of the super-resolution image presented in Figure 19 shows GFP-8 at several LTR-positive endolysosomes and MVB (bottom left in inset). The inset further shows structures budding directly from the membrane, morphologically consistent with shed microvesicles.

To approach the possibility of CINCCKVL sorting to extracellular vesicles, cells transfected with either GFP-RhoB or GFP-8 were treated with C6 ceramide (Figure 41), which has been shown to induce ESCRT-independent formation of ILV that are secreted as exosomes (Trajkovic et al., 2008). An inactive form of this compound, dihydroceramide C6, was used as a negative control.

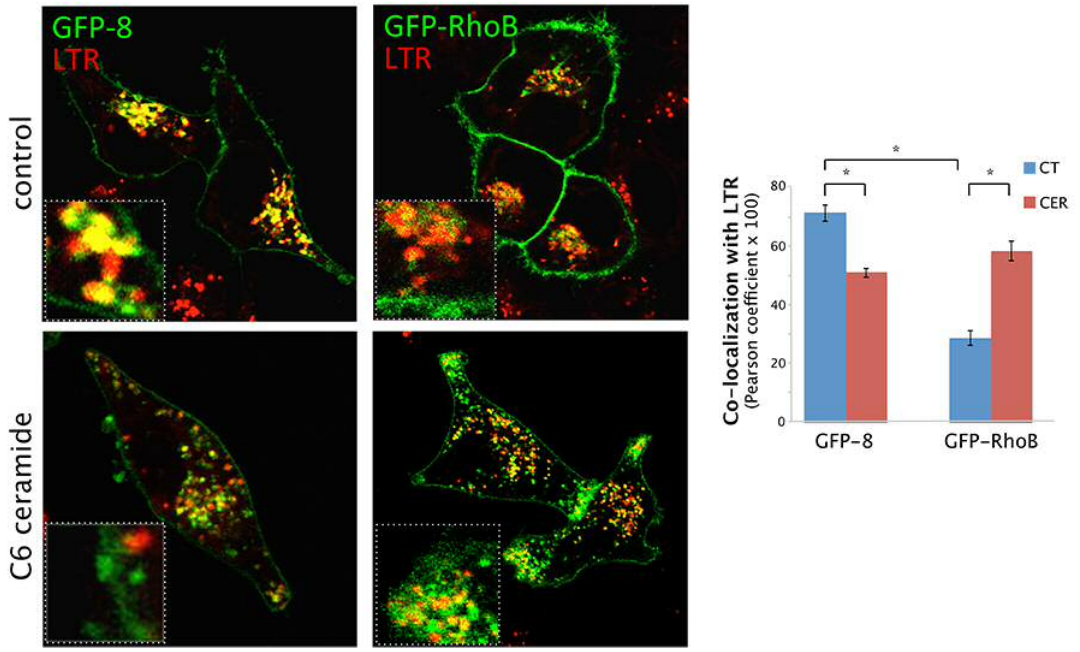

Figure 41. Effect of C6 ceramide on GFP-8 or GFP-RhoB endolysosomal localization.

HeLa cells transfected with the indicated agents were treated with either dihydroceramide C6 (control) or C6 ceramide and stained with LTR prior to live confocal microscopy observation. The graph represents co-localization with LTR of either GFP-8 or GFP-RhoB after the indicated treatments. *$p < 0.001$

As seen in the left panels of Figure 41, upon ceramide treatment, GFP-8 accumulated less at perinuclear, LTR-positive vesicles, its localization at the plasma membrane was in part diminished, and GFP-8-positive material was detected in the proximity of the plasma membrane as well as throughout the culture dish. This behavior was reflected by a significant decrease in co-localization of GFP-8 with LTR upon ceramide treatment (Pearson coefficient = 0.71 ± 0.03 for control compared to 0.51 ± 0.02 after ceramide treatment). However, after treatment with ceramide, GFP-RhoB was retained at the plasma membrane in polarized accumulations that were positive for LTR and did not seem to reach the extracellular space (Figure 41), hence eliciting a significant increase in GFP-RhoB co-localization with LTR (Pearson coefficient = 0.29 ±

0.02 control versus 0.59 ± 0.03). Taken together, these results suggest that CINCCKVL is able to reach the extracellular medium whereas the full-length protein is retained within the cell, possibly due to further sorting signals precluding its secretion or an active role in these processes. These results warrant further studies regarding the extracellular fate of CINCCKVL chimeras and the involvement of the CINCCKVL sequence in this process in the context of full-length RhoB.

3. Small GTPases in pathological scenarios

The plethora of signaling cascades in which small GTPases are involved highlights their importance in maintaining cellular homeostasis. Indeed, as described in the Introduction, members of this protein family have been found to play roles in many pathological processes such as tumorigenesis, inflammation or lysosomal diseases. The experiments described in this section are focused first on exploring GTPase involvement in lysosomal storage diseases, specifically, Chediak-Higashi Syndrome. Secondly, the amenability of several GTPases to be modified by reactive compounds produced during inflammatory or oxidative stress conditions was assessed, for these modifications could alter their subcellular localization and activation, resulting in unfavorable cellular outcomes.

3.1 Endosomal GTPases in cells from patients with lysosomal storage diseases

Cells derived from patients suffering from lysosomal storage disorders are used alongside mouse models not only to study the pathogenesis of these diseases, but also to study the basic processes involved in general trafficking towards the lysosome. Much information about the endocytic route and the trafficking partners involved has been obtained by detection of mutations leading to these pathologies (Ballabio and Gieselmann, 2009). Therefore, GTPase localization was studied in the context of these

models for altered endolysosomal sorting. Several of these cell models have been previously employed in other works from the laboratory (Pérez-Sala et al., 2009; Valero et al., 2010); hence, attention here is focused on Chediak-Higashi Syndrome.

3.1.1 Studies in cells from patients with Chediak-Higashi Syndrome

The enlarged lysosomes found in many cell types of Chediak-Higashi patients were detected by optical microscopy early on and have since been found to accumulate cellular material of different kinds (Oliver et al., 1976). Several lysosomal storage diseases such as NPC present increased cholesterol levels in aberrant compartments as part of their pathogenic scenario. Moreover, a study on the lipid composition of CHS erythrocyte membranes pointed to higher levels of cholesterol (Chico et al., 2000), but to the best of our knowledge, intracellular cholesterol has not been studied in fibroblasts from this disease. Since cholesterol homeostasis can affect sorting of RhoB or CINCCKVL chimeras, unesterified cholesterol levels were assessed in CHS fibroblasts by filipin staining and confocal microscopy observation. As shown in Figure 42, CHS fibroblasts contain significantly higher levels of free cholesterol in their endolysosomes than control cells, quantified to almost double the value of control cells by fluorescence intensity detection.

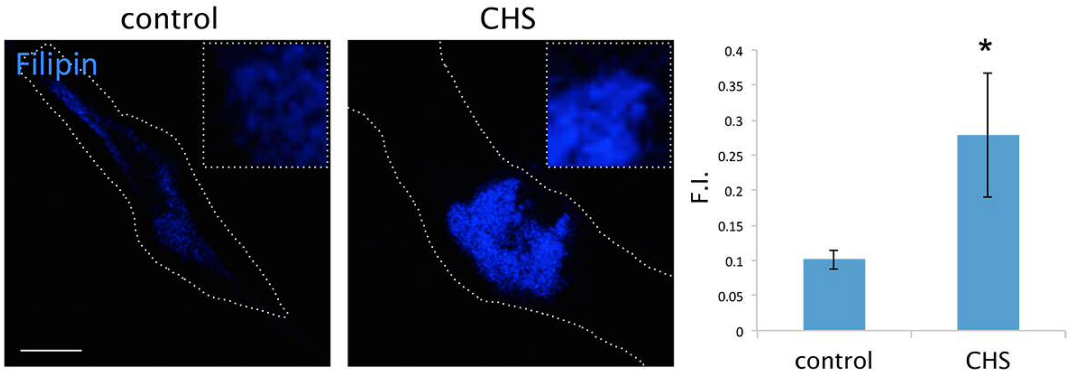

Figure 42. Cholesterol staining in control and Chediak-Higashi fibroblasts.

Confocal imaging of fixed fibroblasts from control subjects versus CHS cells after filipin staining. Images were acquired with identical settings. Quantification of confocal image intensities was performed on wide fields containing several cells and is shown to the right of the images. F.I., fluorescence intensity. *p, 0.05 versus control.

In addition to lipids, several proteins have been found to accumulate at the enlarged endolysosomes of CHS cells, including proteins involved in the endocytic

pathway (Burkhardt et al., 1993). In order to further characterize CHS endolysosomes, a systematic approach was set up whereby the subcellular localization of several endosomal GTPases was compared to endolysosomal markers. Similarly to control fibroblasts, in CHS fibroblasts GFP-Rab7 and Lamp-GFP co-localized with LTR, whereas GFP-Rab5 appeared at smaller, more peripheral vesicles consistent with early endosomes (Oeste et al., unpublished observations). As shown in Figure 43, GFP-RhoB is internalized into the enlarged endolysosomes that appear in CHS cells and co-localizes with LTR at these vesicles. However, GFP-Rab9 elicited an even further enlargement of CHS endolysosomes and was retained at their limiting membrane, in sharp contrast to the normal-sized endolysosomes that contain GFP-Rab9 in control fibroblasts.

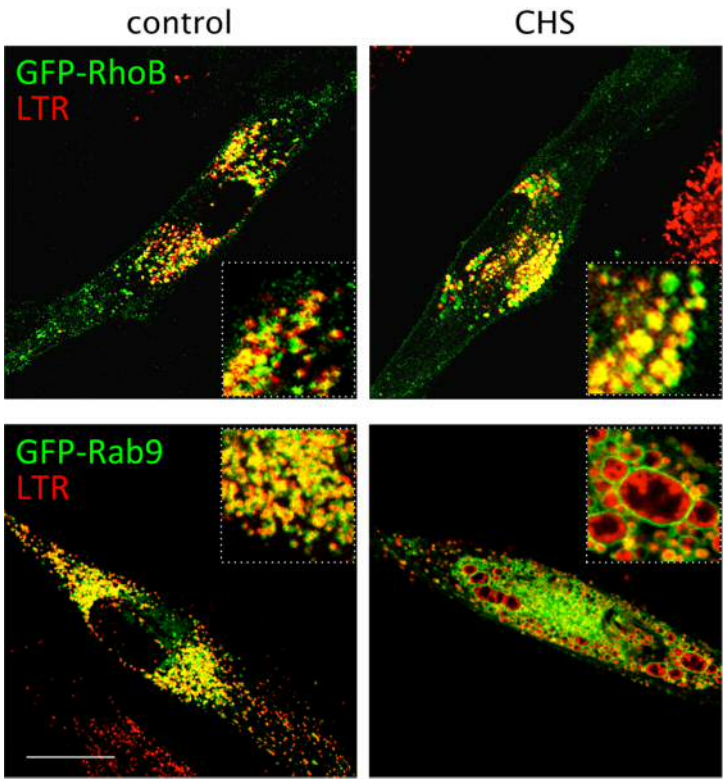

Figure 43. GFP-Rab9 subcellular localization in CHS fibroblasts.

Fibroblasts from control subjects or from CHS patients were transfected with GFP-RhoB or GFP-Rab9 and treated with 25 nM LTR for 15 min prior to live observation by confocal microscopy.

Taken together, these results suggest that the endolysosomal malfunction derived from LYST mutations involves an alteration in lipid composition, as seen by

cholesterol accumulation, that could be responsible for the inadequate localization of Rab9 constructs, as seen in NPC1 cells (Ganley and Pfeffer, 2006).

3.1.2 CINCCKVL localization in cells from lysosomal storage disease patients

Taking into account the aberrant behavior observed in late endolysosomal pathways of lysosomal storage diseases and the results shown above in Chediak-Higashi cells, it was deemed necessary to explore CINCCKVL localization in these lysosomal pathologies. As shown in Figure 44, the distribution of GFP-8 reflected the morphological alterations affecting lysosomal compartments in various diseases.

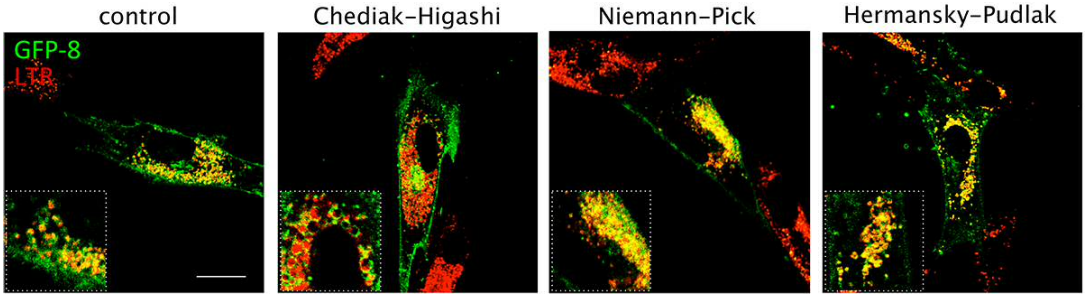

Figure 44. GFP-8 localization in lysosomal storage diseases.

Fibroblasts from control subjects or from patients with the indicated lysosomal diseases were transfected with GFP-8 and treated with 25 nM LTR for 15 min prior to live confocal microscopy observation.

Whereas in control cells, GFP-8 co-localized substantially with lysosomes detected by LTR staining, in fibroblasts from Chediak-Higashi patients, GFP-8 was located at the edge of the abnormally dilated acidic compartments typical of this condition. Interestingly, CHS cells present defects in regulated secretion (Ward et al., 2000). The inset shows that even LTR has difficulty entering the dense lysosomes that accumulate large amounts of ceroid-like material (Figure 44, second panel). On the other hand, as we previously observed (Pérez-Sala et al., 2009), fibroblasts from Niemann Pick type C1 patients, a disease characterized by alterations in intracellular cholesterol traffic, showed increased accumulation of GFP-8 inside lysosomes, probably arising from the altered late endosomal lipid dynamics in this disease. Similarly, fibroblasts from Hermansky-Pudlak Syndrome patients also showed an increase in the

appearance of GFP-8 at LTR-positive compartments. Considering the possible mechanisms responsible for CINCCKVL sorting described in Section 2 of the Results and the altered GFP-8 localization found in CHS cells, further studies could shed light on the sorting mechanisms that are defective in this disease and could find their correlation in other endolysosomal malfunctions.

3.2 Modifications of small GTPase cysteine residues by electrophilic compounds

As described throughout this dissertation, several small GTPases contain cysteine residues at their C-terminal ends that are amenable to palmitoylation and mediate their association with endomembranes of different nature. However, in situations associated with oxidative or electrophilic stress, as occurs in many pathological conditions such as inflammatory processes, diabetes or neurodegeneration, cysteines can suffer non-enzymatic modifications. These include direct oxidation or addition of compounds of electrophilic nature that could preclude palmitoylation and thus proper localization, as previously described for cyPG binding to H-Ras in works from the laboratory (Oeste et al., 2011; Renedo et al., 2007). The assays presented in this section explore whether other small GTPases bearing lipidation cysteines additionally to that of their CAAX box could also be directly modified by cyPG or other small cysteine-reactive compounds, hence eliciting conformation changes in their C-termini that could spread to other areas of the protein, changing their biochemical properties.

3.2.1 Direct binding of cyPG to small GTPases

Previous results from the laboratory established that dienone cyPG such as 15d-PGJ_2 and Δ^{12}-PGJ_2 covalently modify H-Ras at its C-terminal peptide, which bears the palmitoylation cysteines, i.e. C181 and C184 (Renedo et al., 2007). Therefore, binding of biotinylated 15d-PGJ_2 (15d-PGJ_2-B) to other small GTPases containing two palmitoylation cysteines at their C-terminus was assessed. As shown in Figure 45, the

negative control K-Ras4B, which does not have palmitoylatable cysteines in its C-terminus, does not present a detectable biotin signal, as previously reported in cell assays (Renedo et al., 2007). However, binding of 15d-PGJ_2-B was readily observable in the case of H-Ras, RhoB and Rap2B (Figure 45), all of which contain palmitoylation cysteines near the isoprenylation site (see Table 3). Therefore, of the GTPases studied, only those containing cysteine residues that are known to undergo palmitoylation are modified by 15d-PGJ_2-B *in vitro*.

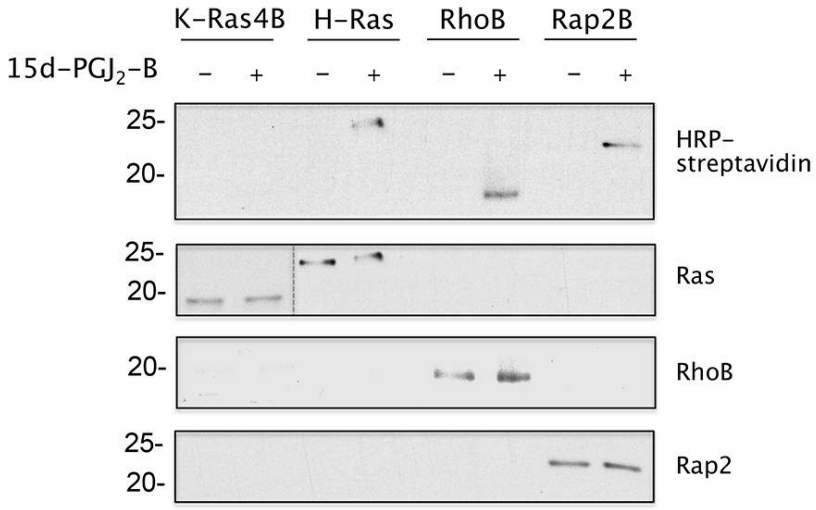

Figure 45. Binding of biotinylated 15d-PGJ_2 to small GTPases.

Human recombinant K-Ras4B, H-Ras, RhoB or His-tagged Rap2B at 5 μM were incubated with 15d-PGJ_2-B at 10 μM for 2 h at room temperature. Incorporation of the biotinylated cyPG was assessed by SDS-PAGE, protein blot and detection with horseradish peroxidase (HRP)-streptavidin (upper panel) or WB with anti-pan Ras, anti-RhoB or anti-Rap2 antibodies. The dashed gray line indicates different exposures due to saturation of the K-Ras4B signal. 20 and 25 kDa markers are shown for reference.

To assess binding of other cyPG to RhoB, *in vitro* studies were carried out with either single enone cyPG or dienone cyPG, as shown in Figure 46. Detection of the biotin signal shows binding of the biotinylated single enones PGA_1 and PGA_2. Interestingly, the *trans* side chain isomer of PGA_2, i.e. the isoprostane 8-iso-PGA_2, displayed a higher biotin signal than its *cis* isomer. Similarly to above, binding of the dienone cyPG 15d-PGJ_2-B was detected, as well. A biotinylated PG devoid of electrophilic carbons, PGE_2, did not bind to RhoB, as expected for this negative control.

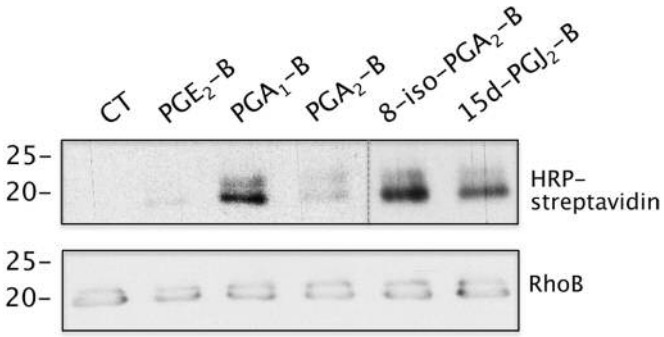

Figure 46. Binding of several cyPG to recombinant RhoB *in vitro*.

Recombinant RhoB at 5 μM was incubated with the indicated biotinylated cyPG at 10 μM for 2 h at room temperature prior to SDS-PAGE analysis, as in Figure 45. The gray dashed line represents two different exposures due to higher biotin levels in the last two lanes.

3.2.2 Binding of small reactive compounds to H-Ras and RhoB

It is possible that other small, bifunctional, thiol-reactive molecules could mimic the behavior of dienone cyPG with respect to binding to GTPases with C-terminal cysteines amenable to palmitoylation. A compound that meets these criteria and is commonly used in cell signaling studies, phenylarsine oxide (PAO, mass 168.02, structure shown in Figure 49B), acts as a tyrosine phosphatase inhibitor that forms adducts with proteins containing sulfhydryl groups close enough to form thioarsine rings (Gerhard et al., 2003; Wang et al., 2003). Indeed, as shown by MALDI-TOF MS in Figure 47A, PAO binding to H-Ras results in a mass increment compatible with addition of a single PAO molecule, which MS-MS analysis detected to be at the C-terminal palmitoylatable cysteines (Oeste et al., 2011). Additionally, since biotinylated 15d-PGJ_2 (15d-PGJ_2-B) binds to full-length H-Ras at its C-terminus, competition assays were performed to determine whether PAO could abrogate dienone cyPG addition. Figure 47B shows that pre-incubation with PAO reduced 15d-PGJ_2-B binding to H-Ras, as reflected by a reduction in biotin detection (28%±7 reduction for PAO versus vehicle-treated Ras). Similarly, the small reactive thiol cross-linker, dibromobimane (DBB, mass 350.01, structure shown in Figure 49B), also elicited a decrease in the biotin signal corresponding to 15d-PGJ_2-B (55% reduction, Figure 47C). The distance between the bromide ions in DBB that are lost upon binding to thiols of cysteines within close range

has been calculated to be approximately 3-6 Å (Sinz and Wang, 2001). Furthermore, DBB is known to undergo a fluorescent shift after bromine loss resulting from cysteine cross-linking (Kim and Raines, 1995), and can indeed be detected directly in gels when incubated with H-Ras (Figure 47C).

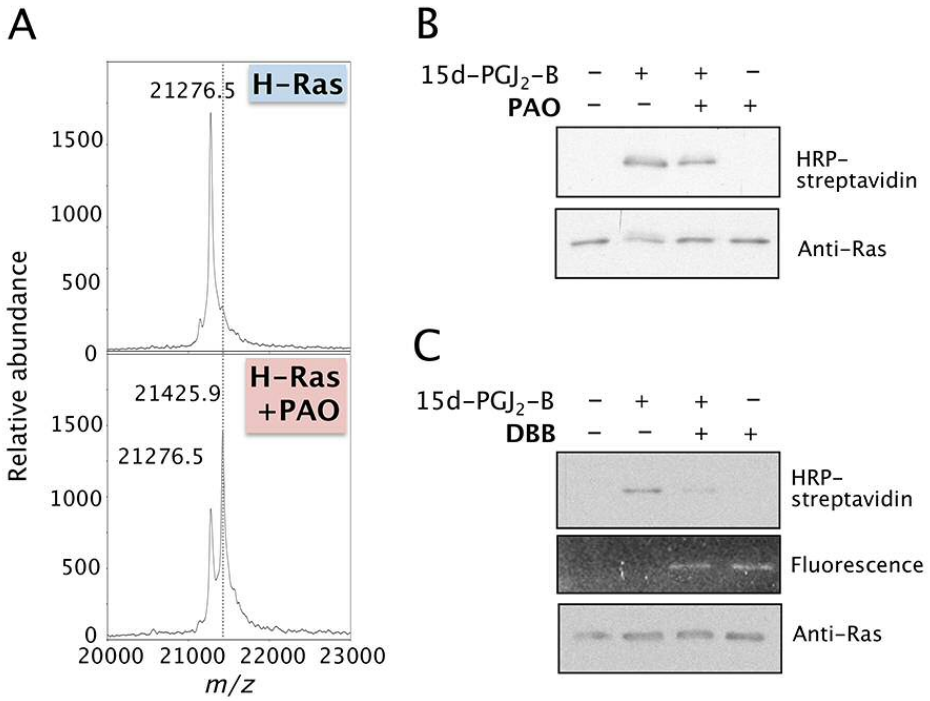

Figure 47. PAO and DBB binding to recombinant H-Ras *in vitro*.

(A) MALDI-TOF MS analysis of human recombinant H-Ras incubated with PAO. (B) Recombinant H-Ras at 5 μM was incubated for 30 min with 50 μM PAO before addition of 1 μM biotinylated 15d-PGJ_2 (15d-PGJ_2-B) for 1 h, where indicated. Incorporation of the biotinylated cyPG was assessed by SDS-PAGE, protein blot and detection with horseradish peroxidase (HRP)-streptavidin (upper panel) or WB with anti-pan Ras antibody (lower panel). (C) Competition of 15d-PGJ_2-B binding to H-Ras by DBB. Full-length H-Ras was incubated similarly to (B) with DBB. Incorporation of DBB was assessed by UV fluorescence detection (middle panel).

In light of the results obtained by SDS-PAGE analysis of RhoB modification by 15d-PGJ_2-B, competition experiments between 15d-PGJ_2-B and PAO or DBB were performed with RhoB, as well. There is a clearly detectable reduction in the biotin signal representing 15d-PGJ_2-B binding when the protein is pre-incubated with either PAO (Figure 48A) or DBB (Figure 48B). Similarly to the results obtained with H-Ras, UV gel fluorescence indicating direct DBB binding was also observed.

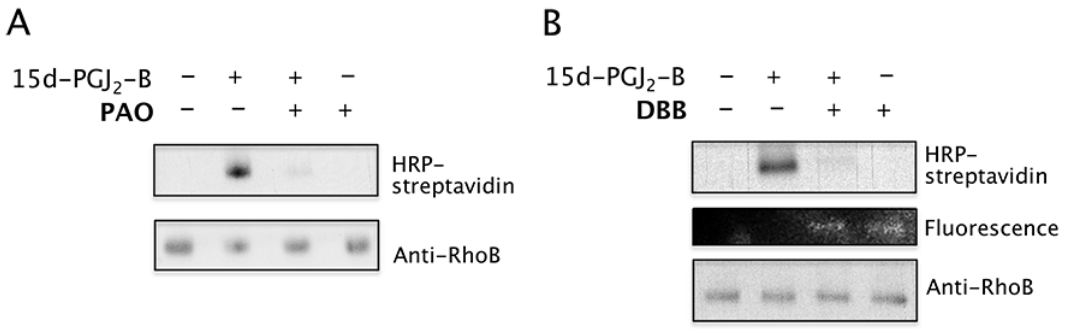

Figure 48. 15d-PGJ_2, PAO and DBB binding to recombinant RhoB *in vitro*.

(A) Recombinant RhoB at 5 μM was incubated for 30 min with 50 μM PAO before addition of 10 μM biotinylated 15d-PGJ_2 (15d-PGJ_2-B) for 1 h, where indicated. Incorporation of the biotinylated cyPG was assessed by SDS-PAGE, protein blot and detection with horseradish peroxidase (HRP)-streptavidin (upper panel) or western blot with anti-RhoB antibody (lower panel). (B) Competition of 15d-PGJ_2-B binding to RhoB by DBB. Full-length RhoB was incubated similarly to (A) with DBB. Incorporation of DBB was assessed by UV fluorescence detection (middle panel).

Several bifunctional reagents have therefore been shown to bind to either full-length H-Ras or RhoB (Figure 47 and Figure 48). Since these proteins contain vicinal cysteines, these compounds could be binding to both cysteine residues simultaneously. Moreover, as mentioned above, direct detection of DBB fluorescence upon incubation of H-Ras or RhoB with this compound indicates that it is bound to two cysteines within 3-6 Å of each other (Kim and Raines, 1995). To directly observe the cross-linking of palmitoylation cysteines elicited by bifunctional compounds, a synthetic peptide corresponding to the H-Ras C-terminus was used as a model in MALDI-TOF MS analyses. This peptide is equivalent to the fragment obtained by tryptic digestion of H-Ras, namely K170-K185 (m/z 1662.7, sequence in Figure 49B), which contains the palmitoylatable cysteines, and presents a more favorable sequence than the equivalent peptide of RhoB, in which the tryptic fragment would include the isoprenylation cysteine in addition to those amenable to palmitoylation. Peptide incubation with 15d-PGJ_2 presents a predominant peak corresponding to the addition of one PG molecule (m/z 1979.80,), as well as two oxidation peaks (m/z 1994.9 and 2010.7), as described in earlier works (Oliva et al., 2003; Renedo et al., 2007).

A

K170–K185: KLNPPDESGPG**C**MS**C**K

	Theoretical *m/z*
Unmodified peptide	1662.73
15d-PGJ_2 adduct (+316.5)	1979.23
PAO adduct (+150)	1812.75
DBB adduct (+188)	1850.73

B

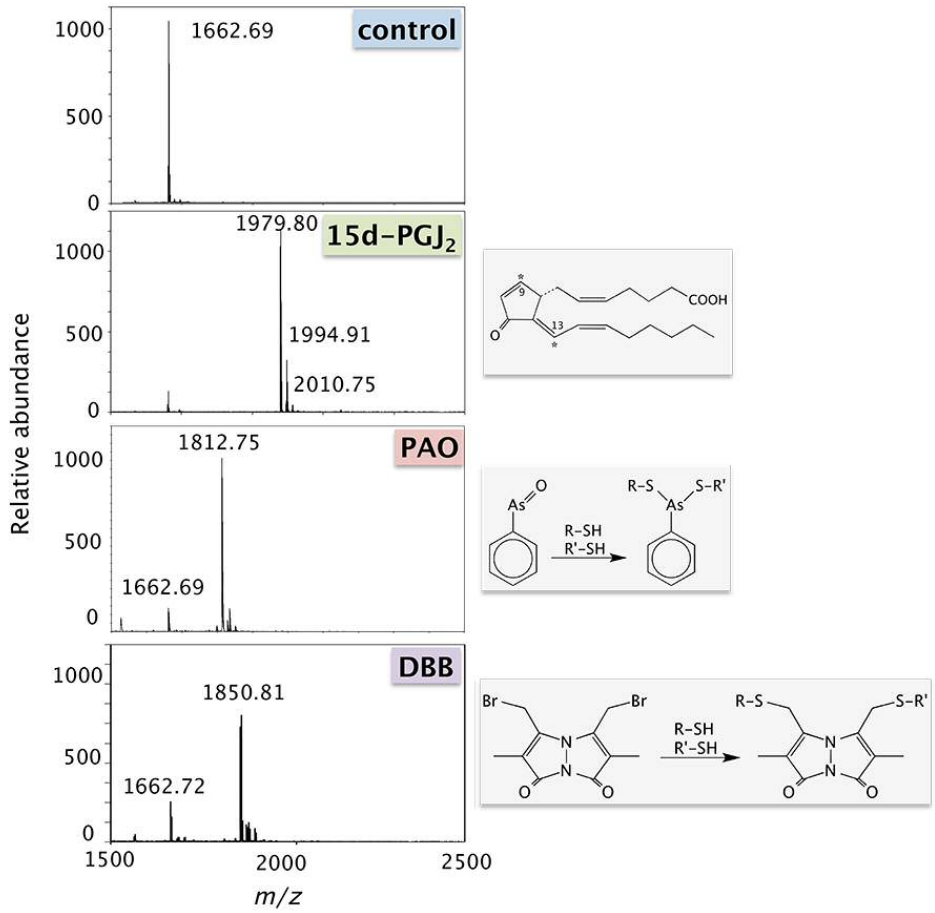

Figure 49. Modification of the K170-K185 H-Ras C-terminal peptide by 15d-PGJ_2, PAO and DBB.

(A) Sequence of the K170-K185 peptide with the modified cysteines in larger, bold font and summary of the theoretical peptide adducts for which compatible peaks were observed by MALDI-TOF mass spectrometry. (B) Incubation of the synthetic H-Ras C-terminal peptide, K170-K185, with either 15d-PGJ_2, PAO or DBB resulted in adducts detected by MALDI-TOF MS. Structures of the compounds employed are shown to the right of the spectra, with a schematic of adduct formation with two thiol groups in the case of PAO and DBB.

Incubation of the K170-K185 peptide with PAO gave rise to a single peak with m/z 1812.7 that represents the simultaneous binding to both cysteines, as depicted to the right of the PAO spectrum (Figure 49B). Likewise, DBB bound to the K170-K185

peptide, resulting in the appearance of a single peak of m/z 1850.81, compatible with a 1:1 adduct of peptide:DBB (Figure 49B). The small span of the DBB reactive groups and the fact that peptide dimers were not detected upon DBB incubation (Oeste et al., 2011) suggest that C181 and C184 are within close range of each other and hence amenable to intramolecular cross-linking by DBB (Figure 49B, bottom).

It should be noted that the H-Ras hypervariable domain does not present a well-defined structure in solution (Thapar et al., 2004), whereas membrane binding induces a more rigid conformation (Gorfe et al., 2007). Therefore, cross-linking of C181 and C184 by 15d-PGJ_2, PAO or DBB binding could potentially stabilize a fixed conformation and disturb H-Ras membrane interactions. These results pave the way for studies in cells to determine the functional repercussion of direct modification by small electrophilic moieties. Assays performed on cells transfected with H-Ras constructs have shown that, indeed, its localization and activation shift from the plasma membrane to endomembranes upon treatment with PAO or DBB (Oeste et al., 2011). Preliminary assays using RhoB have proven unfruitful due to its rapid degradation and low basal levels in cells, though further studies are warranted to determine the cellular effect of binding of these compounds to RhoB.

DISCUSSION

1. Role of the hypervariable motif in small GTPase subcellular localization

Many small GTPases are singly or doubly isoprenylated and some of them undergo further post-translational modifications by palmitoylation. In addition to C-terminal lipidation, the hypervariable region of some Ras superfamily proteins contain basic residue patches that interact with anionic phospholipids that accumulate at particular subcellular membranes and others include further sorting elements such as motifs recognized by adaptors (Bonifacino and Traub, 2003). Significantly, these structural motifs determine subcellular localization patterns that derive from or elicit conformational changes extending to the totality of the protein, which ultimately govern GTPase activation states and signaling functions. In fact, hypervariable regions containing very similar motifs can give rise to different endomembrane sorting on the basis of distinct lipid moiety spacing or even the nature of a few neighboring amino acids.

1.1 Endosomal GTPases appear at distinct subcellular membranes

Studies regarding the hypervariable region sequences of several small GTPases were carried out to assess the structural determinants involved in subcellular localization. Previous studies from the laboratory established the RhoB C-terminal sequence as a motif for sorting to endolysosomes and lysosomal degradation (Pérez-Sala et al., 2009). This behavior depends on its isoprenylation and double palmitoylation, which begged the question of whether other similarly lipidated small GTPases such as H-Ras, Rap2A and B, or TC10 presented similar subcellular localization. As has been performed in detail for H-Ras (Gorfe et al., 2007), short constructs bearing sequences pertaining only to the isoprenylation and palmitoylation motifs of these proteins aided in determining the impact on sorting and degradation of their full-length counterparts.

The results shown in Section 1.1 of the Results indicate that sorting into MVB and subsequent lysosomal degradation is highly specific for RhoB. Though the TC10 C-terminus is very similar to that of RhoB, a basic amino acid patch upstream of the palmitoylation cysteines is responsible for retention at limiting membranes of MVB and

hampers inclusion into ILV (Valero et al., 2010). Indeed, this basic residue motif could mediate an electrostatic interaction of TC10 with the most abundant negatively charged phospholipid, i.e. phosphatidylserine, which is found mainly on the cytosolic surface of endosomes and the plasma membrane (Leventis and Grinstein, 2010; Urade et al., 1988; Yeung et al., 2008), hence obstructing entry into the lumen of MVB and subsequent degradation. Other bipalmitoylated proteins were found similarly retained at the limiting membranes of endolysosomes, such as the Rap2 isoforms (Valero et al., 2010). In this case, the alternate spacing between lipidated residues could confer a distinct overall three-dimensional conformation at the C-terminus of Rap2 proteins that promotes association with membrane microdomains of singular properties. Short constructs derived from the H-Ras C-terminal sequence were mainly present at the plasma membrane, as previously described (Gorfe et al., 2007). It could therefore be postulated that combinations of electrostatic interactions and reversible palmitoylation are responsible for endowing C-termini with conformations that allow binding to membrane regions of well-defined characteristics. Taken together, these results indicate that the isoprenylation and palmitoylation motif of RhoB constitutes a precise structure with affinity for particular membrane domains that determines its selective sorting through the endolysosomal pathway into the lumen of MVB.

1.2 The RhoB C-terminus CINCCKVL is an MVB and endolysosomal marker

Several studies from our laboratory have shown that the fully processed RhoB C-terminal sequence CINCCKVL co-localizes with endolysosomal probes such as LTR, Lamp1, Rab7, Rab9 and CD63 constructs, or LBPA, as well as appearing directly at ILV of MVB (Oeste et al., 2014; Pérez-Sala et al., 2009; Valero et al., 2010). These results were confirmed through the use of several fusion proteins containing this sequence, including varied fluorescent constructs such as GFP, RFP and its photostable forms (tagRFP, tagRFP-T), mCherry, or photoswitchable Dendra2. Intracellular live markers are not devoid of pitfalls, such as endosome enlargement induced by overexpression of Lamp1 or Rab7 constructs and induction of stress fibers by transfecting with full-length RhoB fusion proteins (unpublished observations). In the case of CINCCKVL chimeras, no detectable morphological abnormalities have been encountered during its use, so far.

Furthermore, work from the laboratory in live BAEC and HeLa reported a lack of overlap with several autophagy probes after induction of autophagy such that independent GFP-8-positive structures were clearly distinct from RFP-LC3 autophagosomes (Oeste et al., 2013). CINCCKVL localization to Golgi compartments is also negligible when full modification is allowed (Oeste et al., 2014). As will be discussed below, lipidation status is crucial to CINCCKVL sorting through the endocytic pathway, and can hence be regulated to track subcellular organelles or detect overall isoprenylation precursor status through statin switch assays. Therefore, CINCCKVL fusion proteins may be used as markers amenable to pharmacological modulation for dynamic tracking of MVB and endolysosomes in live cells.

1.3 CINCCKVL localization at endolysosomes depends on lipid modifications

The presence of CINCCKVL proteins at endolysosomes is completely dependent on full post-translational processing by lipids. It is shown in this work that isoprenylated but non-palmitoylated constructs are diffuse within the cytoplasm but exclude the nucleus and are in part retained at the Golgi apparatus, where palmitoyl transferases are usually accumulated, which could represent species that are awaiting palmitoylation, (Aicart-Ramos et al., 2011). In contrast, non-lipidated forms spread throughout the cell, leaving some small, LTR-positive vesicles empty. It therefore becomes apparent that palmitoylation is a *sine qua non* for CINCCKVL entry into endolysosomes, as shown schematically in Figure 50. Similarly, studies involving the Ca^{2+} sensor synaptotagmin 7 described that its palmitoylation elicits association with CD63 and subsequent sorting to lysosomes, whereas non-palmitoylated forms are retained in the Golgi (Flannery et al., 2010). However, these instances are in contrast with the more numerous cases of proteins in which palmitoylation precludes access to lysosomes, as seen in (McCormick et al., 2008; Pérez-Sala et al., 2009). For example, recycling of the M6P receptor from lysosomes to the Golgi is dependent on its N-terminal palmitoylation, for palmitoylation-defective mutants accumulate into dense lysosomes (Schweizer et al., 1996).

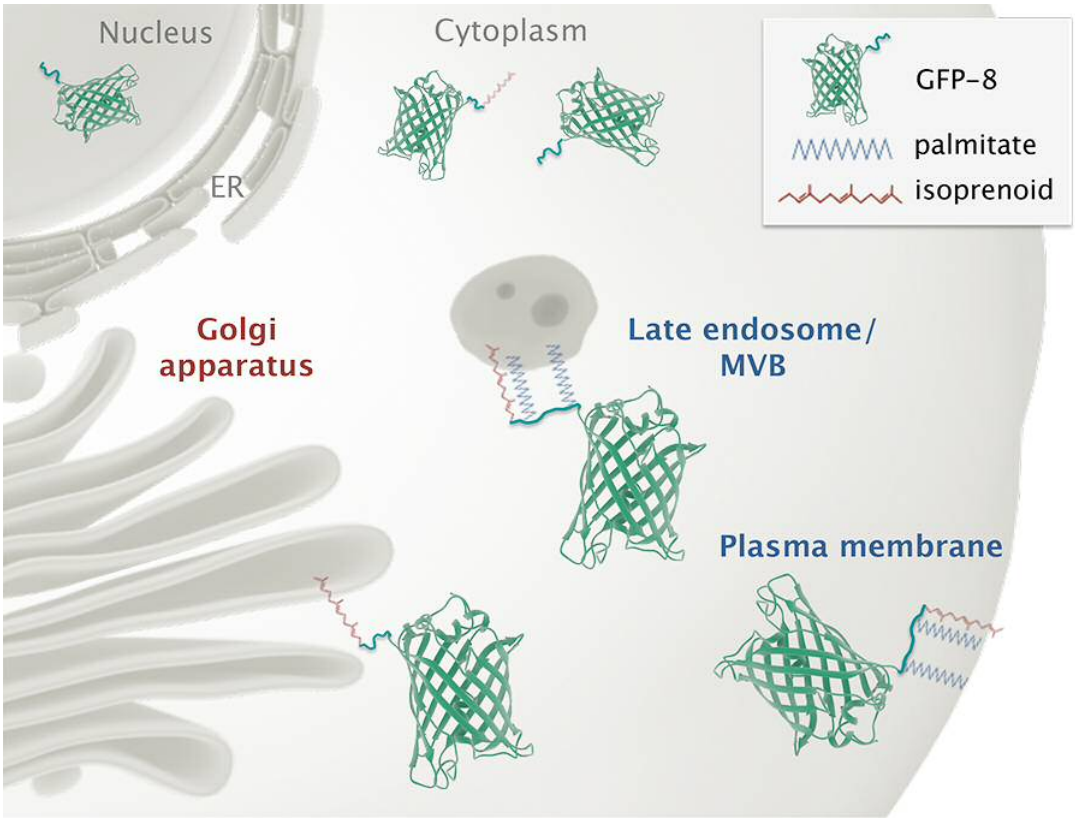

Figure 50. GFP-8 subcellular localization depends on its lipid modifications.

The GFP structure appears as a ribbon diagram in green, with the CINCCKVL motif represented as a green squiggle attached to it. Totally unlipidated forms are completely diffuse throughout the cytoplasm and the nucleus (gray font), whereas isoprenylated forms exclude the nucleus, are predominantly cytosolic and are sometimes associated with the Golgi apparatus (red font). However, isoprenylated and bipalmitoylated GFP-8 appears at late endosomes/MVB and the plasma membrane (blue font). See text for details.

Concerning the GPCR, PAR-1 (protease-activated receptor 1), there seems to be an interplay between its YXXΦ sorting motifs and palmitoylation, such that correct sorting mediated by the tyrosine motif requires correct modification by palmitate and PAR-1 mutants lacking palmitoylation cysteines are degraded in lysosomes to a higher extent (Canto and Trejo, 2013). The yeast protein Vac8 is localized at the vacuolar membrane in yeast, though internalization into this compartment has not been described (Peng et al., 2006). Hence, a general role for palmitoylation in protein sorting is lacking, since the consequences of modification by this lipid seem to be protein-specific and cell-type dependent. Additionally, palmitoylation of RhoB constructs is probably accountable for the lack of interaction between either GFP-8 or GFP-RhoB with RhoGDIα as compared to that detected for GFP-RhoA (Oeste et al., unpublished observations), as previously hypothesized (Michaelson et al., 2001). Nevertheless, it still

remains to be established whether non-palmitoylated RhoB constructs interact with RhoGDI in the cytosol (Ho et al., 2008).

Upon isoprenylation inhibition, full-length RhoB-derived constructs behave as cytosolic proteins, similarly to unprenylated GFP-8 (see Figure 50). Therefore, both membrane and RhoGDI binding cannot occur and RhoB could be degraded through the expected proteasomal pathway followed by soluble proteins. In fact, excessive overexpression of fluorescent RhoB constructs elicits diffuse accumulation in the cytosol, most likely due to saturation of the lipidation machinery and subsequent lack of precursors. Such "extra" proteins could become ubiquitinated and degraded through the proteasome, which is a putative scenario for a study detecting RhoB ubiquitination upon overexpression of RhoB and ubiquitin in cells treated with proteasomal inhibitors (Engel et al., 1998). Indeed, RhoB is an early response gene and its levels can rise quickly within the cell to overcome damage by UV exposure (Canguilhem et al., 2005). It would be interesting to detect whether, following this stimulus, the newly synthesized proteins are capable of becoming isoprenylated and bipalmitoylated to follow the endolysosomal pathway described herein, or whether full lipidation occurs to maintain low RhoB levels principally in resting state conditions.

Pharmacological statin treatment, which is widely prescribed for hypercholesterolemia, greatly increases levels of unprocessed RhoB in the cytosol (Stamatakis et al., 2002). Another report determined that an increase in non-prenylated Rho protein translates into overall elevated levels of GTP-bound Rho as compared to untreated cells expressing normal levels, suggesting that Rho-dependent signaling pathways are more active in statin-treated cells (Turner et al., 2008). Furthermore, it has been previously described that accumulation of unprocessed, soluble forms of Rho proteins (mostly RhoA) are partly responsible for the serious side effects resulting from abrupt statin withdrawal, which implies a sudden lift of the blockade on isoprenoid precursor formation. The accumulated Rho protein is rapidly modified by newly synthesized geranylgeranyl moieties and translocates to the plasma membrane, strongly activating its signaling cascades, including repression of endothelial nitric oxide synthase (eNOS). This phenomenon causes a dangerously abrupt drop in nitric oxide production in cardiac endothelial cells, hence impairing vascular function (Laufs et al., 2000). These effects were studied in detail in the context of RhoA, but the concomitant

increase in unprocessed RhoB concentration in cells from patients undergoing statin treatment warrants further investigation.

1.4 CINCCKVL sorting is conserved from fungi to human cell models

Cells from very diverse species including ascomycetous fungi, insects, amphibians and several mammals are all able to sort RhoB C-terminus constructs to the vacuole or endolysosomes. However, they endogenously express different sets of Ras superfamily proteins, and in some cases a clear RhoB homolog has not been identified or is not localized to endosomes. Mammals and birds express identical RhoB proteins, but organisms studied in this work that are lower on the evolutionary scale differ in their C-terminal RhoB sequence or do not encode a RhoB homolog, as seen in insect cells. In the case of *Schizosaccharomyces pombe,* there is a RhoB homolog termed Rho2 that appears at the plasma membrane, the septation site and growing ends (Hirata et al., 1998). However, this protein contains only one palmitoylated cysteine close to the isoprenylation site (Roth et al., 2006), which is modified by a farnesyl moiety (Ma et al., 2006) in *lieu* of the preferential geranylgeranylation that takes place on RhoB in cells (Roberts et al., 2008). RhoB can become alternatively isoprenylated, though studies with constructs containing CAAX boxes more inclined to either modification, namely GFP-CINCCKVL and GFP-CINCCLVM (geranylgeranylated or farnesylated, respectively), did not present detectable differences as to their endolysosomal localization, so that a crucial role for the length of the C-terminal isoprenoid is not likely (Oeste et al., unpublished observations). Another yeast protein, RasA, is indeed bipalmitoylated, but it accumulates at the plasma membrane and disrupting its palmitoylation elicits a patchy intracellular distribution (Fortwendel et al., 2012). *Aspergillus nidulans* codes for a putative Rho2-like protein expected to be geranylgeranylated and palmitoylated, though a homolog for GGTase I has not yet been biochemically identified in this species.

The instances of lipidated proteins in lower organisms described above highlight the fact that, though these species are able to sort CINCCKVL to endolysosomes, none of their endogenous proteins have been described to follow this route directly. It is therefore worth examining whether the sorting machineries potentially responsible for

RhoB construct sorting in mammals, i.e. Rabs, ESCRT or the tetraspanin CD63, are conserved from fungi to human cells. Indeed, the basic Rab components of the endocytic route are conserved throughout metazoan evolution. In-depth phylogenetic studies on Rab family proteins highlight the existence of a large number of Rabs early on in evolution (Elias et al., 2012; Klöpper et al., 2012). Moreover, it has been proposed that the latest eukaryotic common ancestor (LECA) contained more than 20 core Rab proteins that have suffered expansions by gene duplication or losses throughout eukaryotic evolution (Klöpper et al., 2012). Further human Rabs have arisen from gene duplication of the fundamental Rabs associated either to early endosomes (Rab5), late endosomes (Rab7 and Rab9) recycling endosomes (Rab11) and so on, up to the ten subfamilies identified through phylogenetic studies of mammalian Rabs (Pereira-Leal and Seabra, 2000). Interestingly, CINCCKVL chimeras are present inside vesicles that are marked at their limiting membranes by proteins included in a category containing late endosomal LECA Rabs (group III), such as Rab7.

As is the case for Rab proteins, at least one component from each of the ESCRT-I, -II or –III complexes is present in fungi and metazoans (Wideman et al., 2014). However, outside Ophisthokonta, ESCRT-0 is completely absent, so that other mechanisms for ubiquitin recognition must exist in organisms present before the LECA branched off from other life forms (Leung et al., 2008). Considering the role of ESCRT proteins in MVB biogenesis, it would be expected that organisms with defined intracellular compartments would require their action for correct endosomal sorting. However, *Archaea* have also been shown to contain ESCRT components, though only ESCRT-III and Vps4 (Samson et al., 2008). Such is the case due to the vital role of several ESCRT proteins in membrane abscission during cytokinesis (Rusten et al., 2012). Furthermore, ESCRT proteins are also involved in virus budding, such as human immunodeficiency virus-1 (HIV-1) egress from the plasma membrane, which follows an "inside-out" route from the cytoplasm that is topologically similar to ILV formation (Garrus et al., 2001; Morita and Sundquist, 2004).

Therefore, the Rab and ESCRT proteins found to co-localize with CINCCKVL and RhoB constructs or involved in their sorting could potentially be present in the diverse species studied. In the case of tetraspanin proteins, fungi have been found to contain homologs, though in *Aspergillus nidulans* only a tetraspanin-like protein has

been proposed by sequence homology but has not been characterized (Lambou et al., 2008).

2. RhoB subcellular sorting mechanisms

The structural determinants guiding endosomal small GTPase sorting include lipidation motifs and amino acids of specific characteristics. In the case of RhoB, its C-terminus CINCCKVL represents a unique structure upon lipidation that attaches to the very specific subcellular localization of late endosomal pathway vesicle lumina that is conserved in cells from many organisms. In human cells, targeting to ILV of MVB such as occurs for RhoB does not necessarily mean degradation at lysosomes, though RhoB constructs are indeed degraded mainly through this pathway (Pérez-Sala et al., 2009). As described previously, proteins present at MVB can also be exocytosed by fusing with the plasma membrane or recycled back to the Golgi apparatus as well as being delivered to the lysosome (Futter et al., 1996; Lu and Hong, 2014; Murk et al., 2002; Vlassov et al., 2012). However, there is still debate as to whether the same MVB contains ILV directed towards different sites or if there are specialized MVB that deliver all their ILV to the same subcellular destination (Edgar et al., 2014; van Niel et al., 2011; Vlassov et al., 2012). Therefore, it was crucial to investigate some of the trafficking pathways that lead proteins to and from MVB in eukaryotic cells to determine their role in sorting of RhoB and its last eight amino acids. The interplay between protein sequence and lipid modifications in sorting of these proteins warranted the study not only of protein complexes involved in shuttling material within the cell, but also of the lipid features of the membranes to which they attach.

2.1 Differential role of the ESCRT machinery in sorting of RhoB versus CINCCKVL constructs

Protein sorting into MVB is at the convergence of several endocytic routes, as well as a hub towards other intracellular destinations. ESCRT proteins regulate the canonical pathway described for entry into MVB of many proteins, such as the EGF

receptor. Previous work from the laboratory suggested the involvement of this machinery in RhoB sorting through the use of Vps4 dominant negative constructs in BAEC (Pérez-Sala et al., 2009). Furthermore, other routes to the MVB such as autophagy, microautophagy or chaperone-mediated autophagy are highly unlikely routes for trafficking this GTPase, as discussed in (Oeste et al., 2014). It was therefore possible that the ESCRT machinery played a role in RhoB sorting.

ESCRT-mediated sorting into MVB, when dependent on the whole machinery, begins by ubiquitination of cargo such as EGFR. Ubiquitin-independent mechanisms also exist, but these usually involve only late ESCRT components and ESCRT-III-associated proteins such as Alix. Many attempts at detecting ubiquitination of RhoB constructs were undertaken for this work, including stimulation with EGF, treatment with proteasomal or lysosomal degradation inhibitors, or simvastatin treatment to accumulate RhoB, though none of them resulted in a clear signal of ubiquitinated full-length RhoB or CINCCKVL proteins, rendering these results inconclusive (not shown). Interestingly, the GFP-22 construct that showed a faint ubiquitin signal contains a lysine residue that could become ubiquitinated, but might be less exposed in full-length RhoB, such that regulated processes could mediate its amenability to ubiquitination. However, use of ESCRT siRNA to silence some components of the machinery and observation of GFP-RhoB and GFP-8 by live microscopy revealed differential phenotypes, so that ESCRT could be involved regardless of ubiquitination. Strikingly, by using these constructs in parallel, a distinctive subcellular localization was observed upon depletion of the ESCRT components Hrs and Tsg101. These were the first studies to show differential behavior between full-length RhoB, which showed impaired sorting in cells depleted of these ESCRT, and its chimera, GFP-8, which was sorted into endolysosomes in these cells. It is possible that RhoB is in fact ubiquitinated but we have not achieved its detection, either because its ubiquitination is fast and transient or because it is rapidly degraded in the lysosome upon ubiquitination, or both. In any case, our results suggest that GFP-RhoB would follow an ESCRT-mediated pathway into the lumen of endolysosomes, be it ubiquitin-dependent or -independent. In contrast, GFP-8 would not become ubiquitinated and could therefore follow ceramide and CD63-driven budding into MVB and pinch off to become ILV regardless of alterations in the ESCRT machinery.

Differences encountered between GFP-8 and GFP-RhoB give rise to a working hypothesis for the molecular players involved in RhoB and CINCCKVL localization and sorting. This view is schematized in Figure 51 and will aid in discussing the possible sorting mechanisms throughout the following sections, as well as in future studies.

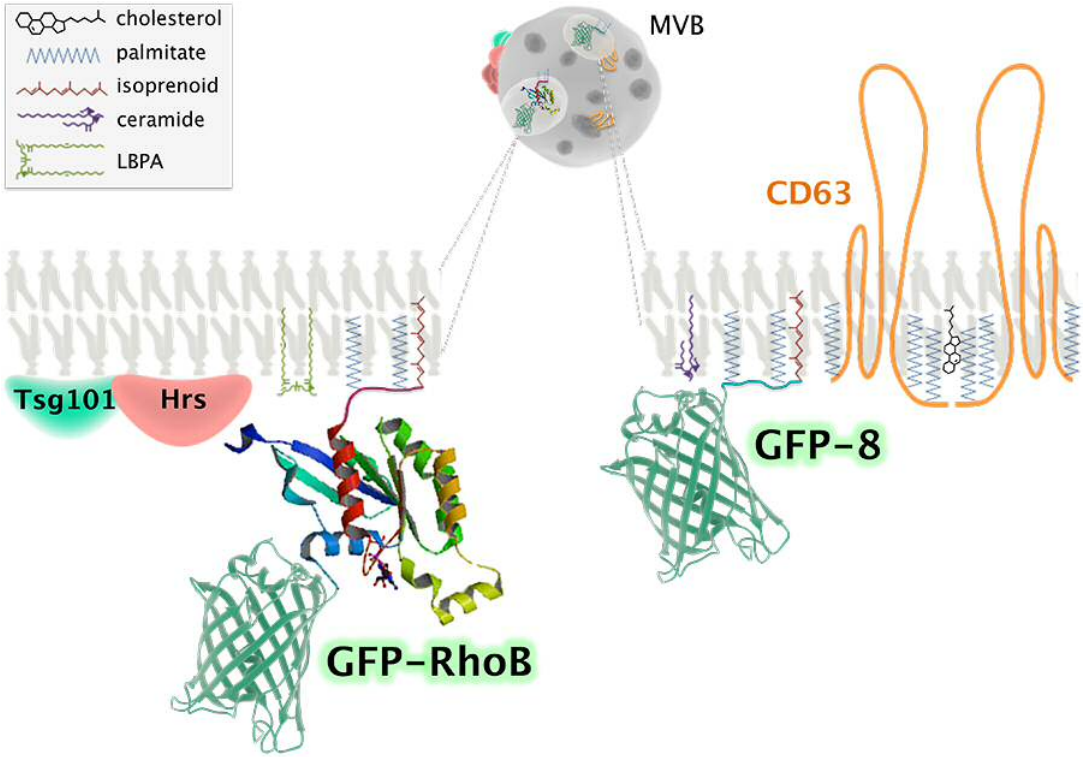

Figure 51. Schematic of possible membrane platforms for GFP-RhoB and GFP-8.

Zoom-in on putative differential ILV of MVB containing either GFP-RhoB or GFP-8. The results shown in this work point to a possible role for the ESCRT proteins Hrs and Tsg101 in GFP-RhoB sorting (left membrane), but not for that of GFP-8. The larger ILV into which GFP-RhoB enters would contain the late endosome lipid, LBPA (light green). In contrast, CD63 could be involved in GFP-8 sorting, as well as cholesterol dynamics (right membrane). Furthermore, ceramide treatment could induce the appearance of GFP-8 in small ILV containing CD63, which could putatively be secreted to the extracellular space.

2.2 Effects of agents altering cellular lipid dynamics on CINCCKVL and full-length RhoB sorting

Apart from the protein machineries involved in intracellular sorting, the lipid composition of endosomal membranes plays a key role in cargo trafficking and MVB biogenesis (Bissig and Gruenberg, 2013; Bissig et al., 2012). In fact, lipid microdomains in the *Saccharomyces cerevisiae* vacuole were recently found to mediate protein

segregation (Toulmay and Prinz, 2013). On one hand, bulk lipids can convey specific conformations to membranes according to their three-dimensional properties, so that conical lipids induce curvature and straight molecules increase membrane order, i.e. diacylglycerol and cholesterol, respectively (Bigay and Antonny, 2012). Altering cholesterol dynamics in several cell types by pharmacological treatment indeed disrupts the association of CINCCKVL constructs to endolysosomes. On one hand, treatment with U18666A, which increases membrane invagination into MVB (Marchetti et al., 2004), gives rise to prominent accumulations of CINCCKVL chimeras within endolysosomes containing LBPA, cholesterol and delimited by markers such as Lamp1-GFP, GFP-Rab7 or -Rab9 (Valero et al., 2010), reflecting their specific association with ILV. On the other hand, inhibiting cholesterol biosynthesis by ZGA treatment induced MVB dilation and a striking retention of proteins at MVB limiting membranes, i.e. GFP-8 or CD63 constructs, which normally internalize into ILV in control cells (Oeste et al., 2014), though this retention was not observed for GFP-RhoB, which still entered endolysosomes upon ZGA treatment (Figure 36).

The results observed for GFP-8 agree with previous reports describing ILV as the major cholesterol-containing vesicles in the endosomal pathway (Möbius et al., 2003). It is possible that overall cholesterol depletion would therefore affect these structures more markedly, hampering the route followed by GFP-8 for invagination into MVB (see Figure 51). In fact, endothelial cells have been shown to contain cholesterol-rich membrane domains in their MVB (Amiya et al., 2013). Moreover, mice deficient in the last enzyme of the cholesterol biosynthetic pathway (Δ24 sterol reductase) present reduced ILV material within their MVB, which follows the same pattern as the reduction of GFP-8 and CD63 constructs in the lumen of MVB upon ZGA treatment (Gilk et al., 2013). Cholesterol has also been found to stabilize particular microdomains containing specialized phosphoinositides (Jiang et al., 2014), so that altering its dynamics could affect these small signaling platforms, as well. Furthermore, specific lipids exist at defined membrane microdomains, as is the case for the curvature-inducing lipid LBPA in endolysosomes (Matsuo et al., 2004), or particular phosphoinositides along the endocytic pathway (Di Paolo and De Camilli, 2006). In this regard, full-length RhoB constructs co-localize to a large extent with LBPA in the endolysosomal lumen (Pérez-Sala et al., 2009), whereas the PI(3)P marker 2xFYVE

appears at small, dispersed vesicles that do not overlap with RhoB or CINCCKVL constructs (Oeste et al., unpublished observations). Therefore, sorting of RhoB constructs is dependent on lipid-mediated mechanisms of ILV formation for which cholesterol and LBPA are essential.

2.3 CD63 overexpression has differential effects on full-length RhoB and CINCCKVL localization

Sorting mediated by tetraspanins and TEM are a telling example of the intrinsic relationship between protein sequence, lipid modifications and membrane organization. In the case of CD63, its four transmembrane domains direct insertion into membranes, its YXXΦ motif guides intracellular trafficking, and palmitoylation at cysteine residues determines attachment to membranes of specific characteristics in a cholesterol-dependent manner (Charrin et al., 2003; Israels and McMillan-Ward, 2010; Pols and Klumperman, 2009; Yang et al., 2002). These features give rise to CD63 sorting to specific membrane microdomains, which are also the destination for RhoB chimeras, i.e. ILV of MVB and the plasma membrane, to a varying extent. In fact, co-localization studies in resting cells show almost total overlap between wild-type CD63 constructs and CINCCKVL chimeras, and to a lesser degree with full-length RhoB constructs. As depicted in Figure 51, it could be hypothesized that GFP-8 is intimately connected to TEM through its palmitate residues by a similar cholesterol-dependent mechanism that keeps CD proteins together (Charrin et al., 2003). The lack of further sorting determinants in GFP-8 would render the protein quite dependent on TEM dynamics. Therefore, disruption of CD63 intracellular trafficking such as that which could take place upon overexpression of CD63 constructs, particularly the Y235A mutant, would hinder binding to AP-3 complexes, which could alter CD63 sorting to TEM at MVB and therefore result in a concomitant misplacement of GFP-8. AP-3 has been shown to contribute to the regulated secretory pathway, as AP-3 depletion reduces regulated secretion of secretogranin II, though it elicits an increase in its constitutive secretion as a compensatory mechanism (Asensio et al., 2010). Therefore, a putative indirect association of GFP-8 to AP-3 via CD63 could be abolished in a scenario of altered CD63 sorting such as cells overexpressing CD63 constructs, sending CINCCKVL proteins

towards constitutive exocytosis. In contrast, additional sorting motifs, interactions with effectors, or an active role in endosomal dynamics could be responsible for full-length RhoB localization at endolysosomes without partaking in secretion mechanisms, regardless of changes in CD63 sorting. In any case, these results set forth the possibility that CINCCKVL chimeras could also appear in the extracellular space, which is congruent with their localization at ILV of MVB containing CD63 and possibly destined for exocytosis.

Biogenesis of ILV destined towards exocytosis, which contain CD63, can occur independently of the ESCRT machinery; instead, the curvature-inducing lipid, ceramide, mediates inward budding from the MVB limiting membrane (Trajkovic et al., 2008). Follow-up studies to determine whether CINCCKVL proteins can be delivered to the extracellular space were performed by exogenous treatment with C6 ceramide. These studies revealed that this lipid elicits an "emptying out" of cells co-transfected with GFP-8 and CD63, with a concomitant appearance of fluorescent extracellular material and reduction of GFP-8/mCherry-CD63 co-localization. On the other hand, GFP-RhoB was retained at several subcortical sites below the plasma membrane and did not appear in secreted membranous structures. Full-length RhoB could therefore contain a motif(s) upstream from the CINCCKVL sequence acting as a retention signal to bar its exit from the cell. Indeed, very few instances of human extracellular vesicle-associated RhoB have been described, including one report in exosomes of colorectal cancer cells, another report describing RhoB in exosomes from urine, and three studies in which microvesicles were found to contain RhoB (www.microvesicles.org). Furthermore, under the conditions employed in preliminary assays for isolating an extracellular vesicle fraction by sequential ultracentrifugation, we were unable to detect RhoB (unpublished observations).

It is worth noting that a study using numerous chimeric proteins postulates that cytosolic proteins with a tendency to oligomerize, when attached to a lipid anchor, become secreted into the extracellular medium. Indeed, a GFP-tagged, oligomeric, cytosolic protein with a RhoB-related isoprenylation and mono-palmitoylation sequence attached (CCKVL) is detectable in an exosome/microvesicle fraction, albeit to a much lesser degree than the positive controls containing either an N-myristoylation tag or a PIP_2-binding domain (Shen et al., 2011). However, throughout this work we

have used different fluorescent proteins besides GFP, some of which are theoretically expressed as monomers and therefore would not necessarily follow this oligomerization trend *per se*, e.g. mCherry, which stands for *m*onomeric Cherry (Shaner et al., 2004). Interestingly, the Hrs domain 2xFYVE is practically incapable of eliciting a secretory phenotype in the study mentioned above. It could be hypothesized that the potential RhoB-Hrs interaction hinted at by Hrs KD cells guides RhoB constructs into ILV destined towards degradation at the lysosome, hindering its entry into exocytic ILV into which GFP-8 is sorted and retaining GFP-RhoB within the cell, as described above. These distinct phenotypes only appear upon altering cellular homeostasis, such as ESCRT depletion or C6 ceramide treatment, but not under resting conditions. Whether these distinct ILV subpopulations exist within the same MVB will be the subject of further studies, though co-transfection of CINCCKVL and RhoB constructs has proven highly toxic, perhaps due to lipid precursor depletion (results not shown).

Considering that lipidated CINCCKVL constructs are fused directly to GFP and have no other RhoB-derived sequences, the differences encountered between these proteins and full-length RhoB constructs point to other sorting, signaling, or interaction sequences upstream of the lipidation sites. A close look at the RhoB sequence does indeed bring up interesting sequences and residues as hypothetical recognition motifs, as shown in Figure 52.

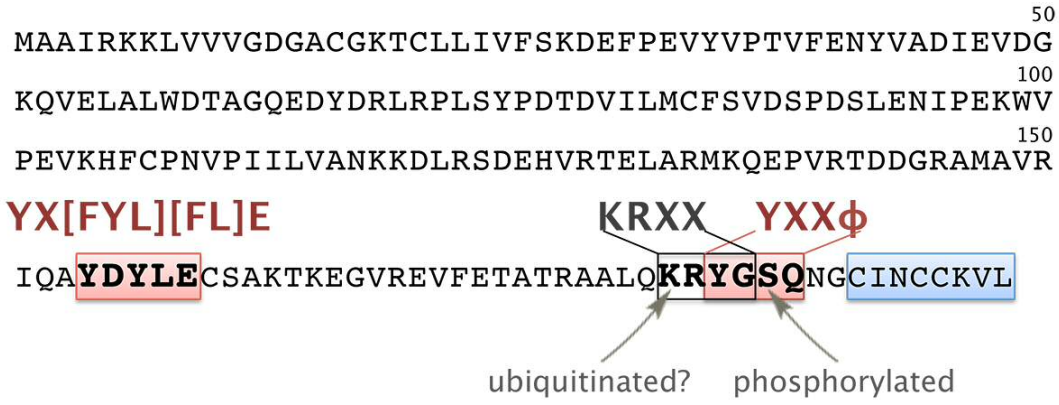

Figure 52. RhoB sequence and possible sorting motifs upstream of its lipidation region.

The full-length human RhoB sequence is shown. The lipidation motif, CINCCKVL is highlighted in blue, while possible AP-interaction motifs are boxed in red or black. The YDYLE sequence fits with a putative motif recognized by AP-4, namely "YX[FYL][FL]E". The second is a putative YXXΦ motif that is recognized by several AP complexes. The "KRXX" sequence is a hypothetical AP-3 binding motif. Arrows mark a possibly ubiquitinated lysine residue and a serine that becomes phosphorylated. See text for details.

Indeed, it has been reported that serine 185 of RhoB, close to its palmitoylation cysteines (see Figure 52), is phosphorylated by casein kinase-1, which hampers stress fiber formation and EGF receptor stabilization (Tillement et al., 2008). As discussed above, a few amino acids upstream, there is a lysine residue included in the GFP-22 construct that could be amenable to ubiquitination. RhoB also possesses a sequence matching a recently described, non-canonical AP-3 interaction motif of interferon-induced transmembrane (IFITM) protein 1, i.e. the dibasic patch "KRXX", as shown in Figure 52. Interestingly, two possible YXXΦ motifs appear in regions upstream of the CAAX box that are unique to RhoB. As seen in Figure 52, that which is closest to the C-terminus, "YGSQ", follows a rather canonical pattern and could hence be recognized by several AP complexes (Bonifacino and Traub, 2003). Furthermore, this sequence includes the phosphorylatable serine and its recognition by AP complexes could therefore depend on its phosphorylation state. The other YXXΦ motif, "YDYLE", appears further upstream (Figure 52), beginning with Tyr154, and is a striking match to the motif that mediates AP-4 binding for trans-Golgi to endosome sorting of the amyloid precursor protein, namely YX[FYL][FL]E (Burgos et al., 2010; Park and Guo, 2014). RhoB interaction with AP-4 would hypothetically be consistent with exit from the Golgi after palmitoylation, *en route* towards its endosomal localization.

Preliminary localization studies were carried out with mutants of tyrosines belonging to these hypothetical YXXΦ motifs, namely, GFP-RhoB-Y154A and GFP-RhoB-Y183A. However, there were no apparent changes in subcellular localization in basal conditions compared to wild-type GFP-RhoB by live confocal microscopy observation. Further studies are needed to address the possibility that response to stimuli such as EGF or alteration of endocytic components such as those used throughout this work would yield discrete phenotypes, or to assess the behavior of these mutants at different time points to detect whether their trafficking is delayed or expedited due to hypothetical disruption with AP complexes.

3. Small GTPases in pathological scenarios

3.1 RhoB constructs appear at endolysosomes in cell models with impaired endolysosomal dynamics

Mutations in several proteins involved in intracellular sorting or lipid homeostasis give rise to an array of lysosomal storage diseases characterized by oculocutaneous albinism, deficiencies in immune processes and neurodegenerative defects (Ballabio and Gieselmann, 2009). These cell models have been widely studied to elucidate intracellular sorting machineries and the routes followed by particular proteins, so that it was deemed necessary to benefit from this approach in the context of RhoB trafficking. Among these disorders, Niemann-Pick Type C Disease is clearly linked to altered cholesterol dynamics, since the mutated protein NPC-1 is responsible for shuttling cholesterol at endolysosomes (Mukherjee and Maxfield, 2004). In turn, Hermansky-Pudlak Syndrome patients develop this disease due to mutation of several proteins, including AP-3 or Rab27, both involved in LRO biogenesis and transport (Wei, 2006). In both of these diseases, GFP-8 appears at intra-endolysosomal accumulations co-localizing with LTR. However, Chediak-Higashi cells, which contain enlarged endolysosomes, show GFP-8 accumulation at their limiting membrane instead of inside the lumen, in spite of the elevated intraluminal cholesterol and LBPA content of these compartments in CHS. Point mutations responsible for CHS occur on the very large scaffolding protein LYST (Karim et al., 2002), of mostly unknown function, though recent studies suggest it could regulate lysosomal size and quantity but not trafficking (Holland et al., 2014). Interestingly, reports using expression constructs of LYST fragments have detected a direct interaction of LYST and the ESCRT component Hrs (Tchernev et al., 2002), further substantiating its involvement in late endosomal dynamics. Considering the results presented in this work with respect to the possible dependence of RhoB sorting on Hrs function, retention of CINCCKVL constructs at the periphery of CHS vesicles could also be due to indirect LYST-mediated mechanisms. However, full-length RhoB constructs do internalize into enlarged CHS endolysosomes, which questions this interpretation.

Another striking phenotype found in CHS fibroblasts was the endolysosomal dilation caused by GFP-Rab9 overexpression, indicating a potential impairment of Rab9-mediated shuttling of material from the trans Golgi network to late endosomes and *vice versa*. In fact, there seems to be an overall entrapment of many small GTPases, i.e. RhoB, Rab7, TC10 and Rab9, co-localizing in endolysosomal compartments, hinting at impaired traffic from that point onwards, be it towards the plasma membrane by exocytosis or endocytic recycling, or towards the Golgi apparatus in biosynthetic recycling (Huynh et al., 2004; Zhang et al., 2007). Another possibility would be that CHS lysosomes possess inefficient degradation mechanisms, though studies with EGFR or RhoB argue against this hypothesis. Recently, degradation of EGFR was found to occur normally in LYST knock-down HeLa cells (Holland et al., 2014). These findings are in line with preliminary studies from the laboratory that showed similar degradation rates for several GTPase constructs in CHS and control fibroblasts (results not shown). These results merit further studies regarding the subcellular functions of the large LYST protein in the context of GTPase involvement in subcellular traffic, ultimately aiming at new therapeutic opportunities for CHS patients.

3.2 Small GTPases as targets for electrophilic lipids

The plethora of posttranslational modifications that can occur on Ras proteins is largely responsible for their ability to act as stimulus sensors from different sites in the cell. In addition to CAAX processing, isoprenylation, palmitoylation or phosphorylation (Hancock et al., 1989; Kim et al., 2009), it has also been established that Ras family proteins (H-Ras, N-Ras or K-Ras) undergo non-enzymatic modifications including nitrosylation, thiolation or addition of lipid electrophiles (Mallis et al., 2001; Oliva et al., 2003). However, the results presented in this work are the first to detect modification by cyPG of RhoB and Rap2B.

Previous results from the laboratory have reported that H-Ras is a target for modification by cyPG and isoprostanes (Oliva et al., 2003; Renedo et al., 2007). Specifically, single enone compounds preferentially modified C118, whereas the dienone compound, 15d-PGJ_2, bound preferentially to C181 and 184 of its C-terminal peptide. Since these latter cysteine residues represent the palmitoylation sites of H-Ras,

binding of 15d-PGJ_2 to RhoB and Rap2B, which also contain palmitoylatable cysteines close to each other at their C-termini, could represent cross-linking of these two residues, similarly to that detected for H-Ras and its synthetic C-terminal peptide (Oeste et al., 2011). In assays addressing modification of RhoB by other cyPG, results showed that biotinylated 15d-PGJ_2 bound to a great extent, as determined by WB. Furthermore, incubation with biotinylated 8-iso-PGA_2 elicited a stronger signal than that of its *cis* isoform, PGA_2. These results suggest that single enones can also bind to RhoB cysteines and that the isoprostane form of PGA_2 is more easily accessible to the cysteine to which it binds. Further experiments are required to ascertain the binding sites of these cyPG and the molecular characteristics responsible for the different signal intensities detected for each cyPG.

As has been described in detail for H-Ras (Oeste et al., 2011), if it is the case in cells that these bipalmitoylated and prenylated proteins are modified by dienone cyPG at the cysteines in their C-termini, their subcellular localization and signaling properties could become significantly altered. The half-life of H-Ras palmitoylation has been estimated as approximately 20 min, which is a small timeframe compared to its 20 h half-life or even the 2-3 h half-life of RhoB, if its palmitoylation dynamics are assumed to be of a similar magnitude (Pérez-Sala et al., 2009; Rocks et al., 2005). Furthermore, Ras activation can induce its depalmitoylation (Omerovic et al., 2007), so that during the palmitoylation-depalmitoylation cycle of H-Ras, it could be that C181 and C184 become available for chemical modification by cyPG or other agents. These modifications could obstruct subsequent rounds of palmitoylation and the microdomain partitioning or subcellular localization prompted by palmitate binding to H-Ras. As will be discussed below, modification of H-Ras by several agents does indeed disrupt its activation patterns and subcellular localization (Oeste et al., 2011). However, whether this is also the case for the other bipalmitoylated and isoprenylated GTPases explored in this work will be the subject of further investigations.

cyPG production is significantly increased upon oxidative stress, suggesting that GTPases that can be modified by these compounds *in vitro* could do so in cells in an oxidative scenario. Furthermore, increased generation of reactive oxygen or nitrogen species that takes place within cells in situations such as inflammation affects unsaturated lipids with a tendency for oxidation (Koenitzer and Freeman, 2010). This is

the case for polyunsaturated fatty acids at membranes, which suffer non-enzymatic oxidations to produce compounds of diverse structure that can modify proteins and affect their subcellular functions (Ceaser et al., 2004). Since the structures and electrophilic groups of these reactive endogenous compounds are similar to those of cyPG, the possibility is set forth that the GTPases studied in this work could become targets for species such as nitrated fatty acids or oxidized phospholipids, which could have a profound impact on their biological actions.

3.3 Electrophilic reagents bind to C-terminal cysteines in H-Ras and RhoB

Additionally to reactive lipids that can be found in biological systems, we have used exogenous, small, bifunctional cysteine reagents as biochemical tools to characterize the structural requirements and functional consequences of C-terminal modification of H-Ras and RhoB. Binding of DBB to two cysteines is only feasible if these are within 3-6 Å of each other, so that the results shown in this work place the palmitoylation cysteines within that range. As addressed above, cyPG could interfere with palmitoylation cycles of H-Ras and hence elicit changes in its subcellular behavior. Similarly, binding of small reactive compounds such as PAO and DBB to C-terminal cysteines can abrogate palmitoylation, though their effects on GTPase activation and localization need not match those of cyPG. Indeed, cells transfected with a fluorescent construct of the Ras binding domain (RBD) of the Ras effector, Raf, and treated with PAO or DBB show that active Ras is recruited to endomembranes. Treatment with these compounds also hampers Ras translocation to the plasma membrane upon EGF stimulation (Oeste et al., 2011). Interestingly, depalmitoylated H-Ras has been shown to travel back to the Golgi complex for addition of new palmitate moieties, and palmitoylation cysteine mutants signal from this localization upon stimulation with growth factors (Chiu et al., 2002). It is therefore possible that PAO or DBB bind to depalmitoylated H-Ras at the Golgi and induce its activation at this site, as summarized in Figure 53. Another approach resulting in alteration of the H-Ras hypervariable region structure is the mutation of C184 for a leucine residue, as appears naturally in N-Ras, which was suggested to replace the palmitate chain that is usually present and results in H-Ras association with the plasma membrane and recycling endosomes (Misaki et al.,

2010). Taken together, cyPG and bifunctional cysteine reagent modification of H-Ras highlights the relevance of hypervariable cysteines and the proximity between them as crucial structural determinants for selectivity of posttranslational modifications.

Modification	Schematic structure	Functional outcome	Reference
Palmitoylation	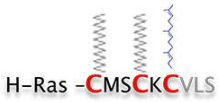	Cycle of palmitoyation/ depalmitoylation and traffic between Golgi and plasma membrane	Hancock, 1989 Rocks, 2005
Lipoxidation (15d-PGJ_2)	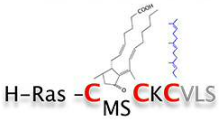	Activation	Oliva, 2003 Renedo, 2007 Oeste, 2011
PAO	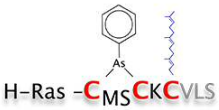	Activation on endomembranes	Oeste, 2011
DBB	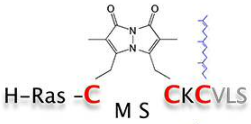	Activation on endomembranes	Oeste, 2011
Guanylation	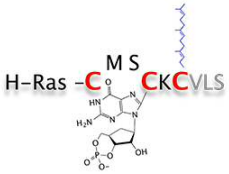	Activation at plasma membrane	Nishida, 2012
Glutathionylation	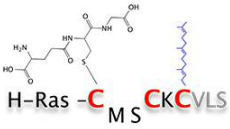	Inhibition of palmitoylation and plasma membrane association	Mallis, 2001 Burgoyne, 2012

Figure 53. H-Ras C-terminal modifications and their functional outcomes.

The three C-terminal H-Ras cysteine residues are shown in red, the last of which becomes irreversibly farnesylated (blue chain). The "-AAX" amino acids removed upon CAAX box processing are shown in gray. Palmitoylation cysteines, i.e. C181 and 184, can undergo modification by electrophilic compounds with varying structures (shown in black), resulting in diverse functional outcomes.

Modification of H-Ras at its C-terminus by compounds with distinct structural features and the functional outcomes that result from them have been explored by our laboratory and others (Figure 53). As described above, binding of several cyPG, including 15d-PGJ_2, elicits H-Ras activation at the plasma membrane, whereas addition of PAO or DBB molecules to the C-terminal cysteines results in activation at endomembranes. Similarly, guanylation of C184 induces Ras activation at the plasma membrane (Nishida et al., 2012). In contrast, glutathionylation of the H-Ras C-terminus in cells hinders palmitoylation and concomitant plasma membrane binding, as well as

inducing apoptosis (Burgoyne et al., 2012). Additionally, this study showed that metabolic stress induces oxidation of reactive cysteine thiolates, which also alters H-Ras palmitoylation, both in cells and mouse models (Burgoyne et al., 2012). Hence a scenario is set forth in which the physicochemical characteristics of the agents that modify palmitoylation cysteines determine the specificity of GTPase subcellular localization or activation.

As seen in this work, small differences in amino acid sequences can have a profound impact on binding to membranes of distinct nature, illustrated by TC10 and RhoB. Furthermore, processed lipidation motifs endow each of these proteins with a defined structural membrane-binding unit. Modification with reactive lipids occurring in pathological settings adds another layer of complexity to the determinants driving intracellular localization of small GTPases such as RhoB. Binding of cyPG or reactive compounds with varied structures to RhoB *in vitro* paves the way for studies in cells to define putative impediments in RhoB palmitoylation due to these modifications, which could alter its subcellular localization pattern and hence its biological actions.

CONCLUSIONS

As a result of the work presented in this dissertation, in which localization and subcellular trafficking of endosomal GTPases have been assessed in the context of their posttranslational modifications, the following conclusions have been arrived at:

1.1. Structural determinants present at the hypervariable region of the endosomal GTPases RhoB and TC10, when exchanged, interconvert their behavior regarding association with distinct subcellular membranes.

1.2. Endolysosomal targeting of RhoB and chimeras of its lipidation motif (CINCCKVL) depends on isoprenylation and palmitoylation at C-terminal cysteines.

1.3. RhoB and CINCCKVL chimeras appear inside endolysosomes and are detected at intraluminal vesicles of multivesicular bodies by super-resolution microscopy.

1.4. CINCCKVL sorting is conserved in cells from diverse model organisms, including fungi, insects, amphibians, and mammals.

These results shed light on the interplay between lipidated residues and other structural determinants in subcellular targeting of GTPases.

2.1 In cells depleted of the ESCRT components Hrs and Tsg101, sorting of full-length RhoB into endolysosomal compartments is impaired, but not that of CINCCKVL chimeras.

2.2 Agents altering late endosomal lipid dynamics differentially disturb RhoB and CINCCKVL chimera localization inside endolysosomes.

2.3 Overexpression of CD63 constructs alters CINCCKVL chimera localization, but not that of full-length RhoB.

Taken together, these results imply that sorting of full-length RhoB and CINCCKVL constructs could be regulated by distinct subcellular trafficking machineries.

3.1 RhoB or CINCCKVL constructs recapitulate endolysosomal defects in cells of patients with lysosomal storage diseases.

3.2 The palmitoylation cysteines of the small GTPases RhoB and H-Ras are targets for modification by structurally diverse electrophilic lipids *in vitro*.

These results suggest that subcellular localization of endosomal GTPases could become altered in pathological scenarios such as genetic diseases or processes involving the generation of reactive species.

SUMMARY IN ENGLISH

Small GTPases of the Ras superfamily are key to cellular processes such as differentiation, proliferation or regulation of the cytoskeleton (Takai et al., 2001). These proteins undergo lipid modifications that elicit their attachment to membranes and are crucial to their activity. Specifically, Ras protein isoprenylation serves as an anchor to the membrane, and Ras proteins are further amenable to reversible palmitoylation, which contributes to their dynamic localization at distinct subcellular compartments (Hancock et al., 1989). Lipid modifications take place at cysteine residues in the C-terminal region. Furthermore, these cysteines can undergo oxidation or addition of electrophilic compounds, e.g. cyclopentenone prostaglandin binding. These compounds are formed by non-enzymatic oxidation of arachidonic acid or from dehydration of other prostaglandins, which endows them with electrophilic carbons (Funk, 2001).

Rho proteins are a group of Ras superfamily proteins that are crucial to cell adhesion and migration, hence modulating cardiovascular pathophysiology and tumorigenic processes (Ridley, 2001). RhoB is a member of this family with roles in vesicular trafficking, tumor suppression and localization of signaling proteins. RhoB lipid modifications (isoprenylation and double palmitoylation) are necessary for its localization to endolysosomes and its degradation through this pathway (Pérez-Sala et al., 2009; Stamatakis et al., 2002). The last eight amino acids of RhoB, which correspond to the lipidation motif, constitute an endolysosomal localization and degradation sequence for chimeric proteins to which this extension is added at their C-terminal end (Pérez-Sala et al., 2009).

In the context of this dissertation, *in vitro* and cell models have been used to study mechanistic and structural aspects of Ras and Rho protein modification, particularly that of RhoB, and its influence on localization and trafficking of these proteins or their chimeras modified by lipids and other compounds. Though lipid modifications of Ras proteins have been described as important regulatory factors, the involvement of lipidation and its interplay with other structural determinants in subcellular targeting of GTPases has not been fully elucidated. Therefore, the role of lipid modifications of RhoB cysteine residues and other important residues at the

hypervariable region on its intracellular sorting has been analyzed. Furthermore, studies were carried out to determine whether the RhoB lipidation motif *per se* (CINCCKVL) is able to mimic the full-length protein. Cell models from different species were used to evaluate whether the latent sorting mechanisms for CINCCKVL proteins are conserved in these model organisms. Using this C-terminal construct in parallel to the full-length protein, the potential involvement of key molecular machineries, i.e. ESCRT complexes, CD63 or lipid dynamics, in their sorting was assessed. Considering the potential alteration of subcellular localization of Ras proteins by modification, targeting of lipidation sequences by other structurally diverse moieties, including reactive species arising in pathological scenarios, was also explored. In addition, assays were carried out to study the potential alteration of endosomal GTPase localization in genetic models of lysosomal disease.

In order to characterize the precise subcellular localization of RhoB, constructs of fluorescent proteins fused to this protein were compared to those of other small GTPases used as markers of endocytic vesicles. Co-localization with fusion proteins of Rab7, Rab9 or Lamp and negligible overlap with early endosome markers, i.e. Rab5 fusion proteins, or the Golgi marker, giantin, underscore RhoB localization within the endolysosomal lumen. These studies also include assays with autophagy probes, with which RhoB or its chimeras show negligible co-localization. The small GTPase, TC10, contains a C-terminal sequence that is very similar to that of RhoB, though a basic amino acid patch upstream of the lipidation sequence elicits retention at the limiting membrane of endolysosomes. Insertion of this basic patch into the RhoB sequence hinders its entry into endolysosomes, highlighting that exchange of structural determinants between these proteins elicits interconversion of their subcellular localization patterns. Furthermore, it has been determined that chimeras bearing the RhoB C-terminal sequence, CINCCKVL, are also internalized into endolysosomes.

It was also described that chimeric proteins fused to the C-terminal sequence of RhoB (CINCCKVL) enter into the endolysosomal lumen. Therefore, studies were carried out to assess whether the CINCCKVL sequence can travel to endolysosomes in cells from diverse species, which in some cases lack an endogenous RhoB homolog sequence. The universality of endolysosomal localization of chimeras bearing the RhoB

C-terminus was set forth by detection of these proteins in endolysosomes of cells as phylogenetically distant as amphibians, insects and fungi.

In order to explore the possible localization mechanisms of RhoB, advanced confocal and super-resolution techniques were employed. By means of these tools, RhoB and CINCCKVL chimeras were unequivocally detected at intraluminal vesicles of multivesicular bodies. Cells were transfected with small interfering RNA to silence components of the ESCRT machinery, which is responsible for endolysosomal trafficking and formation of multivesicular bodies (Raiborg and Stenmark, 2009). By blocking the function of some of these components, RhoB is not internalized into endolysosomes, which reflects a possible role of ESCRT proteins in RhoB endosomal trafficking. However, CINCCKVL chimeras are not similarly affected by ESCRT knock-down. Therefore, other protein and lipid components of multivesicular bodies could play a role in localization of these chimeras, e.g. the tetraspanin CD63. This protein presents a high degree of co-localization with RhoB and related chimeras at multivesicular bodies. Interestingly, it was shown that overexpression of fluorescent constructs of CD63 alter the subcellular localization pattern of CINCCKVL proteins, possibly towards extracellular destinations, but not that of RhoB. To explore the role of lipid dynamics in localization of these proteins, cells were treated with compounds that alter cholesterol dynamics at membranes. In these cells, internalization of C-terminal RhoB chimeras into endolysosomes was reduced, whereas the full-length protein was able to access these compartments. Furthermore, ceramide treatment induced changes in cell morphology that affect RhoB and related protein localization. Taken together, these results suggest that CINCCKVL chimeras can follow a subcellular destination mediated by machineries that are different to those responsible for sorting of full-length RhoB, which implies that RhoB contains further structural determinants for localization or interaction, beyond those that appear at its lipidation sequence.

It has been previously described that RhoB is involved in diverse pathologies such as tumorigenic processes and cardiovascular malfunction (Prendergast, 2001). The results obtained showing RhoB localization to endolysosomal membranes warranted studies in models of lysosomal diseases such as Chediak-Higashi or Niemann-Pick. These disorders result in oculocutaneous albinism, immunodeficiency and cognitive impairment of varying degree (Huizing et al., 2008). Comparing RhoB to other

endosomal GTPases in cells of patients suffering from these diseases, confocal laser microscopy shows that RhoB is localized to the dilated endolysosomes typical of these diseases.

In many pathological scenarios, proteins suffer modifications due to alterations in overall cellular redox status. By means of electrophoretic assays (SDS-PAGE) or proteomic approaches (MALDI-TOF), it was shown that proteins of the Ras superfamily, particularly H-Ras and RhoB, could be modified in vitro at their C-terminal cysteine residues by structurally diverse electrophilic lipids. Specifically, dienone cyclopentenone prostaglandins, derived from non-enzymatic oxidation of arachidonic acid or dehydration of other prostaglandins, bind to these residues. Recombinant RhoB protein is also selectively modified by biotinylated dienone cyclopentenone prostaglandins, as well as by other bifunctional cysteine reagents such as phenylarsine oxide and dibromobimane. It is therefore possible that regulation of small GTPases can occur through processes related to cellular redox status that can have implications beyond the canonical signaling pathways that are mediated by these proteins.

As a result of the work presented in this dissertation, in which localization and subcellular trafficking of endosomal GTPases have been assessed in the context of their posttranslational modifications, several conclusions have been arrived at. Regarding localization sequences at the hypervariable regions of small GTPases, these studies have shown that interplay between lipidated residues and other structural determinants such as basic residue patches elicits specific patterns of subcellular targeting. Furthermore, in the case or RhoB, endolysosomal targeting of full-length or CINCCKVL chimeras depends on isoprenylation and palmitoylation at C-terminal cysteines. These proteins, when fully lipidated, appear inside endolysosomes and are detected at intraluminal vesicles of multivesicular bodies by super-resolution microscopy. Endolysosomal or vacuolar sorting of CINCCKVL chimeras was shown to be conserved in cells from diverse model organisms, including fungi, insects, amphibians, and mammals. As referred to the molecular mechanisms involved in sorting, results imply that sorting of full-length RhoB and CINCCKVL constructs could be regulated by distinct subcellular trafficking machineries, for full-length RhoB sorting is impaired upon ESCRT component depletion, whereas CINCCKVL construct localization is altered in cells

overexpressing CD63 constructs or after treatment with cholesterol-reducing agents. Experiments performed in pathological scenarios such as genetic models of endolysosomal malfunction or processes involving the generation of reactive species show that RhoB or CINCCKVL constructs recapitulate endolysosomal defects in cells of patients with lysosomal storage diseases and that the palmitoylation cysteines of the small GTPases RhoB and H-Ras are targets for modification by structurally diverse electrophilic lipids *in vitro*. These results pave the way for exploring the extent to which diverse modifications of Ras proteins at C-terminal cysteines can disturb their subcellular localization and consequently alter their functional outcomes.

SUMMARY IN SPANISH

1. Introducción

Las GTPasas de bajo peso molecular comprendidas en la superfamilia Ras son proteínas fundamentales para procesos celulares como la diferenciación celular, la regulación del citoesqueleto y la proliferación (Takai et al., 2001). Estas proteínas sufren modificaciones lipídicas que les permiten asociarse con las membranas celulares y son clave para su actividad. En concreto, las proteínas Ras están isopreniladas para anclarse a la membrana, además de ser susceptibles de palmitoilación reversible, lo cual contribuye a su localización dinámica en distintos compartimentos subcelulares (Hancock et al., 1989). Estas modificaciones lipídicas tienen lugar sobre residuos de cisteína en la región carboxilo-terminal (C-terminal). Además, estas cisteínas pueden sufrir oxidaciones o adición de compuestos de naturaleza electrofílica, como por ejemplo, la unión de prostaglandinas ciclopentenonas (Oeste and Pérez-Sala, 2014). Estos compuestos se forman por oxidación no enzimática del ácido araquidónico o por deshidratación de otras prostaglandinas, lo cual las dota de carbonos electrófilos (Funk, 2001).

Las proteínas Rho juegan papeles cruciales en la adhesión y migración celular que repercuten sobre la fisiopatología cardiovascular y procesos tumorigénicos (Ridley, 2001). RhoB es un miembro de esta familia con funciones reguladoras del tráfico vesicular, la supresión de tumores y la localización de proteínas señalizadoras. Las modificaciones lipídicas de RhoB (isoprenilación y doble palmitoilación) son necesarias para su localización endolisosomal y posterior degradación por esta vía (Pérez-Sala et al., 2009; Stamatakis et al., 2002). Los últimos ocho amino ácidos de RhoB, zona donde se encuentran las cisteínas que se lipidan, comprenden una secuencia de localización y degradación endolisosomal para proteínas quiméricas a las que se les añade esta extensión en su extremo carboxilo-terminal (Pérez-Sala et al., 2009).

En el contexto de esta tesis se han estudiado, tanto *in vitro* como en modelos celulares, aspectos mecanísticos y estructurales de la modificación de proteínas Ras y Rho, en concreto RhoB, y su repercusión sobre la localización y tráfico de estas proteínas o sus quimeras modificadas por lípidos y otros compuestos.

2. Objetivos

Las GTPasas de bajo peso molecular ejercen diversas funciones celulares desde localizaciones de membrana específicas. Entre los factores que las regulan, la modificación en secuencias C-terminales juegan un papel crucial, aunque la participación de la lipidación y su interacción con otros determinantes estructurales en la localización subcelular de las GTPasas no ha sido completamente dilucidado. Por ello, el trabajo presentado en esta tesis se centra en analizar el papel de las modificaciones lipídicas en residuos de cisteína de RhoB sobre su tráfico intracelular y determinar si el motivo de lipidación per se es capaz de reproducir el comportamiento de la proteína completa. Además, la posibilidad de que las secuencias de lipidación puedan ser dianas de modificación por otros compuestos de estructura diversa, incluidas especies reactivas que se producen en situaciones patológicas, no se ha explorado. Por tanto, los siguientes objetivos fueron planteados:

- Estudiar el papel de las secuencias C-terminales de GTPasas endosomales en su localización subcelular.
- Valorar la importancia de la isoprenilación y la palmitoilación en la asociación de estas proteínas a vesículas intracelulares.
- Determinar la localización subcelular de quimeras que contienen la secuencia de lipidación del C-terminal de RhoB.
- Evaluar si los mecanismos latentes de localización del C-terminal de RhoB están conservados en células de diversas especies.
- Explorar el posible rol de maquinarias moleculares clave, tales como los complejos ESCRT, CD63 o la dinámica lipídica, en la localización de RhoB y quimeras relacionadas.
- Asentar las bases para estudiar posibles alteraciones en la localización y modificación de GTPasas endosomales en modelos experimentales de enfermedad.

3. Resultados

Se ha llevado a cabo una caracterización de RhoB fusionada a proteínas fluorescentes en el contexto de las endomembranas al comparar su localización y degradación con las de otras GTPasas pequeñas. Su colocalización con proteínas fluorescentes fusionadas a Rab7, Rab9 o Lamp y falta de coincidencia con marcadores de endosomas tempranos (GFP-Rab5) o aparato de Golgi (giantin) atestiguan su localización en el lumen endolisosomal. Los estudios aquí presentados incluyen también la utilización de sondas de la vía autofagocítica, con las cuales ni RhoB ni sus proteínas quimera colocalizan de forma detectable. La GTPasa de bajo peso molecular, TC10, cuya secuencia C-terminal es muy similar a la de RhoB, contiene unos amino ácidos básicos que sin embargo la retienen en la membrana limitante de dichas vesículas. La inserción de la secuencia polibásica de TC10 en la secuencia de RhoB impide su entrada a endolisosomas, lo cual pone de manifiesto que hay determinantes estructurales que al intercambiarse entre estas proteínas dan lugar a patrones subcelulares específicos.

Se describió además que las proteínas quimera fusionadas a la secuencia C-terminal de RhoB (CINCCKVL) también acceden al lumen endolisosomal. Por lo tanto, se exploró si la secuencia CINCCKVL accede a los endolisosomas no sólo en células de mamíferos, sino en células de organismos que pueden contener o no una secuencia endógena para proteínas homólogas a RhoB. La universalidad de la localización endolisosomal de quimeras con el C-terminal de RhoB se pone de manifiesto al detectarse en endolisosomas de células de organismos muy alejados entre sí en la escala filogenética, tales como anfibios, insectos y hongos.

Para explorar los posibles mecanismos de localización de RhoB, se emplearon técnicas de microscopía láser avanzada confocal y de superresolución. Por medio de estas potentes herramientas se ha podido establecer la localización inequívoca de RhoB y quimeras CINCCKVL en vesículas intraluminales de cuerpos multivesiculares. Se transfectaron células con RNA de interferencia para así silenciar componentes de la maquinaria ESCRT, responsable del tráfico endolisosomal y la formación de cuerpos multivesiculares (Raiborg and Stenmark, 2009). Al bloquear la función de algunos de

estos componentes, RhoB no se internaliza en los endolisosomas, lo cual refleja un posible papel de las proteínas ESCRT en el tráfico endosomal de RhoB. Sin embargo, las quimeras CINCCKVL no se ven igualmente afectadas por el bloqueo de componentes ESCRT. Se estudiaron pues otros componentes proteicos y lipídicos de los cuerpos multivesiculares que podrían jugar también un papel en la localización de proteínas CINCCKVL, como por ejemplo la tetraspanina CD63. Esta proteína presenta una alta colocalización con RhoB y quimeras relacionadas en cuerpos multivesiculares. Curiosamente, se observó que la sobreexpresión de construcciones fluorescentes de CD63 cambian el patrón de localización subcelular de quimeras CINCCKVL, posiblemente hacia destinos extracelulares, pero no así el de RhoB. Para explorar el papel de la dinámica lipídica en la localización de estas proteínas, se realizaron ensayos de tratamiento celular con compuestos que alteran la dinámica de colesterol en las membranas. En estas células, se redujo la internalización de quimeras del C-terminal de RhoB hacia el lumen de cuerpos multivesiculares, mientras que la proteína completa siguió su camino hacia el interior de estos compartimentos. Además, el tratamiento con ceramida indujo cambios en la morfología celular que afectan la localización de RhoB y proteínas relacionadas. En conjunto, estos resultados sugieren que las quimeras CINCCKVL pueden seguir un destino subcelular mediado por maquinarias distintas a las responsables del transporte de RhoB completa, lo cual sugiere que RhoB contiene determinantes estructurales de localización o interacción más allá de los que aparecen en su secuencia de lipidación.

Se ha descrito que RhoB interviene en diversas patologías como procesos tumorigénicos y afecciones cardiovasculares (Prendergast, 2001). Debido a los resultados obtenidos sobre la localización de RhoB en membranas endolisosomales, se quiso estudiar su papel en modelos de enfermedades lisosomales como Chediak-Higashi o Niemann-Pick. Estas patologías cursan con albinismo oculocutáneo, inmunodeficiencias y retrasos cognitivos de severidad variada (Huizing et al., 2008). Al comparar RhoB con otras GTPasas endosomales en células de pacientes que sufren estas enfermedades, se detectó por microscopía láser confocal la localización de RhoB en los endolisosomas dilatados típicos de estas patologías.

En muchos escenarios patológicos, las proteínas sufren modificaciones al verse alterado el estado redox global de las células. Se determinó que proteínas de la

superfamilia Ras, en concreto H-Ras y RhoB, se pueden modificar *in vitro* en sus residuos de cisteína del extremo carboxilo-terminal por compuestos electrófilos de diversa índole utilizando ensayos de electroforesis (SDS-PAGE) o métodos proteómicos (MALDI-TOF). En concreto, las prostaglandinas ciclopentenonas dienonas, derivadas de la oxidación no enzimática del ácido araquidónico o deshidratación de otras prostaglandinas, se unen a estos residuos. La proteína recombinante RhoB también se modifica por derivados biotinilados de prostaglandinas ciclopentenonas dienonas de manera selectiva, además de por otros reactivos bifuncionales de unión a cisteínas, como el óxido de fenilo arsénico o el dibromobimano. Se establece así una capacidad reguladora de GTPasas pequeñas por medio de procesos relacionados con el estado redox de la célula que puede tener implicaciones más allá de las vías de señalización canónicas mediadas por estas proteínas.

4. Conclusiones

Como resultado del trabajo presentado en esta tesis, en la que la localización y tráfico subcelular de GTPasas endosomales se han evaluado en el contexto de sus modificaciones postraduccionales, se ha llegado a las siguientes conclusiones:

1.1. Ciertos determinantes estructurales de la región hipervariable de las GTPasas endosomales RhoB y TC10, al intercambiarse, permutan su comportamiento en cuanto a la asociación con membranas subcelulares concretas.

1.2. La localización endolisosomal de RhoB y quimeras de su secuencia de lipidación (CINCCKVL) depende de la isoprenilación y palmitoilación en las cisteínas C-terminales.

1.3. Quimeras de RhoB y CINCCKVL aparecen en el interior de endolisosomas y se detectan en vesículas intraluminales de cuerpos multivesiculares mediante microscopía de superresolución.

1.4. La localización de proteínas CINCCKVL está conservada en células de diversos organismos modelos, incluidos modelos de hongo, insecto, anfibio y mamíferos.

Estos resultados ponen de manifiesto la interacción entre residuos modificados por lípidos y otros determinantes estructurales a la hora de guiar la localización subcelular de GTPasas.

2.1. En células en las que componentes ESCRT (Hrs y Tsg101) han sido silenciados mediante RNA de interferencia, disminuye la localización de la proteína RhoB completa en endolisosomas, pero no así la de quimeras CINCCKVL.

2.2. El uso de compuestos que perturban la dinámica lipídica de endosomas tardíos altera diferencialmente la localización de quimeras de RhoB o CINCCKVL dentro de los endolisosomas.

2.3. La sobreexpresión de construcciones de CD63 altera la localización de quimeras CINCCKVL, pero no así la de RhoB completa.

En conjunto, estos resultados sugieren que la localización de RhoB completa y de construcciones de CINCCKVL podría verse regulada por diferentes maquinarias de tráfico subcelular.

3.1. Las quimeras de RhoB o CINCCKVL recapitulan los defectos endolisosomales en células de pacientes con enfermedades por almacenamiento lisosomal.

3.2. Las cisteínas de palmitoilación de las GTPasas pequeñas RhoB y H-Ras son dianas de modificación *in vitro* por lípidos electrófilos de estructura variada.

Estos resultados sugieren que la localización subcelular de GTPasas endosomales podría verse alterada en situaciones patológicas como enfermedades genéticas o procesos que cursan con generación de especies reactivas.

5. Aportaciones fundamentales

Este trabajo muestra resultados obtenidos mediante técnicas de microscopía avanzada como la microscopía láser confocal y de superresolución, para determinar las localizaciones subcelulares concretas de la proteína RhoB fusionada a diversas proteínas fluorescentes, además de quimeras fluorescentes fusionadas a una secuencia corta derivada del C-terminal de RhoB. Además, se ha determinado la importancia de la lipidación de los residuos de cisteína para la localización endolisosomal de las proteínas de fusión mediante la generación de mutantes no susceptibles de modificación. Por

primera vez, se ha llevado a cabo el estudio de la distribución de la proteína RhoB y quimeras relacionadas en células con alteraciones de la función lisosomal (síndromes de Chediak-Higashi, Niemann-Pick y Hermansky-Pudlak). Por medio de las quimeras fluorescentes del C-terminal de RhoB, se ha caracterizado la especificidad de la localización de dicha secuencia en varias líneas celulares humanas y de especies diversas, incluidos insectos y hongos. Además, estos estudios son los primeros en analizar el papel de mediadores del tráfico intracelular como los complejos ESCRT, la tetraspanina CD63 o la dinámica lipídica en la localización subcelular de RhoB o su secuencia C-terminal.

Se han realizado estudios sobre la modificación de GTPasas de bajo peso molecular, particularmente H-Ras y RhoB, por compuestos que se unen a cisteínas por mecanismos no enzimáticos. Se ha detectado la unión de prostaglandinas ciclopentenonas dienonas a dos residuos del C-terminal de H-Ras. Las diversas técnicas empleadas han servido para caracterizar los motivos estructurales de GTPasas pequeñas que son susceptibles de modificaciones y que pueden repercutir en la actividad o localización de dichas proteínas.

REFERENCES

Abenza JF, Galindo A, Pinar M, Pantazopoulou A, de los Ríos V and Peñalva MA (2012) Endosomal maturation by Rab conversion in *Aspergillus nidulans* is coupled to dynein-mediated basipetal movement. *Mol. Biol. Cell* **23**(10): 1889-1901.

Abenza JF, Pantazopoulou A, Rodríguez JM, Galindo A and Peñalva MA (2009) Long-distance movement of *Aspergillus nidulans* early endosomes on microtubule tracks. *Traffic* **10**(1): 57-75.

Adamson P, Marshall CJ, Hall A and Tilbrook PA (1992) Post-translational modifications of p21rho proteins. *J. Biol. Chem.* **267**(28): 20033-20038.

Adini I, Rabinovitz I, Sun JF, Prendergast GC and Benjamin LE (2003) RhoB controls Akt trafficking and stage-specific survival of endothelial cells during vascular development. *Genes Dev.* **17**(21): 2721-2732.

Ahearn IM, Haigis K, Bar-Sagi D and Philips MR (2012) Regulating the regulator: post-translational modification of RAS. *Nat. Rev. Mol. Cell Biol.* **13**(1): 39-51.

Aicart-Ramos C, Valero RA and Rodríguez-Crespo I (2011) Protein palmitoylation and subcellular trafficking. *Biochim. Biophys. Acta* **1808**(12): 2981-2994.

Amano Y, Yamashita Y, Kojima K, Yoshino K, Tanaka N, Sugamura K and Takeshita T (2011) Hrs recognizes a hydrophobic amino acid cluster in cytokine receptors during ubiquitin-independent endosomal sorting. *J. Biol. Chem.* **286**(17): 15458-15472.

Amiya E, Watanabe M, Takeda N, Saito T, Shiga T, Hosoya Y, Nakao T, Imai Y, Manabe I, Nagai R, Komuro I and Maemura K (2013) Angiotensin II impairs endothelial nitric-oxide synthase bioavailability under free cholesterol-enriched conditions via intracellular free cholesterol-rich membrane microdomains. *J. Biol. Chem.* **288**(20): 14497-14509.

Andreu Z and Yáñez-Mo M (2014) Tetraspanins in extracellular vesicle formation and function. *Front. Immunol.* **5**: 442.

Asensio CS, Sirkis DW and Edwards RH (2010) RNAi screen identifies a role for adaptor protein AP-3 in sorting to the regulated secretory pathway. *J. Cell Biol.* **191**(6): 1173-1187.

Aspenström P, Fransson A and Saras J (2004) Rho GTPases have diverse effects on the organization of the actin filament system. *Biochem. J.* **377**(Pt 2): 327-337.

Babst M (2011) MVB vesicle formation: ESCRT-dependent, ESCRT-independent and everything in between. *Curr. Opin. Cell Biol.* **23**(4): 452-457.

Babst M, Katzmann DJ, Estepa-Sabal EJ, Meerloo T and Emr SD (2002a) ESCRT-III: an endosome-associated heterooligomeric protein complex required for MVB sorting. *Dev. Cell* **3**(2): 271-282.

Babst M, Katzmann DJ, Snyder WB, Wendland B and Emr SD (2002b) Endosome-associated complex, ESCRT-II, recruits transport machinery for protein sorting at the multivesicular body. *Dev. Cell* **3**(2): 283-289.

Babst M, Wendland B, Estepa EJ and Emr SD (1998) The Vps4p AAA ATPase regulates membrane association of a Vps protein complex required for normal endosome function. *EMBO J.* **17**(11): 2982-2993.

Baietti MF, Zhang Z, Mortier E, Melchior A, Degeest G, Geeraerts A, Ivarsson Y, Depoortere F, Coomans C, Vermeiren E, Zimmermann P and David G (2012) Syndecan-syntenin-ALIX regulates the biogenesis of exosomes. *Nat. Cell Biol.* **14**(7): 677-685.

Baixauli F, López-Otín C and Mittelbrunn M (2014) Exosomes and autophagy: coordinated mechanisms for the maintenance of cellular fitness. *Front. Immunol.* **5**: 403.

Ballabio A and Gieselmann V (2009) Lysosomal disorders: from storage to cellular damage. *Biochim. Biophys. Acta* **1793**(4): 684-696.

Bampton ET, Goemans CG, Niranjan D, Mizushima N and Tolkovsky AM (2005) The dynamics of autophagy visualized in live cells: from autophagosome formation to fusion with endolysosomes. *Autophagy* **1**(1): 23-36.

Barbacid M (1987) Ras genes. *Annu. Rev. Biochem.* **56**: 779-827.

Barth S, Glick D and Macleod KF (2010) Autophagy: assays and artifacts. *J. Pathol.* **221**(2): 117-124.

Berg TO, Fengsrud M, Stromhaug PE, Berg T and Seglen PO (1998) Isolation and characterization of rat liver amphisomes. Evidence for fusion of autophagosomes with both early and late endosomes. *J. Biol. Chem.* **273**(34): 21883-21892.

Bigay J and Antonny B (2012) Curvature, lipid packing, and electrostatics of membrane organelles: defining cellular territories in determining specificity. *Dev. Cell* **23**(5): 886-895.

Bishop N and Woodman P (2000) ATPase-defective mammalian Vps4 localizes to aberrant endosomes and impairs cholesterol trafficking. *Mol. Biol. Cell* **11**(1): 227-239.

Bishop NE (2003) Dynamics of endosomal sorting. *Int. Rev. Cytol.* **232**: 1-57.

Bissig C and Gruenberg J (2013) Lipid sorting and multivesicular endosome biogenesis. *Cold Spring Harb. Perspect. Biol.* **5**(10): a016816.

Bissig C, Johnson S and Gruenberg J (2012) Studying lipids involved in the endosomal pathway. *Methods Cell Biol.* **108**: 19-46.

Bogatcheva NV, Sergeeva MG, Dudek SM and Verin AD (2005) Arachidonic acid cascade in endothelial pathobiology. *Microvasc. Res.* **69**(3): 107-127.

Bonifacino JS and Traub LM (2003) Signals for sorting of transmembrane proteins to endosomes and lysosomes. *Annu. Rev. Biochem.* **72**: 395-447.

Boya P, Reggiori F and Codogno P (2013) Emerging regulation and functions of autophagy. *Nat. Cell Biol.* **15**(7): 713-720.

Bucci C, Parton RG, Mather IH, Stunnenberg H, Simons K, Hoflack B and Zerial M (1992) The small GTPase Rab5 functions as a regulatory factor in the early endocytic pathway. *Cell* **70**(5): 715-728.

Bucci C, Thomsen P, Nicoziani P, McCarthy J and van Deurs B (2000) Rab7: a key to lysosome biogenesis. *Mol. Biol. Cell* **11**(2): 467-480.

Burgos PV, Mardones GA, Rojas AL, daSilva LL, Prabhu Y, Hurley JH and Bonifacino JS (2010) Sorting of the Alzheimer's disease amyloid precursor protein mediated by the AP-4 complex. *Dev. Cell* **18**(3): 425-436.

Burgoyne JR, Haeussler DJ, Kumar V, Ji Y, Pimental DR, Zee RS, Costello CE, Lin C, McComb ME, Cohen RA and Bachschmid MM (2012) Oxidation of H-Ras cysteine thiols by metabolic stress prevents palmitoylation in vivo and contributes to endothelial cell apoptosis. *FASEB J.* **26**(2): 832-841.

Burkhardt JK, Wiebel FA, Hester S and Argon Y (1993) The giant organelles in *beige* and Chediak-Higashi fibroblasts are derived from late endosomes and mature lysosomes. *J. Exp. Med.* **178**(6): 1845-1856.

Buschow SI, Nolte-'t Hoen EN, van Niel G, Pols MS, ten Broeke T, Lauwen M, Ossendorp F, Melief CJ, Raposo G, Wubbolts R, Wauben MH and Stoorvogel W (2009) MHC II in dendritic cells is targeted to lysosomes or T cell-induced exosomes via distinct multivesicular body pathways. *Traffic* **10**(10): 1528-1542.

Bustelo XR, Sauzeau V and Berenjeno IM (2007) GTP-binding proteins of the Rho/Rac family: regulation, effectors and functions in vivo. *Bioessays* **29**(4): 356-370.

Callahan JW, Bagshaw RD and Mahuran DJ (2009) The integral membrane of lysosomes: its proteins and their roles in disease. *J. Proteomics* **72**(1): 23-33.

Canguilhem B, Pradines A, Baudouin C, Boby C, Lajoie-Mazenc I, Charveron M and Favre G (2005) RhoB protects human keratinocytes from UVB-induced apoptosis through epidermal growth factor receptor signaling. *J. Biol. Chem.* **280**(52): 43257-43263.

Canto I and Trejo J (2013) Palmitoylation of protease-activated receptor-1 regulates adaptor protein complex-2 and -3 interaction with tyrosine-based motifs and endocytic sorting. *J. Biol. Chem.* **288**(22): 15900-15912.

Carstea ED, Morris JA, Coleman KG, Loftus SK, Zhang D, Cummings C, Gu J, Rosenfeld MA, Pavan WJ, Krizman DB, Nagle J, Polymeropoulos MH, Sturley SL, Ioannou YA, Higgins ME, Comly M, Cooney A, Brown A, Kaneski CR, Blanchette-Mackie EJ, Dwyer NK, Neufeld EB, Chang TY, Liscum L, Strauss JF, 3rd, Ohno K, Zeigler M, Carmi R, Sokol J, Markie D, O'Neill RR, van Diggelen OP, Elleder M, Patterson MC, Brady RO, Vanier MT, Pentchev PG and Tagle DA (1997) Niemann-Pick C1 disease gene: homology to mediators of cholesterol homeostasis. *Science* **277**(5323): 228-231.

Ceaser EK, Moellering DR, Shiva S, Ramachandran A, Landar A, Venkartraman A, Crawford J, Patel R, Dickinson DA, Ulasova E, Ji S and Darley-Usmar VM (2004) Mechanisms of signal transduction mediated by oxidized lipids: the role of the electrophile-responsive proteome. *Biochem. Soc. Trans.* **32**(Pt 1): 151-155.

Cenedella RJ (2009) Cholesterol synthesis inhibitor U18666A and the role of sterol metabolism and trafficking in numerous pathophysiological processes. *Lipids* **44**(6): 477-487.

Cernuda-Morollón E, Pineda-Molina E, Cañada FJ and Pérez-Sala D (2001) 15-Deoxy-Delta 12,14-prostaglandin J2 inhibition of NF-kappaB-DNA binding through covalent modification of the p50 subunit. *J. Biol. Chem.* **276**(38): 35530-35536.

Charrin S, Manie S, Thiele C, Billard M, Gerlier D, Boucheix C and Rubinstein E (2003) A physical and functional link between cholesterol and tetraspanins. *Eur. J. Immunol.* **33**(9): 2479-2489.

Chavrier P, Gorvel JP, Stelzer E, Simons K, Gruenberg J and Zerial M (1991) Hypervariable C-terminal domain of Rab proteins acts as a targeting signal. *Nature* **353**(6346): 769-772.

Chazotte B (2011) Labeling lysosomes in live cells with LysoTracker. *Cold Spring Harb Protoc* **2011**(2): pdb prot5571.

Cherezov V, Rosenbaum DM, Hanson MA, Rasmussen SG, Thian FS, Kobilka TS, Choi HJ, Kuhn P, Weis WI, Kobilka BK and Stevens RC (2007) High-resolution crystal structure of an engineered human beta2-adrenergic G protein-coupled receptor. *Science* **318**(5854): 1258-1265.

Cherfils J and Zeghouf M (2013) Regulation of small GTPases by GEFs, GAPs, and GDIs. *Physiol. Rev.* **93**(1): 269-309.

Chico Y, Lafita M, Ramírez-Duque P, Merino F and Ochoa B (2000) Alterations in erythrocyte membrane lipid and fatty acid composition in Chediak-Higashi syndrome. *Biochim. Biophys. Acta* **1502**(3): 380-390.

Chiu VK, Bivona T, Hach A, Sajous JB, Silletti J, Wiener H, Johnson RL, 2nd, Cox AD and Philips MR (2002) Ras signalling on the endoplasmic reticulum and the Golgi. *Nat. Cell Biol.* **4**(5): 343-350.

Chua CE, Gan BQ and Tang BL (2011) Involvement of members of the Rab family and related small GTPases in autophagosome formation and maturation. *Cell. Mol. Life Sci.* **68**(20): 3349-3358.

Clague MJ and Urbe S (2006) Endocytosis: the DUB version. *Trends Cell Biol.* **16**(11): 551-559.

Colombo M, Moita C, van Niel G, Kowal J, Vigneron J, Benaroch P, Manel N, Moita LF, Thery C and Raposo G (2013) Analysis of ESCRT functions in exosome biogenesis, composition and secretion highlights the heterogeneity of extracellular vesicles. *J. Cell Sci.* **126**(Pt 24): 5553-5565.

Coutinho MF, Prata MJ and Alves S (2012) A shortcut to the lysosome: the mannose-6-phosphate-independent pathway. *Mol. Genet. Metab.* **107**(3): 257-266.

Coyne CB, Shen L, Turner JR and Bergelson JM (2007) Coxsackievirus entry across epithelial tight junctions requires occludin and the small GTPases Rab34 and Rab5. *Cell Host Microbe* **2**(3): 181-192.

Cuervo AM and Dice JF (1996) A receptor for the selective uptake and degradation of proteins by lysosomes. *Science* **273**(5274): 501-503.

Cullen PJ and Korswagen HC (2012) Sorting nexins provide diversity for retromer-dependent trafficking events. *Nat. Cell Biol.* **14**(1): 29-37.

D'Adamo P, Menegon A, Lo Nigro C, Grasso M, Gulisano M, Tamanini F, Bienvenu T, Gedeon AK, Oostra B, Wu SK, Tandon A, Valtorta F, Balch WE, Chelly J and Toniolo D (1998) Mutations in GDI1 are responsible for X-linked non-specific mental retardation. *Nat. Genet.* **19**(2): 134-139.

de Duve D (1969) The peroxisome: a new cytoplasmic organelle. *Proc. R. Soc. Lond. B. Biol. Sci.* **173**(1030): 71-83.

Dell'Angelica EC (2004) The building BLOC(k)s of lysosomes and related organelles. *Curr. Opin. Cell Biol.* **16**(4): 458-464.

Dell'Angelica EC, Mullins C, Caplan S and Bonifacino JS (2000) Lysosome-related organelles. *FASEB J.* **14**(10): 1265-1278.

Desnoyers L, Anant JS and Seabra MC (1996) Geranylgeranylation of Rab proteins. *Biochem. Soc. Trans.* **24**(3): 699-703.

Dessinioti C, Stratigos AJ, Rigopoulos D and Katsambas AD (2009) A review of genetic disorders of hypopigmentation: lessons learned from the biology of melanocytes. *Exp. Dermatol.* **18**(9): 741-749.

Di Paolo G and De Camilli P (2006) Phosphoinositides in cell regulation and membrane dynamics. *Nature* **443**(7112): 651-657.

Dianzani MU (2003) 4-hydroxynonenal from pathology to physiology. *Mol. Aspects Med.* **24**(4-5): 263-272.

Dietrich LE and Ungermann C (2004) On the mechanism of protein palmitoylation. *EMBO Rep* **5**(11): 1053-1057.

Díez-Dacal B and Pérez-Sala D (2010) Anti-inflammatory prostanoids: focus on the interactions between electrophile signaling and resolution of inflammation. *ScientificWorldJournal* **10**: 655-675.

Dirac-Svejstrup AB, Sumizawa T and Pfeffer SR (1997) Identification of a GDI displacement factor that releases endosomal Rab GTPases from Rab-GDI. *EMBO J.* **16**(3): 465-472.

Dores MR, Chen B, Lin H, Soh UJ, Paing MM, Montagne WA, Meerloo T and Trejo J (2012) ALIX binds a YPX(3)L motif of the GPCR PAR1 and mediates ubiquitin-independent ESCRT-III/MVB sorting. *J. Cell Biol.* **197**(3): 407-419.

Dransart E, Olofsson B and Cherfils J (2005) RhoGDIs revisited: novel roles in Rho regulation. *Traffic* **6**(11): 957-966.

Duffield A, Kamsteeg EJ, Brown AN, Pagel P and Caplan MJ (2003) The tetraspanin CD63 enhances the internalization of the H,K-ATPase beta-subunit. *Proc. Natl. Acad. Sci. U. S. A.* **100**(26): 15560-15565.

Dunn WA, Jr. (1994) Autophagy and related mechanisms of lysosome-mediated protein degradation. *Trends Cell Biol.* **4**(4): 139-143.

Dunphy JT, Greentree WK, Manahan CL and Linder ME (1996) G-protein palmitoyltransferase activity is enriched in plasma membranes. *J. Biol. Chem.* **271**(12): 7154-7159.

Durchfort N, Verhoef S, Vaughn MB, Shrestha R, Adam D, Kaplan J and Ward DM (2012) The enlarged lysosomes in *beige j* cells result from decreased lysosome fission and not increased lysosome fusion. *Traffic* **13**(1): 108-119.

Edgar JR, Eden ER and Futter CE (2014) Hrs- and CD63-dependent competing mechanisms make different sized endosomal intraluminal vesicles. *Traffic* **15**(2): 197-211.

Elias M, Brighouse A, Gabernet-Castello C, Field MC and Dacks JB (2012) Sculpting the endomembrane system in deep time: high resolution phylogenetics of Rab GTPases. *J. Cell Sci.* **125**(Pt 10): 2500-2508.

Engel ME, Datta PK and Moses HL (1998) RhoB is stabilized by transforming growth factor beta and antagonizes transcriptional activation. *J. Biol. Chem.* **273**(16): 9921-9926.

Epp N, Rethmeier R, Kramer L and Ungermann C (2011) Membrane dynamics and fusion at late endosomes and vacuoles- Rab regulation, multisubunit tethering complexes and SNAREs. *Eur. J. Cell Biol.* **90**(9): 779-785.

Escola JM, Kleijmeer MJ, Stoorvogel W, Griffith JM, Yoshie O and Geuze HJ (1998) Selective enrichment of tetraspan proteins on the internal vesicles of multivesicular endosomes and on exosomes secreted by human B-lymphocytes. *J. Biol. Chem.* **273**(32): 20121-20127.

Eskelinen EL (2005) Maturation of autophagic vacuoles in mammalian cells. *Autophagy* **1**(1): 1-10.

Fader CM and Colombo MI (2009) Autophagy and multivesicular bodies: two closely related partners. *Cell Death Differ.* **16**(1): 70-78.

Faigle W, Raposo G, Tenza D, Pinet V, Vogt AB, Kropshofer H, Fischer A, de Saint-Basile G and Amigorena S (1998) Deficient peptide loading and MHC class II endosomal sorting in a human genetic immunodeficiency disease: the Chediak-Higashi syndrome. *J. Cell Biol.* **141**(5): 1121-1134.

Falguières T, Luyet PP and Gruenberg J (2009) Molecular assemblies and membrane domains in multivesicular endosome dynamics. *Exp. Cell Res.* **315**(9): 1567-1573.

Falkenstein K and De Lozanne A (2014) Dictyostelium LvsB has a regulatory role in endosomal vesicle fusion. *J. Cell Sci.* **127**(Pt 20): 4356-4367.

Fernández-Borja M, Janssen L, Verwoerd D, Hordijk P and Neefjes J (2005) RhoB regulates endosome transport by promoting actin assembly on endosomal membranes through Dia1. *J. Cell Sci.* **118**(Pt 12): 2661-2670.

Flannery AR, Czibener C and Andrews NW (2010) Palmitoylation-dependent association with CD63 targets the Ca2+ sensor synaptotagmin VII to lysosomes. *J. Cell Biol.* **191**(3): 599-613.

Fortwendel JR, Juvvadi PR, Rogg LE, Asfaw YG, Burns KA, Randell SH and Steinbach WJ (2012) Plasma membrane localization is required for RasA-mediated polarized morphogenesis and virulence of *Aspergillus fumigatus*. *Eukaryot. Cell* **11**(8): 966-977.

Fritz G and Kaina B (1997) RhoB encoding a UV-inducible Ras-related small GTP-binding protein is regulated by GTPases of the Rho family and independent of JNK, ERK, and p38 MAP kinase. *J. Biol. Chem.* **272**(49): 30637-30644.

Fritz G and Kaina B (2000) Ras-related GTPase RhoB forces alkylation-induced apoptotic cell death. *Biochem. Biophys. Res. Commun.* **268**(3): 784-789.

Fuller M, Meikle PJ and Hopwood JJ (2006) Epidemiology of lysosomal storage diseases: an overview, in *Fabry Disease: Perspectives from 5 Years of FOS* (Mehta A, Beck M and Sunder-Plassmann G eds), Oxford.

Funk CD (2001) Prostaglandins and leukotrienes: advances in eicosanoid biology. *Science* **294**(5548): 1871-1875.

Futter CE, Pearse A, Hewlett LJ and Hopkins CR (1996) Multivesicular endosomes containing internalized EGF-EGF receptor complexes mature and then fuse directly with lysosomes. *J. Cell Biol.* **132**(6): 1011-1023.

Gampel A, Parker PJ and Mellor H (1999) Regulation of epidermal growth factor receptor traffic by the small GTPase RhoB. *Curr. Biol.* **9**(17): 955-958.

Ganley IG and Pfeffer SR (2006) Cholesterol accumulation sequesters Rab9 and disrupts late endosome function in NPC1-deficient cells. *J. Biol. Chem.* **281**(26): 17890-17899.

Gao L, Zackert WE, Hasford JJ, Danekis ME, Milne GL, Remmert C, Reese J, Yin H, Tai HH, Dey SK, Porter NA and Morrow JD (2003) Formation of prostaglandins E2 and D2 via the isoprostane pathway: a mechanism for the generation of bioactive prostaglandins independent of cyclooxygenase. *J. Biol. Chem.* **278**(31): 28479-28489.

Garrus JE, von Schwedler UK, Pornillos OW, Morham SG, Zavitz KH, Wang HE, Wettstein DA, Stray KM, Cote M, Rich RL, Myszka DG and Sundquist WI (2001) Tsg101 and the vacuolar protein sorting pathway are essential for HIV-1 budding. *Cell* **107**(1): 55-65.

Garzón B, Oeste CL, Díez-Dacal B and Pérez-Sala D (2011) Proteomic studies on protein modification by cyclopentenone prostaglandins: expanding our view on electrophile actions. *J. Proteomics* **74**(11): 2243-2263.

Gerald D, Adini I, Shechter S, Perruzzi C, Varnau J, Hopkins B, Kazerounian S, Kurschat P, Blachon S, Khedkar S, Bagchi M, Sherris D, Prendergast GC, Klagsbrun M, Stuhlmann H, Rigby AC, Nagy JA and Benjamin LE (2013) RhoB controls coordination of adult angiogenesis and lymphangiogenesis following injury by regulating VEZF1-mediated transcription. *Nat Commun* **4**: 2824.

Gerhard R, John H, Aktories K and Just I (2003) Thiol-modifying phenylarsine oxide inhibits guanine nucleotide binding of Rho but not of Rac GTPases. *Mol. Pharmacol.* **63**(6): 1349-1355.

Geyer M and Wittinghofer A (1997) GEFs, GAPs, GDIs and effectors: taking a closer (3D) look at the regulation of Ras-related GTP-binding proteins. *Curr. Opin. Struct. Biol.* **7**(6): 786-792.

Ghosh P, Dahms NM and Kornfeld S (2003) Mannose 6-phosphate receptors: new twists in the tale. *Nat. Rev. Mol. Cell Biol.* **4**(3): 202-212.

Gibbings DJ, Ciaudo C, Erhardt M and Voinnet O (2009) Multivesicular bodies associate with components of miRNA effector complexes and modulate miRNA activity. *Nat. Cell Biol.* **11**(9): 1143-1149.

Gilk SD, Cockrell DC, Luterbach C, Hansen B, Knodler LA, Ibarra JA, Steele-Mortimer O and Heinzen RA (2013) Bacterial colonization of host cells in the absence of cholesterol. *PLoS Pathog.* **9**(1): e1003107.

Gillooly DJ, Morrow IC, Lindsay M, Gould R, Bryant NJ, Gaullier JM, Parton RG and Stenmark H (2000) Localization of phosphatidylinositol 3-phosphate in yeast and mammalian cells. *EMBO J.* **19**(17): 4577-4588.

Gómez GA and Daniotti JL (2005) H-Ras dynamically interacts with recycling endosomes in CHO-K1 cells: involvement of Rab5 and Rab11 in the trafficking of H-Ras to this pericentriolar endocytic compartment. *J. Biol. Chem.* **280**(41): 34997-35010.

Gorfe AA, Babakhani A and McCammon JA (2007) H-Ras protein in a bilayer: interaction and structure perturbation. *J. Am. Chem. Soc.* **129**(40): 12280-12286.

Hall A (2005) Rho GTPases and the control of cell behaviour. *Biochem. Soc. Trans.* **33**(Pt 5): 891-895.

Hancock JF, Magee AI, Childs JE and Marshall CJ (1989) All Ras proteins are polyisoprenylated but only some are palmitoylated. *Cell* **57**(7): 1167-1177.

Hancock JF and Parton RG (2005) Ras plasma membrane signalling platforms. *Biochem. J.* **389**(Pt 1): 1-11.

Hanson PI, Roth R, Lin Y and Heuser JE (2008) Plasma membrane deformation by circular arrays of ESCRT-III protein filaments. *J. Cell Biol.* **180**(2): 389-402.

Hartman HL, Hicks KA and Fierke CA (2005) Peptide specificity of protein prenyltransferases is determined mainly by reactivity rather than binding affinity. *Biochemistry* **44**(46): 15314-15324.

Hemler ME (2005) Tetraspanin functions and associated microdomains. *Nat. Rev. Mol. Cell Biol.* **6**(10): 801-811.

Henne WM, Stenmark H and Emr SD (2013) Molecular mechanisms of the membrane sculpting ESCRT pathway. *Cold Spring Harb. Perspect. Biol.* **5**(9).

Hirata D, Nakano K, Fukui M, Takenaka H, Miyakawa T and Mabuchi I (1998) Genes that cause aberrant cell morphology by overexpression in fission yeast: a role of a small GTP-binding protein Rho2 in cell morphogenesis. *J. Cell Sci.* **111 (Pt 2)**: 149-159.

Hislop JN, Marley A and Von Zastrow M (2004) Role of mammalian vacuolar protein-sorting proteins in endocytic trafficking of a non-ubiquitinated G protein-coupled receptor to lysosomes. *J. Biol. Chem.* **279**(21): 22522-22531.

Ho TT, Merajver SD, Lapiere CM, Nusgens BV and Deroanne CF (2008) RhoA-GDP regulates RhoB protein stability. Potential involvement of RhoGDIalpha. *J. Biol. Chem.* **283**(31): 21588-21598.

Holland P, Torgersen ML, Sandvig K and Simonsen A (2014) LYST affects lysosome size and quantity, but not trafficking or degradation through autophagy or endocytosis. *Traffic*.

Huang J, Reggiori F and Klionsky DJ (2007a) The transmembrane domain of acid trehalase mediates ubiquitin-independent multivesicular body pathway sorting. *Mol. Biol. Cell* **18**(7): 2511-2524.

Huang M, Duhadaway JB, Prendergast GC and Laury-Kleintop LD (2007b) RhoB regulates PDGFR-beta trafficking and signaling in vascular smooth muscle cells. *Arterioscler. Thromb. Vasc. Biol.* **27**(12): 2597-2605.

Huang M, Kamasani U and Prendergast GC (2006) RhoB facilitates c-Myc turnover by supporting efficient nuclear accumulation of GSK-3. *Oncogene* **25**(9): 1281-1289.

Huizing M, Anikster Y and Gahl WA (2001) Hermansky-Pudlak syndrome and Chediak-Higashi syndrome: disorders of vesicle formation and trafficking. *Thromb. Haemost.* **86**(1): 233-245.

Huizing M, Helip-Wooley A, Westbroek W, Gunay-Aygun M and Gahl WA (2008) Disorders of lysosome-related organelle biogenesis: clinical and molecular genetics. *Annu Rev Genomics Hum Genet* **9**: 359-386.

Huotari J and Helenius A (2011) Endosome maturation. *EMBO J.* **30**(17): 3481-3500.

Huynh C, Roth D, Ward DM, Kaplan J and Andrews NW (2004) Defective lysosomal exocytosis and plasma membrane repair in Chediak-Higashi/*beige* cells. *Proc. Natl. Acad. Sci. U. S. A.* **101**(48): 16795-16800.

Israels SJ and McMillan-Ward EM (2010) Palmitoylation supports the association of tetraspanin CD63 with CD9 and integrin alphaIIbbeta3 in activated platelets. *Thromb. Res.* **125**(2): 152-158.

Janosi L, Li Z, Hancock JF and Gorfe AA (2012) Organization, dynamics, and segregation of Ras nanoclusters in membrane domains. *Proc. Natl. Acad. Sci. U. S. A.* **109**(21): 8097-8102.

Jiang Z, Redfern RE, Isler Y, Ross AH and Gericke A (2014) Cholesterol stabilizes fluid phosphoinositide domains. *Chem. Phys. Lipids* **182**: 52-61.

Kabeya Y, Mizushima N, Ueno T, Yamamoto A, Kirisako T, Noda T, Kominami E, Ohsumi Y and Yoshimori T (2000) LC3, a mammalian homologue of yeast Apg8p, is localized in autophagosome membranes after processing. *EMBO J.* **19**(21): 5720-5728.

Kamasani U, Huang M, Duhadaway JB, Prochownik EV, Donover PS and Prendergast GC (2004) Cyclin B1 is a critical target of RhoB in the cell suicide program triggered by farnesyl transferase inhibition. *Cancer Res.* **64**(22): 8389-8396.

Karim MA, Suzuki K, Fukai K, Oh J, Nagle DL, Moore KJ, Barbosa E, Falik-Borenstein T, Filipovich A, Ishida Y, Kivrikko S, Klein C, Kreuz F, Levin A, Miyajima H, Regueiro J, Russo C, Uyama E, Vierimaa O and Spritz RA (2002) Apparent genotype-phenotype correlation in childhood, adolescent, and adult Chediak-Higashi syndrome. *Am. J. Med. Genet.* **108**(1): 16-22.

Katzmann DJ, Babst M and Emr SD (2001) Ubiquitin-dependent sorting into the multivesicular body pathway requires the function of a conserved endosomal protein sorting complex, ESCRT-I. *Cell* **106**(2): 145-155.

Kim EH and Surh YJ (2006) 15-deoxy-Delta12,14-prostaglandin J2 as a potential endogenous regulator of redox-sensitive transcription factors. *Biochem. Pharmacol.* **72**(11): 1516-1528.

Kim JS and Raines RT (1995) Dibromobimane as a fluorescent cross-linking reagent. *Anal. Biochem.* **225**(1): 174-176.

Kim SE, Yoon JY, Jeong WJ, Jeon SH, Park Y, Yoon JB, Park YN, Kim H and Choi KY (2009) H-Ras is degraded by Wnt/beta-catenin signaling via beta-TrCP-mediated polyubiquitylation. *J. Cell Sci.* **122**(Pt 6): 842-848.

Klöpper TH, Kienle N, Fasshauer D and Munro S (2012) Untangling the evolution of Rab G proteins: implications of a comprehensive genomic analysis. *BMC Biol.* **10**: 71.

Kneen M, Farinas J, Li Y and Verkman AS (1998) Green fluorescent protein as a noninvasive intracellular pH indicator. *Biophys. J.* **74**(3): 1591-1599.

Kobayashi T, Beuchat MH, Lindsay M, Frias S, Palmiter RD, Sakuraba H, Parton RG and Gruenberg J (1999) Late endosomal membranes rich in lysobisphosphatidic acid regulate cholesterol transport. *Nat. Cell Biol.* **1**(2): 113-118.

Koenitzer JR and Freeman BA (2010) Redox signaling in inflammation: interactions of endogenous electrophiles and mitochondria in cardiovascular disease. *Ann. N. Y. Acad. Sci.* **1203**: 45-52.

Kolter T and Sandhoff K (2005) Principles of lysosomal membrane digestion: stimulation of sphingolipid degradation by sphingolipid activator proteins and anionic lysosomal lipids. *Annu. Rev. Cell. Dev. Biol.* **21**: 81-103.

Krzewski K and Cullinane AR (2013) Evidence for defective Rab GTPase-dependent cargo traffic in immune disorders. *Exp. Cell Res.* **319**(15): 2360-2367.

Kypri E, Falkenstein K and De Lozanne A (2013) Antagonistic control of lysosomal fusion by Rab14 and the Lyst-related protein LvsB. *Traffic* **14**(5): 599-609.

Lajoie-Mazenc I, Tovar D, Penary M, Lortal B, Allart S, Favard C, Brihoum M, Pradines A and Favre G (2008) MAP1A light chain-2 interacts with GTP-RhoB to control epidermal growth factor (EGF)-dependent EGF receptor signaling. *J. Biol. Chem.* **283**(7): 4155-4164.

Lambou K, Tharreau D, Kohler A, Sirven C, Marguerettaz M, Barbisan C, Sexton AC, Kellner EM, Martín F, Howlett BJ, Orbach MJ and Lebrun MH (2008) Fungi have three tetraspanin families with distinct functions. *BMC Genomics* **9**: 63.

Laufs U, Endres M, Custodis F, Gertz K, Nickenig G, Liao JK and Bohm M (2000) Suppression of endothelial nitric oxide production after withdrawal of statin treatment is mediated by negative feedback regulation of rho GTPase gene transcription. *Circulation* **102**(25): 3104-3110.

Laulagnier K, Motta C, Hamdi S, Roy S, Fauvelle F, Pageaux JF, Kobayashi T, Salles JP, Perret B, Bonnerot C and Record M (2004) Mast cell- and dendritic cell-derived exosomes display a specific lipid composition and an unusual membrane organization. *Biochem. J.* **380**(Pt 1): 161-171.

Lee J, Giordano S and Zhang J (2012) Autophagy, mitochondria and oxidative stress: cross-talk and redox signalling. *Biochem. J.* **441**(2): 523-540.

Lee SE and Park YS (2013) Role of lipid peroxidation-derived alpha, beta-unsaturated aldehydes in vascular dysfunction. *Oxid. Med. Cell. Longev.* **2013**: 629028.

Leung KF, Baron R and Seabra MC (2006) Thematic review series: lipid posttranslational modifications. geranylgeranylation of Rab GTPases. *J. Lipid Res.* **47**(3): 467-475.

Leung KF, Dacks JB and Field MC (2008) Evolution of the multivesicular body ESCRT machinery; retention across the eukaryotic lineage. *Traffic* **9**(10): 1698-1716.

Leventis PA and Grinstein S (2010) The distribution and function of phosphatidylserine in cellular membranes. *Annu Rev Biophys* **39**: 407-427.

Levonen AL, Landar A, Ramachandran A, Ceaser EK, Dickinson DA, Zanoni G, Morrow JD and Darley-Usmar VM (2004) Cellular mechanisms of redox cell signalling: role of cysteine modification in controlling antioxidant defences in response to electrophilic lipid oxidation products. *Biochem. J.* **378**(Pt 2): 373-382.

Liou W, Geuze HJ, Geelen MJ and Slot JW (1997) The autophagic and endocytic pathways converge at the nascent autophagic vacuoles. *J. Cell Biol.* **136**(1): 61-70.

Lippincott-Schwartz J and Phair RD (2010) Lipids and cholesterol as regulators of traffic in the endomembrane system. *Annu Rev Biophys* **39**: 559-578.

Liu AX, Rane N, Liu JP and Prendergast GC (2001) RhoB is dispensable for mouse development, but it modifies susceptibility to tumor formation as well as cell adhesion and growth factor signaling in transformed cells. *Mol. Cell. Biol.* **21**(20): 6906-6912.

Lobo S, Greentree WK, Linder ME and Deschenes RJ (2002) Identification of a Ras palmitoyltransferase in Saccharomyces cerevisiae. *J. Biol. Chem.* **277**(43): 41268-41273.

Lu L and Hong W (2014) From endosomes to the trans-Golgi network. *Semin. Cell Dev. Biol.* **31**: 30-39.

Ma Y, Kuno T, Kita A, Asayama Y and Sugiura R (2006) Rho2 is a target of the farnesyltransferase Cpp1 and acts upstream of Pmk1 mitogen-activated protein kinase signaling in fission yeast. *Mol. Biol. Cell* **17**(12): 5028-5037.

Madaule P and Axel R (1985) A novel Ras-related gene family. *Cell* **41**(1): 31-40.

Mageswaran SK, Dixon MG, Curtiss M, Keener JP and Babst M (2014) Binding to any ESCRT can mediate ubiquitin-independent cargo sorting. *Traffic* **15**(2): 212-229.

Malcolm T, Ettehadieh E and Sadowski I (2003) Mitogen-responsive expression of RhoB is regulated by RNA stability. *Oncogene* **22**(40): 6142-6150.

Mallis RJ, Buss JE and Thomas JA (2001) Oxidative modification of H-Ras: S-thiolation and S-nitrosylation of reactive cysteines. *Biochem. J.* **355**(Pt 1): 145-153.

Marchetti A, Mercanti V, Cornillon S, Alibaud L, Charette SJ and Cosson P (2004) Formation of multivesicular endosomes in Dictyostelium. *J. Cell Sci.* **117**(Pt 25): 6053-6059.

Matozaki T, Nakanishi H and Takai Y (2000) Small G-protein networks: their crosstalk and signal cascades. *Cell. Signal.* **12**(8): 515-524.

Matsuo H, Chevallier J, Mayran N, Le Blanc I, Ferguson C, Faure J, Blanc NS, Matile S, Dubochet J, Sadoul R, Parton RG, Vilbois F and Gruenberg J (2004) Role of LBPA and Alix in multivesicular liposome formation and endosome organization. *Science* **303**(5657): 531-534.

Maurer-Stroh S, Washietl S and Eisenhaber F (2003) Protein prenyltransferases: anchor size, pseudogenes and parasites. *Biol. Chem.* **384**(7): 977-989.

Maxfield FR and van Meer G (2010) Cholesterol, the central lipid of mammalian cells. *Curr. Opin. Cell Biol.* **22**(4): 422-429.

McCormick PJ, Dumaresq-Doiron K, Pluviose AS, Pichette V, Tosato G and Lefrancois S (2008) Palmitoylation controls recycling in lysosomal sorting and trafficking. *Traffic* **9**(11): 1984-1997.

McMahon HT and Gallop JL (2005) Membrane curvature and mechanisms of dynamic cell membrane remodelling. *Nature* **438**(7068): 590-596.

McTaggart SJ (2006) Isoprenylated proteins. *Cell. Mol. Life Sci.* **63**(3): 255-267.

Mellor H, Flynn P, Nobes CD, Hall A and Parker PJ (1998) PRK1 is targeted to endosomes by the small GTPase, RhoB. *J. Biol. Chem.* **273**(9): 4811-4814.

Menasche G, Feldmann J, Houdusse A, Desaymard C, Fischer A, Goud B and de Saint Basile G (2003) Biochemical and functional characterization of Rab27a mutations occurring in Griscelli syndrome patients. *Blood* **101**(7): 2736-2742.

Michaelson D, Silletti J, Murphy G, D'Eustachio P, Rush M and Philips MR (2001) Differential localization of Rho GTPases in live cells: regulation by hypervariable regions and RhoGDI binding. *J. Cell Biol.* **152**(1): 111-126.

Misaki R, Morimatsu M, Uemura T, Waguri S, Miyoshi E, Taniguchi N, Matsuda M and Taguchi T (2010) Palmitoylated Ras proteins traffic through recycling endosomes to the plasma membrane during exocytosis. *J. Cell Biol.* **191**(1): 23-29.

Mitra S, Cheng KW and Mills GB (2011) Rab GTPases implicated in inherited and acquired disorders. *Semin. Cell Dev. Biol.* **22**(1): 57-68.

Mizushima N, Levine B, Cuervo AM and Klionsky DJ (2008) Autophagy fights disease through cellular self-digestion. *Nature* **451**(7182): 1069-1075.

Mizushima N and Yoshimori T (2007) How to interpret LC3 immunoblotting. *Autophagy* **3**(6): 542-545.

Mizushima N, Yoshimori T and Levine B (2010) Methods in mammalian autophagy research. *Cell* **140**(3): 313-326.

Mizushima N, Yoshimori T and Ohsumi Y (2011) The role of Atg proteins in autophagosome formation. *Annu. Rev. Cell. Dev. Biol.* **27**: 107-132.

Möbius W, van Donselaar E, Ohno-Iwashita Y, Shimada Y, Heijnen HF, Slot JW and Geuze HJ (2003) Recycling compartments and the internal vesicles of multivesicular bodies harbor most of the cholesterol found in the endocytic pathway. *Traffic* **4**(4): 222-231.

Mollinedo F, Pérez-Sala D, Gajate C, Jiménez B, Rodríguez P and Lacal JC (1993) Localization of Rap1 and Rap2 proteins in the gelatinase-containing granules of human neutrophils. *FEBS Lett.* **326**(1-3): 209-214.

Morita E and Sundquist WI (2004) Retrovirus budding. *Annu. Rev. Cell. Dev. Biol.* **20**: 395-425.

Mukherjee S and Maxfield FR (2004) Lipid and cholesterol trafficking in NPC. *Biochim. Biophys. Acta* **1685**(1-3): 28-37.

Murk JL, Stoorvogel W, Kleijmeer MJ and Geuze HJ (2002) The plasticity of multivesicular bodies and the regulation of antigen presentation. *Semin. Cell Dev. Biol.* **13**(4): 303-311.

Narumiya S and Fukushima M (1985) Delta 12-prostaglandin J2, an ultimate metabolite of prostaglandin D2 exerting cell growth inhibition. *Biochem. Biophys. Res. Commun.* **127**(3): 739-745.

Nguyen UT, Goody RS and Alexandrov K (2010) Understanding and exploiting protein prenyltransferases. *ChemBioChem* **11**(9): 1194-1201.

Nishida M, Sawa T, Kitajima N, Ono K, Inoue H, Ihara H, Motohashi H, Yamamoto M, Suematsu M, Kurose H, van der Vliet A, Freeman BA, Shibata T, Uchida K, Kumagai Y and Akaike T (2012) Hydrogen sulfide anion regulates redox signaling via electrophile sulfhydration. *Nat. Chem. Biol.* **8**(8): 714-724.

Oeste CL, Díez-Dacal B, Bray F, García de Lacoba M, de la Torre BG, Andreu D, Ruiz-Sánchez AJ, Pérez-Inestrosa E, García-Domínguez CA, Rojas JM and Pérez-Sala D (2011) The C-terminus of H-Ras as a target for the covalent binding of

reactive compounds modulating Ras-dependent pathways. *PLoS One* **6**(1): e15866.

Oeste CL and Pérez-Sala D (2014) Modification of cysteine residues by cyclopentenone prostaglandins: interplay with redox regulation of protein function. *Mass Spectrom. Rev.* **33**(2): 110-125.

Oeste CL, Pinar M, Schink KO, Martínez-Turrion J, Stenmark H, Peñalva MA and Pérez-Sala D (2014) An isoprenylation and palmitoylation motif promotes intraluminal vesicle delivery of proteins in cells from distant species. *PLoS One* **9**(9): e107190.

Oeste CL, Seco E, Patton WF, Boya P and Pérez-Sala D (2013) Interactions between autophagic and endolysosomal markers in endothelial cells. *Histochem. Cell Biol.* **139**(5): 659-670.

Ohno K, Fujiwara M, Fukushima M and Narumiya S (1986) Metabolic dehydration of prostaglandin E2 and cellular uptake of the dehydration product: correlation with prostaglandin E2-induced growth inhibition. *Biochem. Biophys. Res. Commun.* **139**(2): 808-815.

Oliva JL, Pérez-Sala D, Castrillo A, Martínez N, Cañada FJ, Bosca L and Rojas JM (2003) The cyclopentenone 15-deoxy-delta 12,14-prostaglandin J2 binds to and activates H-Ras. *Proc. Natl. Acad. Sci. U. S. A.* **100**(8): 4772-4777.

Oliver C, Essner E, Zimring A and Haimes H (1976) Age-related accumulation of ceroid-like pigment in mice with Chediak-Higashi syndrome. *Am. J. Pathol.* **84**(2): 225-238.

Omerovic J, Laude AJ and Prior IA (2007) Ras proteins: paradigms for compartmentalised and isoform-specific signalling. *Cell. Mol. Life Sci.* **64**(19-20): 2575-2589.

Pantazopoulou A and Peñalva MA (2009) Organization and dynamics of the *Aspergillus nidulans* Golgi during apical extension and mitosis. *Mol. Biol. Cell* **20**(20): 4335-4347.

Park SY and Guo X (2014) Adaptor protein complexes and intracellular transport. *Biosci. Rep.* **34**(4).

Patterson GH and Lippincott-Schwartz J (2002) A photoactivatable GFP for selective photolabeling of proteins and cells. *Science* **297**(5588): 1873-1877.

Peñalva MA, Galindo A, Abenza JF, Pinar M, Calcagno-Pizarelli AM, Arst HN and Pantazopoulou A (2012) Searching for gold beyond mitosis: Mining intracellular membrane traffic in *Aspergillus nidulans*. *Cell Logist* **2**(1): 2-14.

Peng Y, Tang F and Weisman LS (2006) Palmitoylation plays a role in targeting Vac8p to specific membrane subdomains. *Traffic* **7**(10): 1378-1387.

Peplowska K, Markgraf DF, Ostrowicz CW, Bange G and Ungermann C (2007) The CORVET tethering complex interacts with the yeast Rab5 homolog Vps21 and is involved in endolysosomal biogenesis. *Dev. Cell* **12**(5): 739-750.

Pereira-Leal JB and Seabra MC (2000) The mammalian Rab family of small GTPases: definition of family and subfamily sequence motifs suggests a mechanism for functional specificity in the Ras superfamily. *J. Mol. Biol.* **301**(4): 1077-1087.

Pérez-Hernández D, Gutiérrez-Vázquez C, Jorge I, López-Martín S, Ursa A, Sánchez-Madrid F, Vázquez J and Yáñez-Mo M (2013) The intracellular interactome of tetraspanin-enriched microdomains reveals their function as sorting machineries toward exosomes. *J. Biol. Chem.* **288**(17): 11649-11661.

Pérez-Sala D (2007) Protein isoprenylation in biology and disease: general overview and perspectives from studies with genetically engineered animals. *Front. Biosci.* **12**: 4456-4472.

Pérez-Sala D, Boya P, Ramos I, Herrera M and Stamatakis K (2009) The C-terminal sequence of RhoB directs protein degradation through an endo-lysosomal pathway. *PLoS One* **4**(12): e8117.

Pérez-Sala D, Tan EW, Cañada FJ and Rando RR (1991) Methylation and demethylation reactions of guanine nucleotide-binding proteins of retinal rod outer segments. *Proc. Natl. Acad. Sci. U. S. A.* **88**(8): 3043-3046.

Platt FM, Boland B and van der Spoel AC (2012) The cell biology of disease: lysosomal storage disorders: the cellular impact of lysosomal dysfunction. *J. Cell Biol.* **199**(5): 723-734.

Platta HW and Stenmark H (2011) Endocytosis and signaling. *Curr. Opin. Cell Biol.* **23**(4): 393-403.

Pols MS and Klumperman J (2009) Trafficking and function of the tetraspanin CD63. *Exp. Cell Res.* **315**(9): 1584-1592.

Poteryaev D, Datta S, Ackema K, Zerial M and Spang A (2010) Identification of the switch in early-to-late endosome transition. *Cell* **141**(3): 497-508.

Prada-Delgado A, Carrasco-Marín E, Peña-Macarro C, Del Cerro-Vadillo E, Fresno-Escudero M, Leyva-Cobián F and Álvarez-Domínguez C (2005) Inhibition of Rab5a exchange activity is a key step for *Listeria monocytogenes* survival. *Traffic* **6**(3): 252-265.

Prendergast GC (2001) Actin' up: RhoB in cancer and apoptosis. *Nat. Rev. Cancer* **1**(2): 162-168.

Prior IA, Harding A, Yan J, Sluimer J, Parton RG and Hancock JF (2001) GTP-dependent segregation of H-Ras from lipid rafts is required for biological activity. *Nat. Cell Biol.* **3**(4): 368-375.

Raiborg C, Bache KG, Mehlum A, Stang E and Stenmark H (2001) Hrs recruits clathrin to early endosomes. *EMBO J.* **20**(17): 5008-5021.

Raiborg C and Stenmark H (2009) The ESCRT machinery in endosomal sorting of ubiquitylated membrane proteins. *Nature* **458**(7237): 445-452.

Raposo G and Stoorvogel W (2013) Extracellular vesicles: exosomes, microvesicles, and friends. *J. Cell Biol.* **200**(4): 373-383.

Raymond CK, Howald-Stevenson I, Vater CA and Stevens TH (1992) Morphological classification of the yeast vacuolar protein sorting mutants: evidence for a prevacuolar compartment in class E vps mutants. *Mol. Biol. Cell* **3**(12): 1389-1402.

Recchi C and Seabra MC (2012) Novel functions for Rab GTPases in multiple aspects of tumour progression. *Biochem. Soc. Trans.* **40**(6): 1398-1403.

Reddy A, Caler EV and Andrews NW (2001) Plasma membrane repair is mediated by Ca(2+)-regulated exocytosis of lysosomes. *Cell* **106**(2): 157-169.

Renedo M, Gayarre J, García-Domínguez CA, Pérez-Rodríguez A, Prieto A, Cañada FJ, Rojas JM and Pérez-Sala D (2007) Modification and activation of Ras proteins by electrophilic prostanoids with different structure are site-selective. *Biochemistry* **46**(22): 6607-6616.

Ridley AJ (2001) Rho proteins: linking signaling with membrane trafficking. *Traffic* **2**(5): 303-310.

Rink J, Ghigo E, Kalaidzidis Y and Zerial M (2005) Rab conversion as a mechanism of progression from early to late endosomes. *Cell* **122**(5): 735-749.

Roberts PJ, Mitin N, Keller PJ, Chenette EJ, Madigan JP, Currin RO, Cox AD, Wilson O, Kirschmeier P and Der CJ (2008) Rho Family GTPase modification and dependence on CAAX motif-signaled posttranslational modification. *J. Biol. Chem.* **283**(37): 25150-25163.

Rocks O, Peyker A, Kahms M, Verveer PJ, Koerner C, Lumbierres M, Kuhlmann J, Waldmann H, Wittinghofer A and Bastiaens PI (2005) An acylation cycle regulates localization and activity of palmitoylated Ras isoforms. *Science* **307**(5716): 1746-1752.

Rojas AM, Fuentes G, Rausell A and Valencia A (2012) The Ras protein superfamily: evolutionary tree and role of conserved amino acids. *J. Cell Biol.* **196**(2): 189-201.

Rondanino C, Rojas R, Ruiz WG, Wang E, Hughey RP, Dunn KW and Apodaca G (2007) RhoB-dependent modulation of postendocytic traffic in polarized Madin-Darby canine kidney cells. *Traffic* **8**(7): 932-949.

Rotblat B, Yizhar O, Haklai R, Ashery U and Kloog Y (2006) Ras and its signals diffuse through the cell on randomly moving nanoparticles. *Cancer Res.* **66**(4): 1974-1981.

Roth AF, Feng Y, Chen L and Davis NG (2002) The yeast DHHC cysteine-rich domain protein Akr1p is a palmitoyl transferase. *J. Cell Biol.* **159**(1): 23-28.

Roth AF, Wan J, Bailey AO, Sun B, Kuchar JA, Green WN, Phinney BS, Yates JR, 3rd and Davis NG (2006) Global analysis of protein palmitoylation in yeast. *Cell* **125**(5): 1003-1013.

Rous BA, Reaves BJ, Ihrke G, Briggs JA, Gray SR, Stephens DJ, Banting G and Luzio JP (2002) Role of adaptor complex AP-3 in targeting wild-type and mutated CD63 to lysosomes. *Mol. Biol. Cell* **13**(3): 1071-1082.

Rusten TE and Simonsen A (2008) ESCRT functions in autophagy and associated disease. *Cell Cycle* **7**(9): 1166-1172.

Rusten TE, Vaccari T and Stenmark H (2012) Shaping development with ESCRTs. *Nat. Cell Biol.* **14**(1): 38-45.

Sadowski L, Pilecka I and Miaczynska M (2009) Signaling from endosomes: location makes a difference. *Exp. Cell Res.* **315**(9): 1601-1609.

Sadowski M, Suryadinata R, Tan AR, Roesley SN and Sarcevic B (2012) Protein monoubiquitination and polyubiquitination generate structural diversity to control distinct biological processes. *IUBMB Life* **64**(2): 136-142.

Saftig P and Klumperman J (2009) Lysosome biogenesis and lysosomal membrane proteins: trafficking meets function. *Nat. Rev. Mol. Cell Biol.* **10**(9): 623-635.

Sagne C and Gasnier B (2008) Molecular physiology and pathophysiology of lysosomal membrane transporters. *J. Inherit. Metab. Dis.* **31**(2): 258-266.

Samson RY, Obita T, Freund SM, Williams RL and Bell SD (2008) A role for the ESCRT system in cell division in archaea. *Science* **322**(5908): 1710-1713.

Sánchez-Gómez FJ, Cernuda-Morollón E, Stamatakis K and Pérez-Sala D (2004) Protein thiol modification by 15-deoxy-Delta12,14-prostaglandin J2 addition in mesangial cells: role in the inhibition of pro-inflammatory genes. *Mol. Pharmacol.* **66**(5): 1349-1358.

Sánchez-Gómez FJ, Gayarre J, Avellano MI and Pérez-Sala D (2007) Direct evidence for the covalent modification of glutathione-S-transferase P1-1 by electrophilic

prostaglandins: implications for enzyme inactivation and cell survival. *Arch. Biochem. Biophys.* **457**(2): 150-159.

Sandilands E, Cans C, Fincham VJ, Brunton VG, Mellor H, Prendergast GC, Norman JC, Superti-Furga G and Frame MC (2004) RhoB and actin polymerization coordinate Src activation with endosome-mediated delivery to the membrane. *Dev. Cell* **7**(6): 855-869.

Schink KO, Raiborg C and Stenmark H (2013) Phosphatidylinositol 3-phosphate, a lipid that regulates membrane dynamics, protein sorting and cell signalling. *Bioessays* **35**(10): 900-912.

Schmidt-Glenewinkel H, Vacheva I, Hoeller D, Dikic I and Eils R (2008) An ultrasensitive sorting mechanism for EGF receptor endocytosis. *BMC Syst. Biol.* **2**: 32.

Schmitz AA, Govek EE, Bottner B and Van Aelst L (2000) Rho GTPases: signaling, migration, and invasion. *Exp. Cell Res.* **261**(1): 1-12.

Schröder J, Lullmann-Rauch R, Himmerkus N, Pleines I, Nieswandt B, Orinska Z, Koch-Nolte F, Schröder B, Bleich M and Saftig P (2009) Deficiency of the tetraspanin CD63 associated with kidney pathology but normal lysosomal function. *Mol. Cell. Biol.* **29**(4): 1083-1094.

Schwartz AL and Ciechanover A (2009) Targeting proteins for destruction by the ubiquitin system: implications for human pathobiology. *Annu. Rev. Pharmacol. Toxicol.* **49**: 73-96.

Schweizer A, Kornfeld S and Rohrer J (1996) Cysteine34 of the cytoplasmic tail of the cation-dependent mannose 6-phosphate receptor is reversibly palmitoylated and required for normal trafficking and lysosomal enzyme sorting. *J. Cell Biol.* **132**(4): 577-584.

Seabra MC, Brown MS and Goldstein JL (1993) Retinal degeneration in choroideremia: deficiency of Rab geranylgeranyl transferase. *Science* **259**(5093): 377-381.

Seabra MC, Ho YK and Anant JS (1995) Deficient geranylgeranylation of Ram/Rab27 in choroideremia. *J. Biol. Chem.* **270**(41): 24420-24427.

Seals DF, Eitzen G, Margolis N, Wickner WT and Price A (2000) A Ypt/Rab effector complex containing the Sec1 homolog Vps33p is required for homotypic vacuole fusion. *Proc. Natl. Acad. Sci. U. S. A.* **97**(17): 9402-9407.

Shaner NC, Campbell RE, Steinbach PA, Giepmans BN, Palmer AE and Tsien RY (2004) Improved monomeric red, orange and yellow fluorescent proteins derived from *Discosoma sp.* red fluorescent protein. *Nat. Biotechnol.* **22**(12): 1567-1572.

Shaner NC, Lin MZ, McKeown MR, Steinbach PA, Hazelwood KL, Davidson MW and Tsien RY (2008) Improving the photostability of bright monomeric orange and red fluorescent proteins. *Nat. Methods* **5**(6): 545-551.

Sharpe HJ, Stevens TJ and Munro S (2010) A comprehensive comparison of transmembrane domains reveals organelle-specific properties. *Cell* **142**(1): 158-169.

Shen B, Wu N, Yang JM and Gould SJ (2011) Protein targeting to exosomes/microvesicles by plasma membrane anchors. *J. Biol. Chem.* **286**(16): 14383-14395.

Shibata T, Kondo M, Osawa T, Shibata N, Kobayashi M and Uchida K (2002) 15-deoxy-delta 12,14-prostaglandin J2. A prostaglandin D2 metabolite generated during inflammatory processes. *J. Biol. Chem.* **277**(12): 10459-10466.

Shim S, Merrill SA and Hanson PI (2008) Novel interactions of ESCRT-III with LIP5 and Vps4 and their implications for ESCRT-III disassembly. *Mol. Biol. Cell* **19**(6): 2661-2672.

Shiraki T, Kamiya N, Shiki S, Kodama TS, Kakizuka A and Jingami H (2005) Alpha,beta-unsaturated ketone is a core moiety of natural ligands for covalent binding to peroxisome proliferator-activated receptor gamma. *J. Biol. Chem.* **280**(14): 14145-14153.

Simons M and Raposo G (2009) Exosomes-vesicular carriers for intercellular communication. *Curr. Opin. Cell Biol.* **21**(4): 575-581.

Sinensky M (2000) Recent advances in the study of prenylated proteins. *Biochim. Biophys. Acta* **1484**(2-3): 93-106.

Sinz A and Wang K (2001) Mapping protein interfaces with a fluorogenic cross-linker and mass spectrometry: application to nebulin-calmodulin complexes. *Biochemistry* **40**(26): 7903-7913.

Smith AC, Heo WD, Braun V, Jiang X, Macrae C, Casanova JE, Scidmore MA, Grinstein S, Meyer T and Brumell JH (2007) A network of Rab GTPases controls phagosome maturation and is modulated by *Salmonella enterica* serovar *Typhimurium*. *J. Cell Biol.* **176**(3): 263-268.

Smotrys JE and Linder ME (2004) Palmitoylation of intracellular signaling proteins: regulation and function. *Annu. Rev. Biochem.* **73**: 559-587.

Smotrys JE, Schoenfish MJ, Stutz MA and Linder ME (2005) The vacuolar DHHC-CRD protein Pfa3p is a protein acyltransferase for Vac8p. *J. Cell Biol.* **170**(7): 1091-1099.

Sobo K, Le Blanc I, Luyet PP, Fivaz M, Ferguson C, Parton RG, Gruenberg J and van der Goot FG (2007) Late endosomal cholesterol accumulation leads to impaired intra-endosomal trafficking. *PLoS One* **2**(9): e851.

Solinger JA and Spang A (2013) Tethering complexes in the endocytic pathway: CORVET and HOPS. *FEBS J.* **280**(12): 2743-2757.

Stachowiak JC, Brodsky FM and Miller EA (2013) A cost-benefit analysis of the physical mechanisms of membrane curvature. *Nat. Cell Biol.* **15**(9): 1019-1027.

Stamatakis K, Cernuda-Morollón E, Hernández-Perera O and Pérez-Sala D (2002) Isoprenylation of RhoB is necessary for its degradation. A novel determinant in the complex regulation of RhoB expression by the mevalonate pathway. *J. Biol. Chem.* **277**(51): 49389-49396.

Stamatakis K and Pérez-Sala D (2006) Prostanoids with cyclopentenone structure as tools for the characterization of electrophilic lipid-protein interactomes. *Ann. N. Y. Acad. Sci.* **1091**: 548-570.

Stamatakis K, Sánchez-Gómez FJ and Pérez-Sala D (2006) Identification of novel protein targets for modification by 15-deoxy-Delta12,14-prostaglandin J2 in mesangial cells reveals multiple interactions with the cytoskeleton. *J. Am. Soc. Nephrol.* **17**(1): 89-98.

Stenmark H (2009) Rab GTPases as coordinators of vesicle traffic. *Nat. Rev. Mol. Cell Biol.* **10**(8): 513-525.

Stepanek O, Draber P and Horejsi V (2014) Palmitoylated transmembrane adaptor proteins in leukocyte signaling. *Cell. Signal.* **26**(5): 895-902.

Stinchcombe J, Bossi G and Griffiths GM (2004) Linking albinism and immunity: the secrets of secretory lysosomes. *Science* **305**(5680): 55-59.

Stinchcombe JC, Page LJ and Griffiths GM (2000) Secretory lysosome biogenesis in cytotoxic T lymphocytes from normal and Chediak Higashi syndrome patients. *Traffic* **1**(5): 435-444.

Stipp CS, Kolesnikova TV and Hemler ME (2003) Functional domains in tetraspanin proteins. *Trends Biochem. Sci.* **28**(2): 106-112.

Straus DS and Glass CK (2001) Cyclopentenone prostaglandins: new insights on biological activities and cellular targets. *Med. Res. Rev.* **21**(3): 185-210.

Strauss K, Goebel C, Runz H, Möbius W, Weiss S, Feussner I, Simons M and Schneider A (2010) Exosome secretion ameliorates lysosomal storage of cholesterol in Niemann-Pick type C disease. *J. Biol. Chem.* **285**(34): 26279-26288.

Stuffers S, Sem Wegner C, Stenmark H and Brech A (2009) Multivesicular endosome biogenesis in the absence of ESCRTs. *Traffic* **10**(7): 925-937.

Takai Y, Sasaki T and Matozaki T (2001) Small GTP-Binding Proteins. *Physiol. Rev.* **81**(1): 153-208.

Tan EW, Pérez-Sala D, Cañada FJ and Rando RR (1991) Identifying the recognition unit for G protein methylation. *J. Biol. Chem.* **266**(17): 10719-10722.

Tchernev VT, Mansfield TA, Giot L, Kumar AM, Nandabalan K, Li Y, Mishra VS, Detter JC, Rothberg JM, Wallace MR, Southwick FS and Kingsmore SF (2002) The Chediak-Higashi protein interacts with SNARE complex and signal transduction proteins. *Mol. Med.* **8**(1): 56-64.

Terebiznik MR, Vázquez CL, Torbicki K, Banks D, Wang T, Hong W, Blanke SR, Colombo MI and Jones NL (2006) *Helicobacter pylori* VacA toxin promotes bacterial intracellular survival in gastric epithelial cells. *Infect. Immun.* **74**(12): 6599-6614.

Thapar R, Williams JG and Campbell SL (2004) NMR characterization of full-length farnesylated and non-farnesylated H-Ras and its implications for Raf activation. *J. Mol. Biol.* **343**(5): 1391-1408.

Theos AC, Truschel ST, Tenza D, Hurbain I, Harper DC, Berson JF, Thomas PC, Raposo G and Marks MS (2006) A lumenal domain-dependent pathway for sorting to intralumenal vesicles of multivesicular endosomes involved in organelle morphogenesis. *Dev. Cell* **10**(3): 343-354.

Tillement V, Lajoie-Mazenc I, Casanova A, Froment C, Penary M, Tovar D, Marquez R, Monsarrat B, Favre G and Pradines A (2008) Phosphorylation of RhoB by CK1 impedes actin stress fiber organization and epidermal growth factor receptor stabilization. *Exp. Cell Res.* **314**(15): 2811-2821.

Touchot N, Chardin P and Tavitian A (1987) Four additional members of the Ras gene superfamily isolated by an oligonucleotide strategy: molecular cloning of YPT-related cDNAs from a rat brain library. *Proc. Natl. Acad. Sci. U. S. A.* **84**(23): 8210-8214.

Toulmay A and Prinz WA (2013) Direct imaging reveals stable, micrometer-scale lipid domains that segregate proteins in live cells. *J. Cell Biol.* **202**(1): 35-44.

Trajkovic K, Hsu C, Chiantia S, Rajendran L, Wenzel D, Wieland F, Schwille P, Brugger B and Simons M (2008) Ceramide triggers budding of exosome vesicles into multivesicular endosomes. *Science* **319**(5867): 1244-1247.

Turner SJ, Zhuang S, Zhang T, Boss GR and Pilz RB (2008) Effects of lovastatin on Rho isoform expression, activity, and association with guanine nucleotide dissociation inhibitors. *Biochem. Pharmacol.* **75**(2): 405-413.

Uechi Y, Bayarjargal M, Umikawa M, Oshiro M, Takei K, Yamashiro Y, Asato T, Endo S, Misaki R, Taguchi T and Kariya K (2009) Rap2 function requires palmitoylation and recycling endosome localization. *Biochem. Biophys. Res. Commun.* **378**(4): 732-737.

Ullrich O, Horiuchi H, Bucci C and Zerial M (1994) Membrane association of Rab5 mediated by GDP-dissociation inhibitor and accompanied by GDP/GTP exchange. *Nature* **368**(6467): 157-160.

Ullrich O, Reinsch S, Urbe S, Zerial M and Parton RG (1996) Rab11 regulates recycling through the pericentriolar recycling endosome. *J. Cell Biol.* **135**(4): 913-924.

Ullrich O, Stenmark H, Alexandrov K, Huber LA, Kaibuchi K, Sasaki T, Takai Y and Zerial M (1993) Rab GDP dissociation inhibitor as a general regulator for the membrane association of rab proteins. *J. Biol. Chem.* **268**(24): 18143-18150.

Urade R, Hayashi Y and Kito M (1988) Endosomes differ from plasma membranes in the phospholipid molecular species composition. *Biochim. Biophys. Acta* **946**(1): 151-163.

Valero RA, Oeste CL, Stamatakis K, Ramos I, Herrera M, Boya P and Pérez-Sala D (2010) Structural determinants allowing endolysosomal sorting and degradation of endosomal GTPases. *Traffic* **11**(9): 1221-1233.

van Niel G, Charrin S, Simoes S, Romao M, Rochin L, Saftig P, Marks MS, Rubinstein E and Raposo G (2011) The tetraspanin CD63 regulates ESCRT-independent and -dependent endosomal sorting during melanogenesis. *Dev. Cell* **21**(4): 708-721.

Vega FM, Colomba A, Reymond N, Thomas M and Ridley AJ (2012) RhoB regulates cell migration through altered focal adhesion dynamics. *Open Biol* **2**(5): 120076.

Veit M, Sollner TH and Rothman JE (1996) Multiple palmitoylation of synaptotagmin and the t-SNARE SNAP-25. *FEBS Lett.* **385**(1-2): 119-123.

Verkruyse LA and Hofmann SL (1996) Lysosomal targeting of palmitoyl-protein thioesterase. *J. Biol. Chem.* **271**(26): 15831-15836.

Vlassov AV, Magdaleno S, Setterquist R and Conrad R (2012) Exosomes: current knowledge of their composition, biological functions, and diagnostic and therapeutic potentials. *Biochim. Biophys. Acta* **1820**(7): 940-948.

Vogt AB, Spindeldreher S and Kropshofer H (2002) Clustering of MHC-peptide complexes prior to their engagement in the immunological synapse: lipid raft and tetraspan microdomains. *Immunol. Rev.* **189**: 136-151.

Walsh CT, Garneau-Tsodikova S and Gatto GJ, Jr. (2005) Protein posttranslational modifications: the chemistry of proteome diversifications. *Angew. Chem. Int. Ed. Engl.* **44**(45): 7342-7372.

Wang DA and Sebti SM (2005) Palmitoylated cysteine 192 is required for RhoB tumor-suppressive and apoptotic activities. *J. Biol. Chem.* **280**(19): 19243-19249.

Wang M, Guo L, Wu Q, Zeng T, Lin Q, Qiao Y, Wang Q, Liu M, Zhang X, Ren L, Zhang S, Pei Y, Yin Z, Ding F and Wang HR (2014) ATR/Chk1/Smurf1 pathway determines cell fate after DNA damage by controlling RhoB abundance. *Nat Commun* **5**: 4901.

Wang Q, Pfeiffer GR, 2nd and Gaarde WA (2003) Activation of SRC tyrosine kinases in response to ICAM-1 ligation in pulmonary microvascular endothelial cells. *J. Biol. Chem.* **278**(48): 47731-47743.

Wang W, Yang L and Huang HW (2007) Evidence of cholesterol accumulated in high curvature regions: implication to the curvature elastic energy for lipid mixtures. *Biophys. J.* **92**(8): 2819-2830.

Ward DM, Griffiths GM, Stinchcombe JC and Kaplan J (2000) Analysis of the lysosomal storage disease Chediak-Higashi syndrome. *Traffic* **1**(11): 816-822.

Watson RT, Furukawa M, Chiang SH, Boeglin D, Kanzaki M, Saltiel AR and Pessin JE (2003) The exocytotic trafficking of TC10 occurs through both classical and nonclassical secretory transport pathways in 3T3L1 adipocytes. *Mol. Cell. Biol.* **23**(3): 961-974.

Wei ML (2006) Hermansky-Pudlak syndrome: a disease of protein trafficking and organelle function. *Pigment Cell Res.* **19**(1): 19-42.

Wennerberg K and Der CJ (2004) Rho-family GTPases: it's not only Rac and Rho (and I like it). *J. Cell Sci.* **117**(Pt 8): 1301-1312.

Wherlock M, Gampel A, Futter C and Mellor H (2004) Farnesyltransferase inhibitors disrupt EGF receptor traffic through modulation of the RhoB GTPase. *J. Cell Sci.* **117**(Pt 15): 3221-3231.

Whyte DB, Kirschmeier P, Hockenberry TN, Nunez-Oliva I, James L, Catino JJ, Bishop WR and Pai JK (1997) K- and N-Ras are geranylgeranylated in cells treated with farnesyl protein transferase inhibitors. *J. Biol. Chem.* **272**(22): 14459-14464.

Wideman JG, Leung KF, Field MC and Dacks JB (2014) The cell biology of the endocytic system from an evolutionary perspective. *Cold Spring Harb. Perspect. Biol.* **6**(4): a016998.

Williams RL and Urbe S (2007) The emerging shape of the ESCRT machinery. *Nat. Rev. Mol. Cell Biol.* **8**(5): 355-368.

Wubbolts R, Leckie RS, Veenhuizen PT, Schwarzmann G, Möbius W, Hoernschemeyer J, Slot JW, Geuze HJ and Stoorvogel W (2003) Proteomic and biochemical analyses of human B cell-derived exosomes. Potential implications for their function and multivesicular body formation. *J. Biol. Chem.* **278**(13): 10963-10972.

http://www.lipidlibrary.aocs.org

http://www.microvesicles.org

Yang X, Claas C, Kraeft SK, Chen LB, Wang Z, Kreidberg JA and Hemler ME (2002) Palmitoylation of tetraspanin proteins: modulation of CD151 lateral interactions, subcellular distribution, and integrin-dependent cell morphology. *Mol. Biol. Cell* **13**(3): 767-781.

Yang Z and Klionsky DJ (2010) Eaten alive: a history of macroautophagy. *Nat. Cell Biol.* **12**(9): 814-822.

Yeung T, Gilbert GE, Shi J, Silvius J, Kapus A and Grinstein S (2008) Membrane phosphatidylserine regulates surface charge and protein localization. *Science* **319**(5860): 210-213.

Yoshida T, Kawano Y, Sato K, Ando Y, Aoki J, Miura Y, Komano J, Tanaka Y and Koyanagi Y (2008) A CD63 mutant inhibits T-cell tropic human immunodeficiency virus type 1 entry by disrupting CXCR4 trafficking to the plasma membrane. *Traffic* **9**(4): 540-558.

Zhang H, Fan X, Bagshaw RD, Zhang L, Mahuran DJ and Callahan JW (2007) Lysosomal membranes from *beige* mice contain higher than normal levels of endoplasmic reticulum proteins. *J. Proteome Res.* **6**(1): 240-249.

Zheng H, Pearsall EA, Hurst DP, Zhang Y, Chu J, Zhou Y, Reggio PH, Loh HH and Law PY (2012) Palmitoylation and membrane cholesterol stabilize mu-opioid receptor homodimerization and G protein coupling. *BMC Cell Biol.* **13**: 6.